Published for SISSA by Springer

Received: *February 28, 2025*
Revised: *September 1, 2025*
Accepted: *September 10, 2025*
Published: *October 16, 2025*

Remarks on the Higgs branch of 5d conformal matter

Mario De Marco[b,e], **Michele Del Zotto**[a,c,b,e], **Julius F. Grimminger**[d] **and Andrea Sangiovanni**[a,c,b,e]

[a] *Mathematics Institute, Uppsala University, Box 480, SE-75106 Uppsala, Sweden*
[b] *Centre for Geometry and Physics, Uppsala University, Box 480, SE-75106 Uppsala, Sweden*
[c] *Department of Physics and Astronomy, Uppsala University, Box 516, SE-75120 Uppsala, Sweden*
[d] *Mathematical Institute, University of Oxford, Andrew Wiles Building, Woodstock Road, Oxford, OX2 6GG, U.K.*
[e] *Physique Théorique et Mathématique and International Solvay Institutes, Université Libre de Bruxelles, C.P. 231, 1050 Brussels, Belgium*

E-mail: mario.de.marco@ulb.be, michele.delzotto@math.uu.se, julius.grimminger@maths.ox.ac.uk, andrea.sangiovanni@math.uu.se

Abstract: Among the elementary building blocks in the atomic classification of 5d SCFTs there are 5d bifundamental conformal matter theories of various kinds. In this work we study the Higgs branch of these models and of the corresponding molecules arising from their fusion. To this aim we use two complementary independent strategies. On the one hand for the type A and D conformal matter, we identify dual (p, q) brane webs in IIB and exploit them to read off the corresponding magnetic quivers. On the other hand, we exploit circle reductions and study the resulting 4d $\mathcal{N} = 2$ SCFTs, giving an alternative derivation of their Higgs branches which extend also to the E types.

Keywords: Brane Dynamics in Gauge Theories, Extended Supersymmetry, Field Theories in Higher Dimensions, Supersymmetric Gauge Theory

ArXiv ePrint: 2502.04431

https://doi.org/10.1007/JHEP10(2025)144

Contents

1 Introduction

For a long time in the history of quantum fields it was believed that field theories in dimension greater than four were limited to systems of free fields. This was based on a Lagrangian prejudice and was proved wrong about 30 years ago with the discovery of interacting

JHEP10(2025)144

superconformal field theories (SCFTs) in 5 and 6 dimensions [1–8]. These systems have been since then a constant source of inspiration throughout formal QFT and mathematics. An interesting pathway to study these models is to resort to various combinations of stringy techniques — in particular string dualities and geometric engineering — and field theoretical methods such as (twisted) compactifications. Very often a non-Lagrangian SCFT in higher dimensions can be thus related to Lagrangian field theories in lower dimensions that can be exploited to learn about features of their higher dimensional progenitor. This is the strategy we will adopt also in this work to learn about a recently introduced class of 5d SCFTs, giving the first examples of 5d Conformal Matter (CM) [9] — 5d avatars of the 6d Conformal Matter [10], introduced to provide a 5d version of the atomic classification of 6d SCFTs and LSTs [11–13]. Our main aim is to explore their Higgs branches via a concerted effort that involves studying RG flows, circle compactifications (identifying suitable 4d $\mathcal{N} = 2$ systems along their extended KK Coulomb branch), as well as their dual fivebrane realizations to extract magnetic quivers. These techniques generate a coherent picture that passes several strict consistency checks operating across dimensions, and also serve to test new 5d dualities, clearly establishing the role of 5d Conformal Matter theories in the 5d SCFT landscape.

After the initial spark provided by [4–8, 14–19], 5d $\mathcal{N} = 1$ SCFTs have received a great deal of attention in the recent years: this renewed endeavour has fostered steadfast progress in their classification, relying on geometric approaches involving M-theory setups reduced on a non-compact canonical Calabi-Yau threefold[1] (CY3) [21–38], (p, q)-web constructions [39–49], as well as dimensional reduction from 6d SCFTs realized via F-theory on elliptic CY3 [50–54]. These are clearly interconnected technologies that completely agree on realms where they overlap. Eyes have been particularly set on characterizing the Coulomb and Higgs branches of the 5d SCFTs of interest: while the former can be analyzed with relatively straightforward methods,[2] in the context of geometric engineering Higgs branches receive quantum corrections due to M2-brane instantons, thus essentially hindering their understanding from an M-theory perspective. In order to overcome such difficulties, it is useful to resort to string-theoretic dualities. It turns out that 5d Higgs branches, which are typically singular hyper-Kähler cones, can be conveniently interpreted as Coulomb branches of suitably chosen 3d $\mathcal{N} = 4$ theories called magnetic quivers. The quantum corrections to these Coulomb branches, due to monopole operators, are under control [55] and are hence vastly more amenable to an explicit examination. Arguably the most successful recipe to extract magnetic quivers is via brane webs [56–70], if available. This is the case for all 5d Conformal Matter theories of types A and D. Building on the gauge theory phases identified in [9], in this work we give explicit (p, q) web realizations for all of these systems, thus establishing further dictionaries between networks of branes and M-theory singularities. As a byproduct of this analysis, we obtain magnetic quivers for all 5d CM theories of types A and D. But what about the 5d CM theories of type E? In order to determine the corresponding Higgs branches we exploit a different strategy, a circle compactification to 4d. On the one hand, this gives a

[1] Oftentimes, it is assumed that a suitable complete Calabi-Yau metric exists for canonical CY3. This is a subtle assumption that requires great care — see e.g. [20] for a recent work examining this aspect.

[2] E.g., in the context of M-theory backgrounds on CY3 $\times\mathbb{R}^{4,1}$, by performing a crepant resolution of the singularities of CY3.

JHEP10(2025)144

nice independent consistency check on the magnetic quiver results, on the other hand this allows to obtain information about the exceptional 5d CM theories.

The 5d CM theories can be organized in two broad families in the atomic classification spirit: we have 5d CMs that serve as atoms, and molecules that can be interpreted as fusions of several 5d CM systems. We denote these 5d SCFTs with $\mathcal{T}_X$, where X is the CY3 employed to engineer them in M-theory. Fusion is a 5d process which is reminiscent of the 6d fusion [71] (a generalization of the process of conformal gauging in 4d to higher dimensional systems). We say that a 5d SCFT is a fusion of several atoms whenever along the 5d Coulomb branch of the given system, we find a non-Lagrangian gauge theory phase that can be interpreted as a generalized linear quiver that has CM atoms as edges and gauge nodes of type $\mathfrak{g}$. We denote such gauge theory phase $\widetilde{\mathsf{Q}}_X$. For a generalized bifundamental atom of type $\mathfrak{g}$, $\widetilde{\mathsf{Q}}_X = \mathcal{T}_X$ since by definition this theory does not have any gauge nodes of type $\mathfrak{g}$ [9]. All bifundamental CM theories also have a Lagrangian gauge theory phase, corresponding to a suitable decoration of the Dynkin quiver of type $\mathfrak{g}$ by SU(N) gauge nodes, which we denote Q_X. These two gauge theory phases, being points on the extended Coulomb branch of the same 5d SCFT, are related by a 5d duality.[3] The behavior of 5d atoms and 5d molecules upon circle reduction is slightly different and we summarize it in figures 1 and 2. In the figures we represent in red the extended 5d CB, and in blue the 4d KK Coulomb branch. Along the 4d KK Coulomb branch there are special loci, analogous to Argyres-Douglas points [72], where a 4d $\mathcal{N} = 2$ SCFT arises. It is of particular interest to determine the point which corresponds to the circle reduction of the undeformed 5d SCFT. We denote $D^{\circ}_{S^1}\mathcal{T}_X$ the resulting 4d $\mathcal{N} = 2$ SCFT. In the case of the circle reduction of the 5d CM atoms we consider in this paper the result is a class-$\mathcal{S}$ trinion, that we can determine uniquely thanks to the extensive work on their classification [73–82]. This identification also determines the corresponding Higgs branch, as the latter does not receive correction upon circle compactification. In the case of the circle reduction of the 5d CM molecules $D^{\circ}_{S^1}\mathcal{T}_X$ is no longer arising from regular punctures in class-$\mathcal{S}$ — see figure 2. The class-$\mathcal{S}$ avatar we find along the 4d KK Coulomb branch is a circle reduction of the gauge theory phase $\widetilde{\mathsf{Q}}_X$. We can still use this result to provide a conjecture about the dimension of the Higgs branch of $D^{\circ}_{S^1}\mathcal{T}_X$, which is confirmed by the magnetic quiver analysis in types A and D. In particular, this predicts the existence of ADE families of generalized bifundamental 4d $\mathcal{N} = 2$ SCFTs with flavor symmetry $\mathfrak{g} \times \mathfrak{g} \times F_X$ with $\mathfrak{g} \in ADE$ and F_X an enhanced flavor symmetry we can explicitly determine that cannot be constructed via regular punctures in class-$\mathcal{S}$.

This work is organized as follows. In section 2 we review the construction of 5d conformal matter atoms and molecules of [9]. In section 3 the S^1 reduction of 5d conformal matter atoms to 4d $\mathcal{N} = 2$ class-$\mathcal{S}$ fixtures is discussed. In section 4 the brane web constructions of A- and D-type 5d conformal matter atoms are presented and their magnetic quivers are derived, testing, as a by-product, the construction in section 3. In section 5 the S^1 reduction of 5d conformal matter molecules is addressed; by turning on specific masses for the 5d conformal matter molecule the S^1 reduction leads to a 4d $\mathcal{N} = 2$ class-$\mathcal{S}$ theory, which is provided. In section 6 the brane web constructions of A- and D-type 5d conformal matter molecules are

[3] Employing standard terminology, we say that two different 5d gauge theories are related by a 5d UV duality if and only if they can be obtained as different mass deformations of the *same* 5d UV fixed point.

JHEP10(2025)144

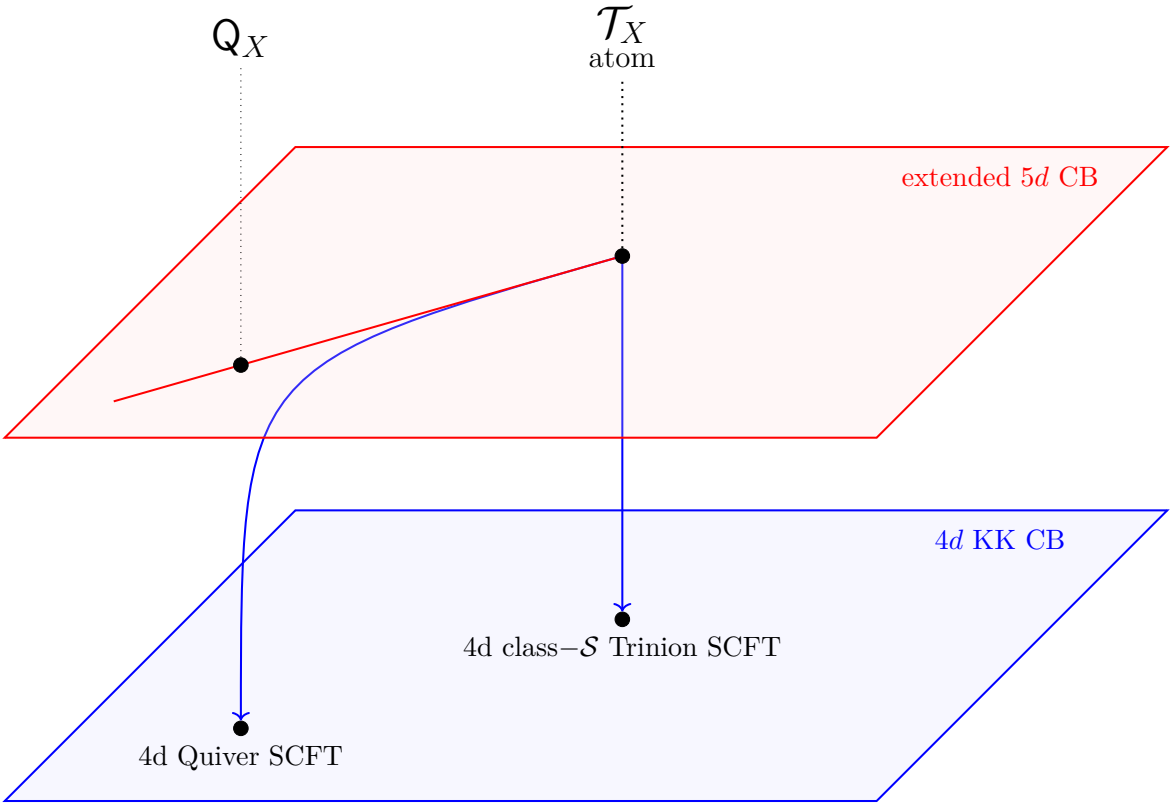

Figure 1. Illustration of toroidal compactifications of a 5d conformal matter atom. The red shaded area is a schematic depiction of the 5d extended Coulomb branch (including mass deformations) of the SCFT $\mathcal{T}_X$. The red line emanating from the origin of the CB corresponds to the mass deformation of the SCFT to the Dynkin quiver phase. Blue arrows depict RG flows to 4 dimensions. The area shaded in blue is a schematic depiction of the 4d KK Coulomb branch. The atom $\mathcal{T}_X$ can be directly compactified to a 4d class$-\mathcal{S}$ trinion SCFT, which we may call 4d class$-\mathcal{S}$ atom. Turning on the mass deformation going to the left it can also be compactified to a 4d Lagrangian SCFT. For an atom we have $\underset{\text{atom}}{\mathcal{T}_X} = \tilde{\mathsf{Q}}_X$.

presented and their magnetic quivers are derived, furthermore a precise description of the mass deformation of section 5 is described. Section 7 serves as the conclusion and provides an outlook on future work. Appendix A summarises specific low energy quiver descriptions of 5d conformal matter atoms and molecules, which were provided in [9]. Appendix B addresses the question of identifying Higgs branch moduli of 5d a $\mathcal{N} = 1$ SCFT from the geometry of a local CY3 which engineers it. In appendix C breaking patterns of the flavor group are explored. In appendix D our notation for quivers and brane webs is reviewed.

We conclude this section by summarizing the notation used in this paper in table 1 for the convenience of our readers.

2 Atomic classification of 5d conformal matter theories

In this section we summarise key features of 5d conformal matter theories, which were recently introduced in [9].

JHEP10(2025)144

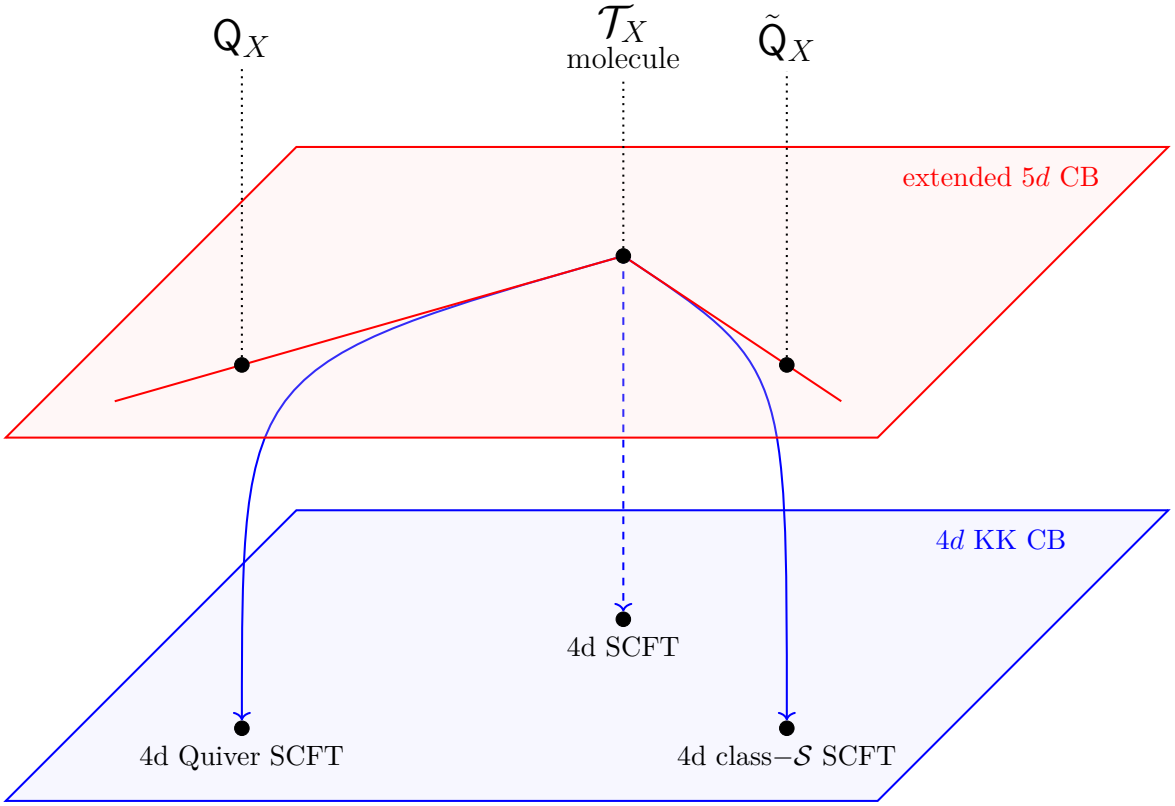

Figure 2. Illustration of toroidal compactifications of a 5d conformal matter molecule. The red shaded area is a schematic depiction of the 5d extended Coulomb branch (including mass deformations) of the SCFT $\mathcal{T}_X$. The red line emanating from the origin of the CB to the left corresponds to the mass deformation of the SCFT to the Dynkin quiver phase. The red line emanating to the right corresponds to the mass deformation of the SCFT to the 'generalized quiver' phase. Blue arrows depict RG flows to 4 dimensions. The area shaded in blue is a schematic depiction of the 4d KK Coulomb branch. The atom $\mathcal{T}_X$ cannot be directly compactified to a 4d class$-\mathcal{S}$ theory, and we don't know a good description of this theory in 4d. Turning on the mass deformation going to the left the theory can be compactified to a 4d Lagrangian SCFT. Turning on the mass deformation going to the right the theory can be compactified to a 4d class$-\mathcal{S}$ theory which is the gauging of 4d class$-\mathcal{S}$ atoms.

These are interacting 5d SCFTs, displaying at least $\mathfrak{g} \times \mathfrak{g}$ flavor symmetry, with $\mathfrak{g} \in ADE$. Further, they all admit a low-energy gauge theory phase, which can be employed to explicitly glean the UV flavor symmetry thanks to the techniques of [83].

2.1 Atoms of 5d conformal matter

Concretely, 5d conformal matter bifundamental theories are obtained via M-theory geometric engineering on a specific class of threefolds with canonical non-isolated singularities. The starting point of our construction are the ADE (or Du Val) surface singularities:

$$P_{\mathfrak{g}}(x_1, x_2, x_3) = 0 \qquad \mathfrak{g} \in ADE, \tag{2.1}$$

JHEP10(2025)144

$\mathcal{T}_{5d}$ or $\mathcal{T}_{X_{\mathfrak{g}}^{(1^{n_1},2^{n_2},3^{n_3})}}$	The 5d SCFT engineered by a conformal matter atom or molecule.
$\mathsf{Q}_{X_{\mathfrak{g}}^{(1^{n_1},2^{n_2},3^{n_3})}}$	The 5d low-energy Dynkin quiver phase corresponding to our preferred choice of resolution, outlined in section 2.2.
$\tilde{\mathsf{Q}}_{X_{\mathfrak{g}}^{(1^{n_1},2^{n_2},3^{n_3})}}$	The generalized 5d conformal matter quiver that directly descends to some class-$\mathcal{S}$ theory. This coincides with $\mathcal{T}_{X_{\mathfrak{g}}^{(1^{n_1},2^{n_2},3^{n_3})}}$ *only for atoms.*
$\mathcal{T}_{4d}$	The 4d class-$\mathcal{S}$ theory that descends from $\tilde{\mathsf{Q}}_{X_{\mathfrak{g}}^{(1^{n_1},2^{n_2},3^{n_3})}}$.
$\mathsf{MQ}(\ldots)$	Magnetic quiver of '…' some SQFT.
HB(…)	Higgs branch of '…' some SQFT.
$\mathrm{CB}_{5d}(\ldots)$	5d Coulomb branch of '…' some 5d $\mathcal{N}=1$ SQFT.
$\mathrm{CB}_{4d}(\ldots)$	4d Coulomb branch of '…' some 4d $\mathcal{N}=2$ SQFT.
$\mathrm{CB}_{3d}(\ldots)$	3d Coulomb branch of '…' some 3d $\mathcal{N}=4$ SQFT.

Table 1. Notation chosen for the present work.

where we are using the conventional form:

$$\begin{cases} P_{A_k}(x_1,x_2,x_3) = x_1^2 + x_2^2 - x_3^{k+1} \\ P_{D_k}(x_1,x_2,x_3) = x_1^2 + x_3 x_2^2 + x_3^{k-1} \\ P_{E_6}(x_1,x_2,x_3) = x_1^2 + x_2^3 + x_3^4 \\ P_{E_7}(x_1,x_2,x_3) = x_1^2 + x_2^3 + x_2 x_3^3 \\ P_{E_8}(x_1,x_2,x_3) = x_1^2 + x_2^3 + x_3^5, \end{cases} \tag{2.2}$$

Replacing one of the $x_i \to uv$ we get a threefold:

$$X_{\mathfrak{g}}^{(i)} \quad : \quad \begin{cases} P_{\mathfrak{g}}(x_1,x_2,x_3) = 0 \\ x_i = uv \end{cases} \quad . \tag{2.3}$$

Notice that the threefold $X_{\mathfrak{g}}^{(i)}$ possesses two non-compact complex lines of singularities of type $\mathfrak{g}$, on top of $u=0$ and $v=0$ respectively, intersecting at the origin $x_1=x_2=x_3=u=v=0$. The central claim of [9] can then be phrased as:

> *M-theory reduced on the singularities $X_{\mathfrak{g}}^{(i)}$ geometrically engineers interacting 5d SCFTs with at least $\mathfrak{g}\times\mathfrak{g}$ flavor symmetry. We call these theories the fundamental "atoms" of 5d conformal matter.*

One can directly prove this claim by explicitly performing a crepant resolution of the singularities $X_{\mathfrak{g}}^{(i)}$: it turns out that one such resolution always exists, and that the 5d SCFT admits a low-energy quiver gauge theory phase, that can readily be inferred from the

JHEP10(2025)144

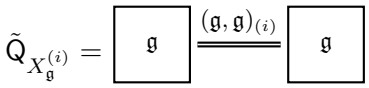

Figure 3. Generalised quiver representing an atom of 5d conformal matter of type $(\mathfrak{g},\mathfrak{g})_{(i)}$.

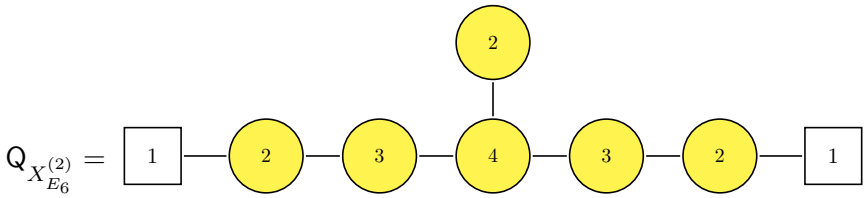

Figure 4. Low-energy Dynkin quiver description for the $X_{E_6}^{(2)}$ 5d conformal matter theory. Yellow gauge nodes represent special unitary factors in the gauge group.

resolution procedure. A list of the low-energy quiver gauge theories is provided in appendix A directly taken from [9]. The crucial consequence of this analysis is:

> *For each $\mathfrak{g} \in ADE$ there exist inequivalent atoms of 5d conformal matter, corresponding to the choice of i in $X_{\mathfrak{g}}^{(i)}$.*

"Inequivalent" means that they engineer different 5d SCFTs, which have different low-energy quiver gauge theory descriptions.

Only some of the 5d conformal matter atoms are dimensional reductions of 6d conformal matter atoms. All remaining 5d CM atoms are Higgsings thereof, as we will show in [84].

We may represent a single "atom" of 5d conformal matter as a *generalized quiver*, like in figure 3, where the two $\mathfrak{g}$ flavor factors are highlighted. Notice that the edge *is* an interacting 5d SCFT,[4] and thus it is labelled by $(\mathfrak{g},\mathfrak{g})_{(i)}$, with i one among $1, 2, 3$. We denote these generalised quivers as $\tilde{\mathsf{Q}}_{X_{\mathfrak{g}}^{(i)}}$.

In general, the 5d conformal matter SCFT atom in figure 3 has the following properties:

- The SCFT is specified by the edge $(\mathfrak{g},\mathfrak{g})_{(i)}$. One can also represent the atom via an ordinary quiver (namely, a quiver where the edges are genuine bifundamental hypermultiplets) dual to figure 3, corresponding to the low-energy gauge theory phase arising from a specific choice of resolution (that will be reviewed in section (2.2)) of $X_{\mathfrak{g}}^{(i)}$. We denote these quivers as $\mathsf{Q}_{X_{\mathfrak{g}}^{(i)}}$.

  E.g. in the case $X_{E_6}^{(2)}$, one obtains the ordinary quiver of figure 4, which is an E_6 Dynkin quiver.

  See [9] and appendix A for the explicit Dynkin quiver realizations for all algebras.

- The flavor symmetry in the UV is:[5]

$$F_{UV} = \mathfrak{g} \times \mathfrak{g} \times F_{\text{rest}},$$

[4] In comparison a conventional edge in a quiver corresponding to a hypermultiplet may be considered a free SCFT.

[5] In this work we avoid discussions on the global form of the symmetry groups.

JHEP10(2025)144

with F_{rest} a product of $\mathfrak{su}$ and $\mathfrak{u}(1)$ factors, with known rank. F_{UV} can be computed employing the techniques of [83] applied to the Dynkin quiver in figure 4.

2.2 Summary of the resolution procedure

We quickly recall, for later reference, the recipe to obtain the specific resolution performed in [9]:

1. Perform the resolution of the $Y_{\mathfrak{g}}$ Du Val *surface* singularity displayed in (2.2), obtaining the following expressions:
$$\begin{cases} x_1 = x_1(a_j, b_j), \\ x_2 = x_2(a_j, b_j), \\ x_3 = x_3(a_j, b_j), \end{cases} \tag{2.4}$$
where $(a_j, b_j) \in \mathbb{C}^2$ form an atlas of the *resolved* Du Val surface and the functions $x_i(a_j, b_j)$ describes the blowdown map;

2. substitute $x_i = uv$ inside (2.4), obtaining a threefold $\widetilde{X}^{(i)}_{\mathfrak{g}}$, that partially resolves $X^{(i)}_{\mathfrak{g}}$. We note that, at this point, the remaining equations $x_k = x_k(a_j, b_j)$, with $k \neq i$, are spurious and can be dropped.

This procedure fully resolves the singularities outside the origin of (2.3) and corresponds to lifting to the *resolved* Du Val surface $\widetilde{Y}_{\mathfrak{g}}$ the base-change that we used to obtain $X^{(i)}_{\mathfrak{g}}$ from the *singular* Du Val surface $Y_{\mathfrak{g}}$. We call $\widetilde{X}^{(i)}_{\mathfrak{g}}$ the partially resolved threefold obtained in this way and ε the partial resolution map

$$\varepsilon : \quad \widetilde{X}^{(i)}_{\mathfrak{g}} \longrightarrow X^{(i)}_{\mathfrak{g}}. \tag{2.5}$$

The singular locus of $\widetilde{X}^{(i)}_{\mathfrak{g}}$ lies within the subvariety $\varepsilon^{-1}(0)$ that is blown-down to the origin. $\varepsilon^{-1}(0)$ is collection of $\mathbb{P}^1_i$'s, with $i = 1, \ldots, \text{rank}(\mathfrak{g})$. Each of these $\mathbb{P}^1_i$'s supports a line of singularities of type A_{r_i} with $r_i \geq 0$, from which we can read off the quivers obtained in [9]. We pictorially represent the geometry of $\widetilde{X}^{(i)}_{\mathfrak{g}}$ in figure 5, for the $\mathfrak{g} = E_6$ example: we copied the *resolved* $Y_{\mathfrak{g}}$ singularity along the two non-compact lines $u = 0$ and $v = 0$. Over each point of these lines we have a collection of rank($\mathfrak{g}$) $\mathbb{P}^1$'s that intersect each other according to the $\mathfrak{g}$ Dynkin diagram and that can be "translated"[6] along the considered line. These two collections of "movable" $\mathbb{P}^1$'s fuse together on the $\varepsilon^{-1}(0)$, creating a singular collection of $\mathbb{P}^1$'s.

A key feature of 5d conformal matter theories is that, for fixed $\mathfrak{g}$, there come physically inequivalent "species", labelled by (i), displaying different CB dimensions and different flavor groups. Geometrically, this comes from the fact that the resolution maps $x_i(a_j, b_j)$ differs from $x_k(a_j, b_j)$ for $k \neq i$.

2.3 Molecules of 5d conformal matter

The atomic analogy for 5d conformal matter can be pushed further: atoms can be fused together to form complex molecules, that in turn correspond to well-defined 5d SCFTs. Indeed, one of the advantages of the geometric approach is that the Calabi-Yau condition furnishes an

[6] More precisely, their normal bundle contains a $\mathcal{O}(0)$ summand.

JHEP10(2025)144

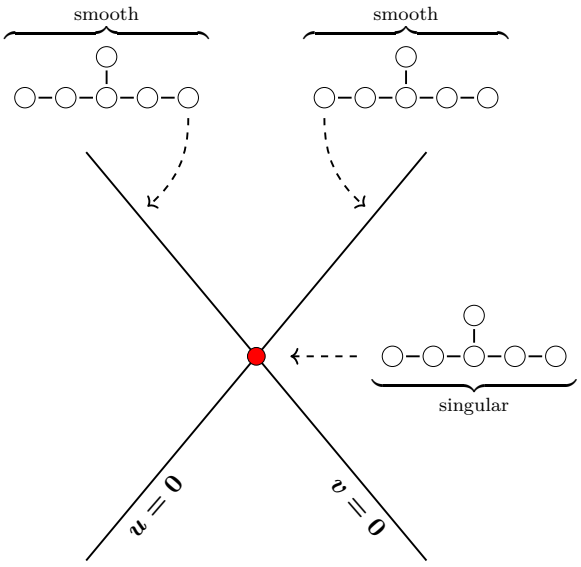

Figure 5. Pictorial representation of $\widetilde{X}^{(i)}_{E_6}$. The red point corresponds to the origin and its preimage under ϵ consists of a collection of singular $\mathbb{P}^1$'s, arranged like a E_6 Dynkin diagram.

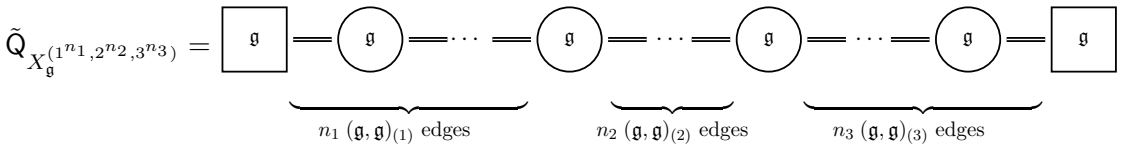

Figure 6. The most general molecule of 5d conformal matter.

easy criterion to understand whether we can fuse a $\mathfrak{g}$ symmetry. The result is that, in order to preserve the Calabi-Yau condition, we can gauge together the diagonal combination of at most two flavor nodes of the 5d conformal matter atoms depicted in figure 3, as proven in [9]. The most general molecule satisfying this criterion can be engineered from the threefold:

$$X_{\mathfrak{g}}^{(1^{n_1},2^{n_2},3^{n_3})}: \quad \begin{cases} P_{\mathfrak{g}}(x_1,x_2,x_3)=0 \\ UV = x_1^{n_1}x_2^{n_2}x_3^{n_3} \end{cases}, \tag{2.6}$$

with n_1, n_2, n_3 integers equal or greater than 0 (and at least one of them non-vanishing). This theory can be represented by the generalized quiver in figure 6, which is obtained by gluing together many of the atoms depicted in figure 3. We remark that the edges are to be thought as carrying non-trivial gauge content, labeled by $(\mathfrak{g},\mathfrak{g})_{(i)}$. In turn, for every threefold of the (2.6) kind, one can explicitly write down a Dynkin quiver with special unitary nodes corresponding to a 5d low-energy gauge theory phase. As an example, for the threefold

$$X_{E_6}^{(2^{n_2})}: \quad \begin{cases} P_{E_6}(x_1,x_2,x_3)=0 \\ UV = x_2^{n_2} \end{cases}, \tag{2.7}$$

the corresponding low-energy quiver gauge theory is depicted in figure 7.

We refer to [9] for all the other realizations.

JHEP10(2025)144

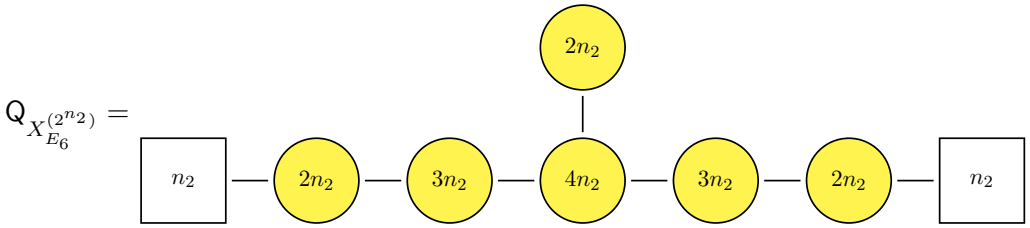

Figure 7. Low-energy quiver phase corresponding to the molecule with $\mathfrak{g} = E_6$, $n_1 = n_3 = 0$ and n_2 arbitrary.

In summary, given the expression (2.6) for the threefold canonical singularity, one needs to choose the following data, in order to specify a 5d conformal matter molecule:

- the algebra $\mathfrak{g}$, that yields the $\mathfrak{g} \times \mathfrak{g}$ flavor symmetry factor;
- the exponents n_1, n_2, n_3 in (2.6), that dictate how many atoms compose the molecule, and the kind of atoms that compose it.[7]

Physically, this data fixes the gauge symmetry of the corresponding 5d SCFT, as well as the rank of the flavor symmetry, which is of the form

$$F_{UV} = \mathfrak{g} \times \mathfrak{g} \times F_{\text{rest}}, \tag{2.8}$$

with F_{rest} depending on n_1, n_2, n_3.

All in all, the aforementioned data (namely, the choice of $\mathfrak{g}$ and n_i) furnishes the sought-after atomic classification of the class of 5d conformal matter SCFTs introduced in [9].[8]

3 5d conformal matter atoms and class $\mathcal{S}$ constructions

We now turn to the toroidal compactifications of 5d conformal matter atoms. It turns out that, for all the 5d conformal matter *atoms* we have exhibited, there exists a 4d $\mathcal{N} = 2$ descendant, based on a class-$\mathcal{S}$ construction. Such claim is substantiated explicitly by checking that the following well-known facts hold [86, 87]:

- the number of (real-valued) $\mathcal{T}_{5d}$ CB modes must coincide with the number of (complex-valued) $\mathcal{T}_{4d}$ CB modes;
- the global symmetries of $\mathcal{T}_{5d}$ and $\mathcal{T}_{4d}$ must be the same;[9]
- if there is no 1-form symmetry in $\mathcal{T}_{5d}$, then there is none also in $\mathcal{T}_{4d}$.

[7] Of course, molecules can be arbitrarily long, and single atoms such as figure 3 are recovered setting all exponents n_1, n_2, n_3 to zero, except for one set to 1.

[8] Notice that the low-energy phases of the 5d conformal matter theories with $n_1 = n_2 = 0$ in (2.6) were already explored in [24] (for the case $n_3 = 1$) and [85]. These are the direct dimensional reduction of 6d conformal matter theories. One might wonder whether also all the other 5d conformal matter theories reviewed in this work descend from 6d, along the lines of [53]: we will clarify this aspect in upcoming work [84].

[9] For some caveats to this claim, that will not enter our discussion, see [87].

JHEP10(2025)144

We begin, in section 3.1, finding a set of theories $\mathcal{T}_{4d}$ satisfying all the above points, by means of a class-$\mathcal{S}$ setup involving regular punctures. Such $\mathcal{T}_{4d}$ are strong candidates to be the descendants of the 5d conformal matter atomic theories $\mathcal{T}_{5d}$ via circle reduction. We will then, in section 3.2, match the Higgs branch dimensions between $\mathcal{T}_{5d}$ and $\mathcal{T}_{4d}$, carefully taking into account the contributions of the instantonic particles and tracking them back in the geometry of the threefolds $X_{\mathfrak{g}}^{(i)}$.

3.1 4d reduction of 5d conformal matter atoms

The logic to extract the 4d reduction $\mathcal{T}_{4d}$ of 5d conformal matter fundamental atoms $\mathcal{T}_{5d}$ from bottom-up is straightforward and can be implemented by way of a step-by-step procedure.

Start by picking the conformal matter theory $\mathcal{T}_{5d}$ related to the threefold $X_{\mathfrak{g}}^{(i)}$, that we have recalled in section 2. To access the 4d picture, consider the 6d $\mathcal{N} = (2, 0)$ theory of type $\mathfrak{g}$ reduced on a sphere with three regular punctures (with a suitable topological twist). Recall that each regular puncture is related to[10] a nilpotent orbit $\mathcal{O}_i$ of $\mathfrak{g}$, and that the Coulomb branch dimension of the 4d theory is:

$$\dim \mathrm{CB}_{4d}(\mathcal{T}_{4d}) = \frac{1}{2} \sum_{i=1}^{n_{\text{punctures}}} (\dim(\mathcal{O}_i)) - \dim(\mathfrak{g}). \tag{3.1}$$

Moreover, the contribution of each puncture to the flavor symmetry is given by the stabilizers of the Langlands dual of $\mathcal{O}_i$, that we denote with $\mathcal{O}_i^L$ [75].

Given the flavor symmetry of $\mathcal{T}_{5d}$, say (coherently with the notation of the previous sections)

$$F_{UV} = \mathfrak{g} \times \mathfrak{g} \times F_{\text{rest}}, \tag{3.2}$$

the punctures are chosen according to:

- Two punctures are maximal punctures related to the algebra $\mathfrak{g}$. This ensures that we obtain a $\mathfrak{g} \times \mathfrak{g}$ factor in the flavor symmetry, precisely as in the 5d parent.
- The third puncture $\mathcal{O}_{III}$ is chosen in such a way to match the expected CB dimension (i.e. the dimension of the CB of $\mathcal{T}_{5d}$). Non-trivially, the third puncture must also account for the F_{rest} flavor symmetry factor of $\mathcal{T}_{5d}$.[11]

It is easy to check that the above criteria for the class-$\mathcal{S}$ construction uniquely constrain the choice of the three regular punctures.[12]

[10] More precisely, the Hitchin field associated to the class $\mathcal{S}$ theory must have a simple pole

$$\Phi(w) = \frac{\Phi_{-1}}{w - w_p} + O(1)$$

at the puncture $w = w_p$, with w a coordinate on the Gaiotto curve. In the conformal limit, Φ_{-1} is nilpotent, and belongs to a nilpotent orbit $\mathcal{O}_i$ of $\mathfrak{g}$.

[11] In a follow up work [84] we uncover an interesting relationship between the $\mathcal{O}_{III}$ orbit and the Dynkin quiver. Nevertheless, as is done in this work, it is enough to use a small set of physical data to fix the orbit.

[12] There are rare exceptions to this claim: e.g. for the $X_{D_7}^{(2)}$ theory we could have chosen $\mathcal{O}'_{III} = [3^2, 1^8]$ instead of $\mathcal{O}_{III} = [2^6, 1^2]$, keeping the CB dimension and the flavor symmetry unchanged. The orbit $\mathcal{O}'_{III}$, though, would not fit into the infinite family of table 2 labelled by j, and thus we choose to set it aside.

JHEP10(2025)144

In table 2 we gather all the information needed to construct the 4d $\mathcal{N}=2$ class-$\mathcal{S}$ theory, listing the threefolds $X_{\mathfrak{g}}^{(i)}$ corresponding to its 5d parent, the nilpotent orbit $\mathcal{O}_{III}$ whose numbers dictate [74] the row lengths of the "Hitchin partition" Young tableaux of the third puncture, its Langlands dual $\mathcal{O}_{III}^{L}$ (whose numbers dictate the column heights of the "Nahm partition" Young tableaux of the third puncture), the rank of the 4d CB and the total 4d flavor symmetry. We employ the standard notation of [88] to label nilpotent orbits. In this notation,

- the Hitchin partition of a full puncture of type A_j is denoted as $[j+1]$. The Hitchin partition of a full puncture for a D_j algebra is denoted as $[2j-1,1]$;
- the Nahm partition of a full puncture of type A_j is denoted as $[1^{j+1}]$. The Nahm partition of a full puncture D_j algebra is denoted as $[1^{2j}]$. The Young tableaux of the Nahm partition can be obtained, for D_j, from the Hitchin one by the "D-collapse" procedure [74] (and taking care of reading the height of columns instead of the row length). The Young tableaux of the Nahm partition for the A_j case coincides with the Young tableaux of the Hitchin partition (where, in the first case, we read the heights of the columns, and in the second the lengths of the rows).

Furthermore, notice that, according to [89], class-$\mathcal{S}$ theories on a sphere with only untwisted regular punctures admit no 1-form symmetries. This is in agreement with the result found in [9]:

- since all line operators are screened in $\mathcal{T}_{5d}$, there can be no electric one-form symmetry in its descendant $\mathcal{T}_{4d}$,
- since all magnetically charged surface operators in $\mathcal{T}_{5d}$ are screened, there must be no magnetically charged lines in $\mathcal{T}_{4d}$.

Notice the perfect agreement between the rank of the 5d and 4d CB dimensions, as well as the full flavor symmetry.

As a fitting conclusion to this section, we point out that a completely rigorous description of the 4d descendants of our 5d theories $X_{\mathfrak{g}}^{(i)}$ would have to go through their Type IIA description, obtained from circle reduction: the corresponding Type IIB mirror geometry precisely enforces the class-$\mathcal{S}$ construction, that we have depicted above based on consistency arguments. We leave such analysis for future work.

3.2 5d conformal matter atoms and Higgs branch dimension

In this section we compute the quaternionic Higgs branch dimension of the 5d conformal matter theories reviewed in section 2, both from the purely 5d perspective and the class-$\mathcal{S}$ 4d point of view, showing their agreement. This relies on the fact that such dimension is protected under circle compactification, and provides a further consistency check of our constructions.

We start by computing the number of Higgs branch modes in the low-energy quiver phase of 5d conformal matter atoms of type $\mathfrak{g}$. These are the modes that are unlifted by the partial resolution (2.5). We then account for extra Higgs branch directions that open up in the infinite coupling limit, due to instantonic particles becoming massless, following [83]. We geometrically interpret the appearance of these instantonic particles in terms of the

JHEP10(2025)144

Singularity	$\mathcal{O}_{III}$	${\mathcal{O}_{III}}^L$	$\mathbf{rank}\,\mathbf{CB}_{\mathcal{T}_{4d}}$	F_{UV}
$X^{(1)}_{A_{2j+1}}$	$[2^{j+1}]$	$[(j+1)^2]$	j^2	$A_{2j+1} \times A_{2j+1} \times \mathfrak{u}(1)$
$X^{(1)}_{A_{2j}}$	$[2^j, 1]$	$[j+1, j]$	$j(j-1)$	$A_{2j} \times A_{2j} \times \mathfrak{u}(1)$
$X^{(3)}_{A_j}$	$[2, 1^{j-1}]$	$[j, 1]$	0	$A_j \times A_j \times \mathfrak{u}(1)$
$X^{(1)}_{D_{2j+2}}$	$[3^2, 2^{2j-2}, 1^2]$	$[(2j+1)^2, 1^2]$	$j(2j+3)$	$D_{2j+2} \times D_{2j+2} \times \mathfrak{u}(1)^2$
$X^{(1)}_{D_{2j+3}}$	$[3^2, 2^{2j-2}, 1^4]$	$[2j+3, 2j+1, 1^2]$	$j(2j+5)+1$	$D_{2j+3} \times D_{2j+3} \times \mathfrak{u}(1)$
$X^{(2)}_{D_{2j+2}}$	$[2^{2j}, 1^4]$	$[2j+3, 2j+1]$	$2j^2+j-2$	$D_{2j+2} \times D_{2j+2}$
$X^{(2)}_{D_{2j+3}}$	$[2^{2j+2}, 1^2]$	$[(2j+3)^2]$	$j(2j+3)$	$D_{2j+3} \times D_{2j+3} \times \mathfrak{u}(1)$
$X^{(3)}_{D_j}$	$[3, 1^{2j-3}]$	$[2j-3, 1^3]$	$j-2$	$D_j \times D_j \times \mathfrak{su}(2)$
$X^{(1)}_{E_6}$	A_2	$E_6(a_3)$	15	$E_6 \times E_6$
$X^{(2)}_{E_6}$	$2A_1$	D_5	10	$E_6 \times E_6 \times \mathfrak{u}(1)$
$X^{(3)}_{E_6}$	A_1	$E_6(a_1)$	5	$E_6 \times E_6$
$X^{(1)}_{E_7}$	A_2+A_1	$E_6(a_1)$	31	$E_7 \times E_7 \times \mathfrak{u}(1)$
$X^{(2)}_{E_7}$	$(3A_1)''$	E_6	20	$E_7 \times E_7 \times \mathfrak{su}(2)$
$X^{(3)}_{E_7}$	A_1	$E_7(a_1)$	10	$E_7 \times E_7$
$X^{(1)}_{E_8}$	A_2+A_1	$E_8(a_4)$	60	$E_8 \times E_8$
$X^{(2)}_{E_8}$	$2A_1$	$E_8(a_2)$	38	$E_8 \times E_8$
$X^{(3)}_{E_8}$	A_1	$E_8(a_1)$	21	$E_8 \times E_8$

Table 2. class-$\mathcal{S}$ data to construct the 4d descendants of the 5d conformal matter atoms.

transformation of M2-brane "vector-like" modes into M2-brane "Higgs-branch modes" at the collision point of the two lines of Du Val singularities.

Finally, we compute the Higgs branch dimension of the candidate class-$\mathcal{S}$ 4d reduction of 5d conformal matter atoms, showing complete agreement with the 5d Higgs branch dimension at the UV point.

Let us kick off our computation from the 5d perspective and examine the theories engineered by M-theory on $X^{(i)}_{\mathfrak{g}}$, whose low-energy ordinary quiver gauge theory phases were written down in [9]. We have shown an example of such quivers in figure 4. Therefore, the dimension of the Higgs branch at finite coupling can be computed directly from the quiver, namely:

$$\dim_{\mathbb{H}} \mathrm{HB}\left(\mathsf{Q}_{X^{(i)}_{\mathfrak{g}}}\right) = n_H - n_V, \tag{3.3}$$

with n_H the number of hypermultiplets and n_V the number of vector multiplets. We have

JHEP10(2025)144

to be careful, though, because this computation *neglects* the contribution of deformations that have been obstructed by the resolution map ϵ in (2.5). From the quiver perspective, this comes from the fact that (3.3) just captures the number of perturbative Higgs branch modes, and is blind to the instantonic particles becoming massless in the infinite coupling limit. These additional Higgs branch directions open up at the UV point, and can be detected by contracting the curves inflated by ϵ, which are arranged as the $\mathfrak{g}$ Dynkin diagram. Indeed, the instantonic particles of the quiver are exactly labeled by the root system of $\mathfrak{g}$ [83], with the single-instantons being the simple roots and the multi-instantons being the other roots.

In order to characterize them explicitly, let us consider $\widetilde{X}_{\mathfrak{g}}^{(i)}$: we can zoom in on a region centered on one of the two non-compact lines of *resolved* Du Val singularities of $\widetilde{X}_{\mathfrak{g}}^{(i)}$, away from their intersection point. There, the threefold locally looks like $\mathbb{C} \times \widetilde{Y}_{\mathfrak{g}}$, where $\widetilde{Y}_{\mathfrak{g}}$ is the *resolved* Du Val singularity and $\mathbb{C}$ is spanned, say, by u (equivalently, by v). We can now wrap M2-branes on the compact curves ruled over the non-compact line of resolved $\mathfrak{g}$ singularities. These curves exactly coincide with the $\mathbb{P}^1$'s resolving the (say) $u = 0$ line of Du Val singularity (away from the $v = 0$ point). These M2-branes become, in the limit of vanishing volume of the $\mathbb{P}^1$'s, states localized at the points where the $\mathbb{P}^1$'s get contracted. In this case, the M2-branes must be interpreted as 7d *vector* multiplets because

- the normal bundle of each $\mathbb{P}^1$ is $\mathcal{O}(0) \times \mathcal{O}(-2)$ and hence we have no first-order obstruction to a translation (along the $\mathcal{O}(0)$ direction) of the M2-brane. Mathematically, this comes from the existence of an holomorphic non-zero section of the normal bundle. Physically, this means that the corresponding M2-state is localized in 7d (rather than in 5d);
- there are also no higher-order obstructions.

In general, if one of these two conditions fails to be true, the M2-brane state gets localized to 5d, and generates 5d *Higgs branch* modes [29–31, 34, 35, 90].

It is a well-known result [91–93] that not all the elements in the compact homology $H_2(Y_{\mathfrak{g}}, \mathbb{Z})$ support an M2 BPS brane state, but, rather, the homology classes supporting an M2 state correspond to the root system of $\mathfrak{g}$. More precisely, the Poincaré duals of the $\mathbb{P}^1$'s resolving $Y_{\mathfrak{g}}$ correspond to the dual roots α_j^* of the $\mathfrak{g}$ Dynkin diagram. Furthermore, let α_j be the simple roots of $\mathfrak{g}$ and consider a two-cycle

$$\nu = \sum_{j=1}^{\text{rank}(\mathfrak{g})} n_j [\alpha_j] \tag{3.4}$$

with $[\alpha_j] \in H_2(\widetilde{Y}_{\mathfrak{g}}, \mathbb{Z})$ the homology class of the j-th. $\mathbb{P}^1$. Then, ν supports a M2 BPS state if and only if $\sum_{j=1}^{\text{rank}(\mathfrak{g})} n_j \alpha_j$ is a root of $\mathfrak{g}$.

We can specialize this general picture to the partially resolved threefold $\widetilde{X}_{\mathfrak{g}}^{(i)}$. As we can see from figure 5, away from the (red) intersection point the M2-branes wrapped on the compact $\mathbb{P}^1$'s become 7d vector multiplets, producing the W-bosons of the $\mathfrak{g} \times \mathfrak{g}$ flavor algebra. The *singular* $\mathbb{P}^1$'s contracted to the origin display obstructed deformation theory inside $\widetilde{X}_{\mathfrak{g}}^{(i)}$, and hence the corresponding M2 states are Higgs branch modes (rather than being part of a vector multiplet). This is in agreement with the 4d class-$\mathcal{S}$ picture, as we

JHEP10(2025)144

will show momentarily. In other words, at the intersection of the two lines of resolved Du Val singularities the M2-branes wrapping the $\mathbb{P}^1$'s can *not* be holomorphically "translated" along the non-compact direction, and hence they localize to 5d hypermultiplets. Indeed, as the size of the $\mathbb{P}^1$'s is different from zero (proportional to the square of the inverse gauge couplings) in the ordinary quiver phase, the aforementioned modes are massive and then do not contribute to (3.3). From a field theory perspective, the resolution (2.5) corresponds to giving a v.e.v. to the Cartan elements of a diagonal factor $\mathfrak{g}_{\text{diag}} \subset \mathfrak{g} \times \mathfrak{g}$ 5d flavor group of M-theory on $X_{\mathfrak{g}}^{(i)}$. Under a minimal coupling interaction $q_Q \widetilde{Q} M Q$, this lifts all the 5d Higgs branch modes with charge $q_Q \neq 0$ under g_{diag}, restricting the Higgs-branch dimension. The number of these states is the number of M2-branes wrapped on the "undeformable" $\mathbb{P}^1$'s contracting on the origin, and exactly matches the number of roots of $\mathfrak{g}$.

In appendix B we exhibit an explicit example of our choice of partial resolution of a 5d singular threefold, highlighting the curves wrapped by the M2-brane states that get trapped at the origin, thus giving rise to HB modes. Such an example involves the famous 5d T_N trinion theories, for a bipartite reason: it allows us to rely on toric geometry (although it is by no means a necessary choice) and, above all, shows this previously unnoticed behavior in such a well-known set of theories.

For the purpose of computing the UV Higgs branch dimension of 5d conformal matter atoms, the previous discussion implies that (3.3) gets modified as:

$$\dim_{\mathbb{H}} \text{HB}\left(\mathcal{T}_{X_{\mathfrak{g}}^{(i)}}\right) = n_H - n_V + \#\text{roots}(\mathfrak{g}). \tag{3.5}$$

Let us finally make contact with the 4d class-$\mathcal{S}$ picture. The dimension of the Higgs branch for the 4d $\mathcal{N} = 2$ theory can be computed according to [75], simply from the data of the regular punctures:

$$\dim_{\mathbb{H}} \text{HB}\left(\mathcal{T}_{4d}\right) = \frac{1}{2} \sum_i \left(\dim_{\mathbb{C}}(\mathfrak{g}) - \text{rank}(\mathfrak{g}) - \dim_{\mathbb{C}}(\mathcal{O}_i^L)\right) + \text{rank}(\mathfrak{g}), \tag{3.6}$$

with the choices of $\mathcal{O}_i^L$ of table (2).

Let us collect the results from the 5d and 4d computation in table 3, where we have listed the 5d HB dimension from the low-energy quiver phase, the 4d HB dimension, the difference between them (which corresponds to degrees of freedom that become massless in the infinite coupling limit of the 5d gauge theory, as many as the number of roots of the appropriate $\mathfrak{g}$), as well as the UV 5d HB dimension. Notice that the UV 5d HB dimension precisely agrees with the 4d HB dimension, as expected from the circle reduction.

4 5d conformal matter atoms, brane webs and magnetic quivers

Let us now to turn to a brane web construction for 5d conformal matter atoms, which exists for A- and D-type. For the A-type the atoms are realised on standard brane webs of (p, q)5-branes. For D-type one needs to include an ON5-plane. Our conventions for brane webs are summarised in appendix D.2.

JHEP10(2025)144

Singularity	$\dim_{\mathbb{H}}\mathrm{HB}(\mathsf{Q}_{X_{\mathfrak{g}}^{(i)}})$	$\dim_{\mathbb{H}}\mathrm{HB}(\mathcal{T}_{4d})$	$\dim_{\mathbb{H}}\mathrm{HB}(\mathcal{T}_{4d})-\dim_{\mathbb{H}}\mathrm{HB}(\mathsf{Q}_{X_{\mathfrak{g}}^{(i)}})$	$\dim_{\mathbb{H}}\mathrm{HB}(\mathcal{T}_{X_{\mathfrak{g}}^{(i)}})$
$X^{(1)}_{A_{2j+1}}$	$3j+2$	$4j^2+9j+4$	$2(2j^2+3j+1)$	$4j^2+9j+4$
$X^{(1)}_{A_{2j}}$	$3j$	$j(4j+5)$	$2j(2j+1)$	$j(4j+5)$
$X^{(3)}_{A_j}$	$j+1$	$(j+1)^2$	$j(j+1)$	$(j+1)^2$
$X^{(1)}_{D_{2j+2}}$	$3j+4$	$8j^2+15j+8$	$4(2j^2+3j+1)$	$8j^2+15j+8$
$X^{(1)}_{D_{2j+3}}$	$3j+5$	$8j^2+23j+17$	$4(2j^2+5j+3)$	$8j^2+23j+17$
$X^{(2)}_{D_{2j+2}}$	$3j+2$	$8j^2+15j+6$	$4(2j^2+3j+1)$	$8j^2+15j+6$
$X^{(2)}_{D_{2j+3}}$	$3j+4$	$8j^2+23j+16$	$4(2j^2+5j+3)$	$8j^2+23j+16$
$X^{(3)}_{D_j}$	$j+2$	$2j^2-j+2$	$2j(j-1)$	$2j^2-j+2$
$X^{(1)}_{E_6}$	9	81	72	81
$X^{(2)}_{E_6}$	8	80	72	80
$X^{(3)}_{E_6}$	7	79	72	79
$X^{(1)}_{E_7}$	11	137	126	137
$X^{(2)}_{E_7}$	10	136	126	136
$X^{(3)}_{E_7}$	8	134	126	134
$X^{(1)}_{E_8}$	12	252	240	252
$X^{(2)}_{E_8}$	10	250	240	250
$X^{(3)}_{E_8}$	9	249	240	249

Table 3. Higgs branch dimension from the low-energy quiver 5d phase $\mathsf{Q}_{X_{\mathfrak{g}}^{(i)}}$, the class-$\mathcal{S}$ 4d perspective $\mathcal{T}_{4d}$, and the infinite coupling 5d phase $\mathcal{T}_{X_{\mathfrak{g}}^{(i)}}$.

JHEP10(2025)144

4.1 A-type

4.1.1 $X^{(1)}_{A_{2j+1}}$

The low energy Dynkin quiver description $\mathsf{Q}_{X^{(1)}_{A_{2j+1}}}$ of the 5d SCFT $\mathcal{T}_{X^{(1)}_{A_{2j+1}}}$ associated to the $X^{(1)}_{A_{2j+1}}$ singularity is [9]

$\mathsf{Q}_{X^{(1)}_{A_{2j+1}}} =$

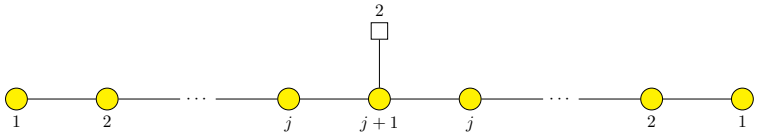

. (4.1)

A brane web for this theory (with both flavours massive) is

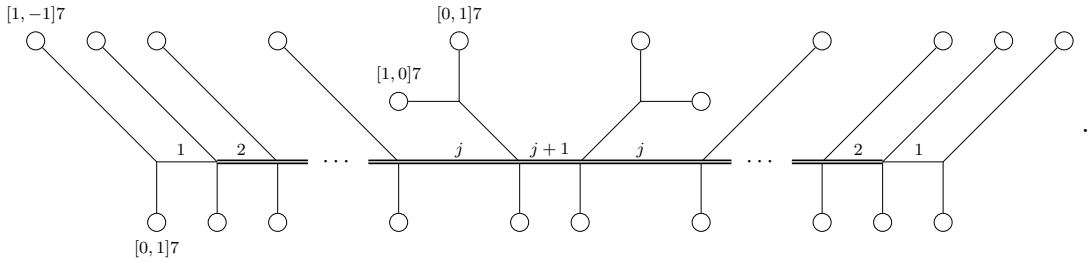

(4.2)

The parallel D5 branes support the SU gauge groups, and the two D7 branes ($[1,0]7$) provide the two flavours to the central SU gauge group. The vertical position of the D7 branes corresponds to the mass of the flavours.

After some Hanany-Witten moves (brane creation) we obtain

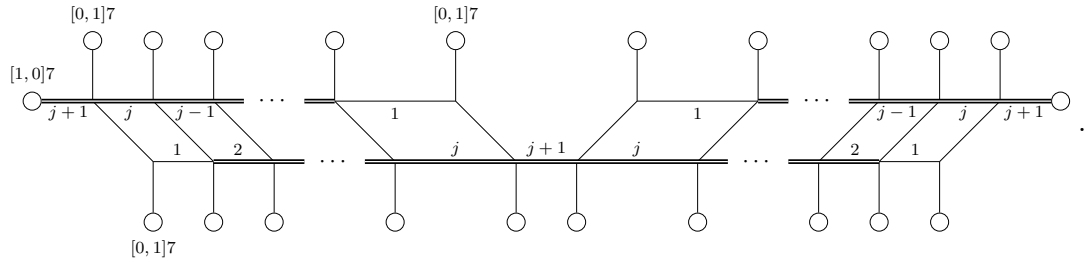

(4.3)

Taking the masses to zero we obtain

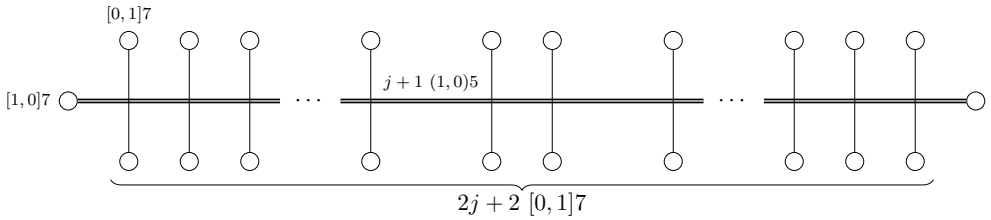

(4.4)

From this brane web the magnetic quiver for the finite coupling electric quiver (4.1) can be read using the prescriptions in [60]:

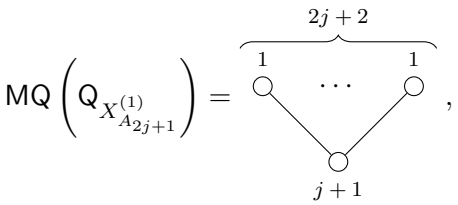

(4.5)

which is the 3d mirror of (4.1). From the magnetic quiver it is easy to identify the Higgs branch symmetry of the finite coupling quiver (4.1) to be $\mathrm{U}(1)^{2j+2}$, which matches exactly the $\mathrm{U}(1)^{2j+2}$ baryonic symmetries of said quiver. We have

$$\dim_{\mathbb{H}}\mathrm{CB}_{3d}\left(\mathsf{MQ}\left(\mathsf{Q}_{X^{(1)}_{A_{2j+1}}}\right)\right) = 3j+2 = \dim_{\mathbb{H}}\mathrm{HB}\left(\mathsf{Q}_{X^{(1)}_{A_{2j+1}}}\right) , \tag{4.6}$$

which matches table 3.

JHEP10(2025)144

Taking the couplings to infinity we obtain the brane web

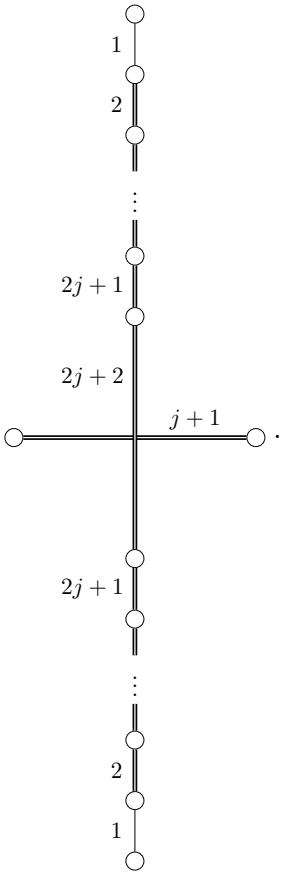

(4.7)

The corresponding GTP is

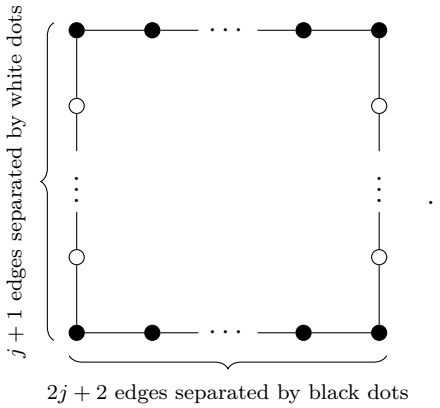

(4.8)

From this brane web we can read the magnetic quiver for the infinite coupling SCFT $\mathcal{T}_{X^{(1)}_{A_{2j+1}}}$

of (4.1) (i.e. the SCFT associated to the singular $X^{(1)}_{A_{2j+1}}$), which is

$$\mathsf{MQ}\left(\mathcal{T}_{X^{(1)}_{A_{2j+1}}}\right) =$$

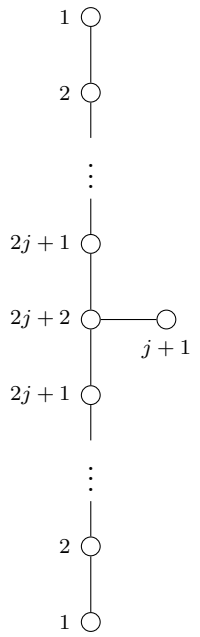

. (4.9)

From this magnetic quiver it is easy to identify the $\mathfrak{su}(2j+2) \times \mathfrak{su}(2j+2) \times \mathfrak{u}(1)$ symmetry of the SCFT, which enhances to E_7 for $j = 1$, and which enhances to $\mathfrak{sp}(4)$ for $j = 0$ where the magnetic quiver has Coulomb branch $\mathbb{H}^4$ indicating that the SCFT consists of free hypers. We have

$$\dim_{\mathbb{H}}\mathrm{CB}_{3d}\left(\mathsf{MQ}\left(\mathcal{T}_{X^{(1)}_{A_{2j+1}}}\right)\right) = 4j^2+9j+4 = (3j+2)+2(2j^2+3j+1) = \dim_{\mathbb{H}}\mathrm{HB}\left(\mathcal{T}_{X^{(1)}_{A_{2j+1}}}\right), \tag{4.10}$$

which matches table 3.

UV dual quiver descriptions. As a little aside we point out two more low energy quiver descriptions of the SCFT associated to $X^{(1)}_{A_{2j+1}}$, which can be read from the brane web. In order to see this we first perform an S-duality (along with a rotation) on our brane web, and obtain

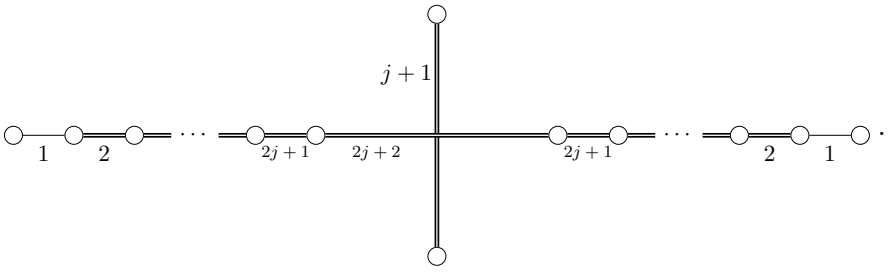

. (4.11)

After partially going on the extended Coulomb branch, and then performing some Hanany-Witten moves, we can obtain a brane web with quiver description

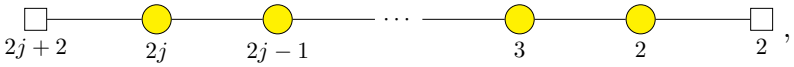

, (4.12)

JHEP10(2025)144

which has a manifest $\mathfrak{su}(2j+2)$ symmetry. At the level of the threefold, this operation amounts to performing another resolution of the singularity w.r.t. the one we presented in Section 2.2. We notice that some of the instantonic particles of the quiver (4.1) are now local degrees of freedom for (4.12).

One can go to a different leaf in the extended Coulomb branch, and after again performing Hanany-Witten transitions obtain a brane web with quiver description

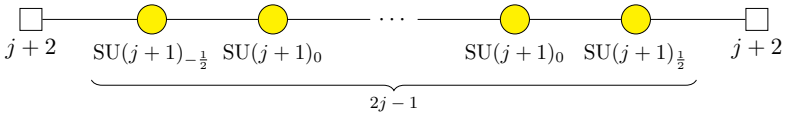

, (4.13)

which however does not have a manifest $\mathfrak{su}(2j+2)$ symmetry.

4.1.2 $X^{(1)}_{A_{2j}}$

The discussion of the brane web for the 5d SCFT associated to the $X^{(1)}_{A_{2j}}$ singularity is analogous to the previous section. We only present the infinite coupling brane web and corresponding magnetic quiver.

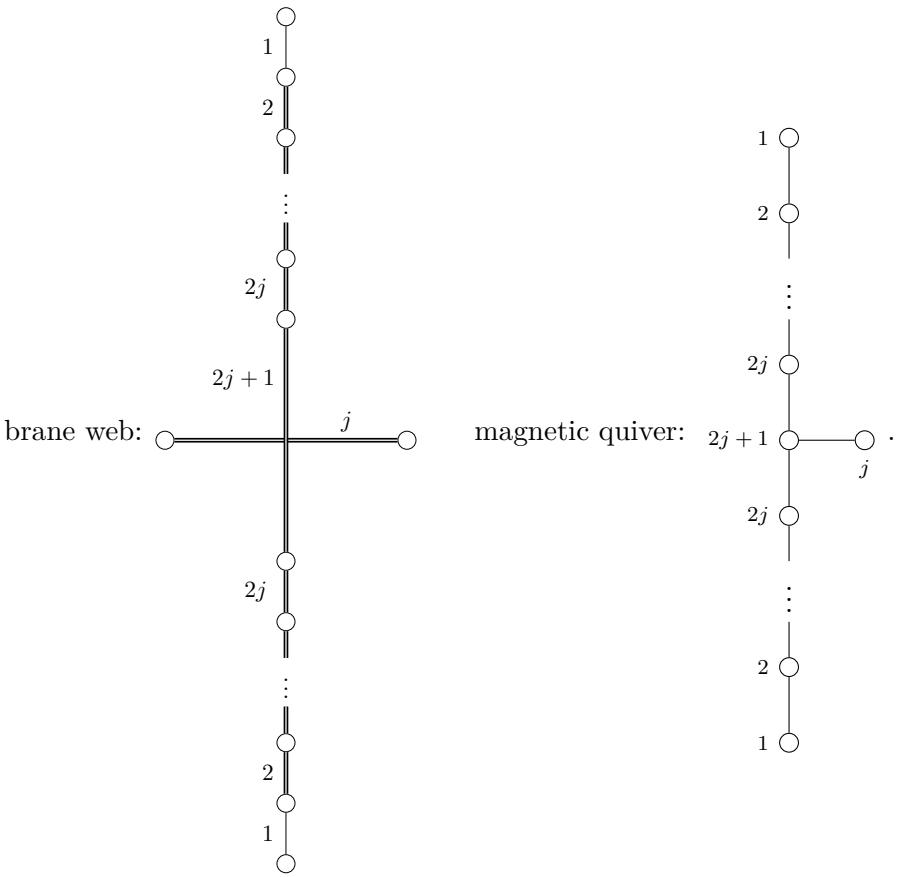

. (4.14)

The CB symmetry of this magnetic quiver is $\mathfrak{su}(2j+1)\times\mathfrak{su}(2j+1)\times\mathfrak{u}(1)$, which enhances to $\mathfrak{su}(10)$ for $j=2$, and enhances to $\mathfrak{sp}(9)$ for $j=1$ where the magnetic quiver has Coulomb branch $\mathbb{H}^9$ indicating that the SCFT consists of free hypers. We have

$$\dim_{\mathbb{H}}\left(\mathrm{CB}^{3d}\left(\mathsf{MQ}\left(\mathcal{T}_{X^{(1)}_{A_{2j}}}\right)\right)\right)=4j^2+5j=\dim_{\mathbb{H}}\left(\mathrm{HB}\left(\mathcal{T}_{X^{(1)}_{A_{2j}}}\right)\right)\,, \tag{4.15}$$

which matches table 3.

JHEP10(2025)144

4.2 D-type

4.2.1 $X^{(1)}_{D_{2j+2}}$

A low energy quiver description of the 5d SCFT associated to the $X^{(1)}_{D_{2j+2}}$ singularity is [9]

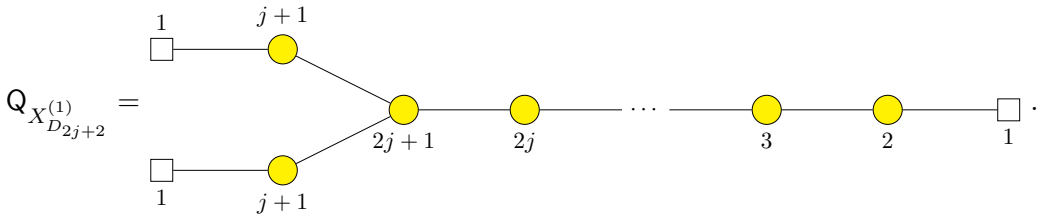

(4.16)

The D-type bifurcation in the gauge nodes can be realised on a brane web with ON5$^-$ (drawn as a green vertical line), similar to the constructions in [94]. The brane web with both flavours massive is

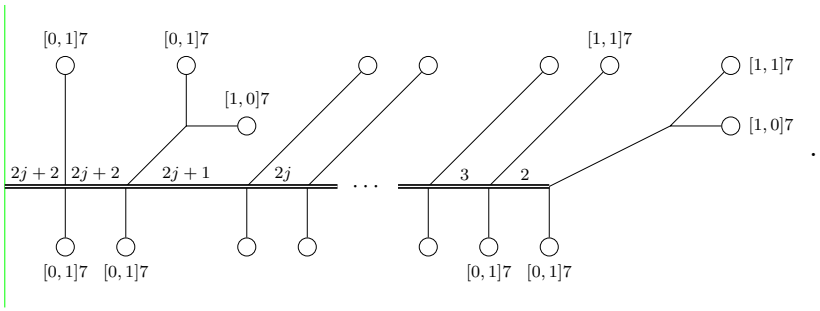

(4.17)

After some Hanany-Witten moves and taking the masses to zero we obtain

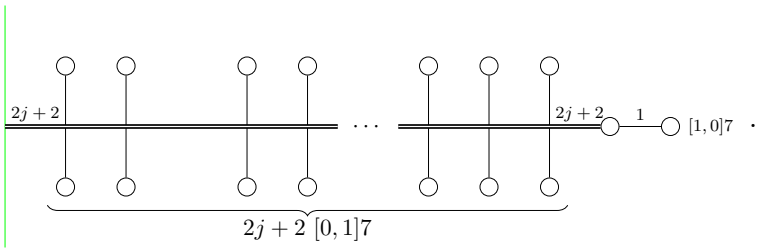

(4.18)

The magnetic quiver for the finite coupling electric quiver (4.16) can be read from the brane web using the prescriptions in [66]:[13]

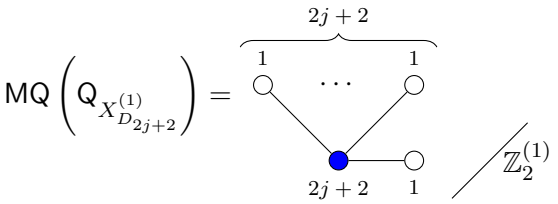

(4.19)

where $/\mathbb{Z}_2^{(1)}$ denotes gauging the $\mathbb{Z}_2$ 1-form symmetry of the quiver, which is achieved on the level of the monopole formula by considering the half-integer magnetic lattice [95]. The

[13] Ref. [66] deals with brane webs in the presence of O5 orientifold branes, such a setup is reached by performing an S-duality on our brane web.

JHEP10(2025)144

Coulomb branch global symmetry of the magnetic quiver is $\mathrm{U}(1)^{2j+3}$. We have

$$\dim_{\mathbb{H}}\mathrm{CB}_{3d}\left(\mathsf{MQ}\left(\mathsf{Q}_{X^{(1)}_{D_{2j+2}}}\right)\right) = 3j+4 = \dim_{\mathbb{H}}\mathrm{HB}\left(\mathsf{Q}_{X^{(1)}_{D_{2j+2}}}\right)\,, \tag{4.20}$$

which matches table 3.

Taking the couplings to infinity we obtain the brane web (now with both ON5$^-$ and $\widetilde{\mathrm{ON}}5^-$ planes, where $\widetilde{\mathrm{ON}}5^-$ is drawn in orange and corresponds to an ON5$^-$ with a stuck $\frac{1}{2}(0,1)5$ on top, see appendix D.2)

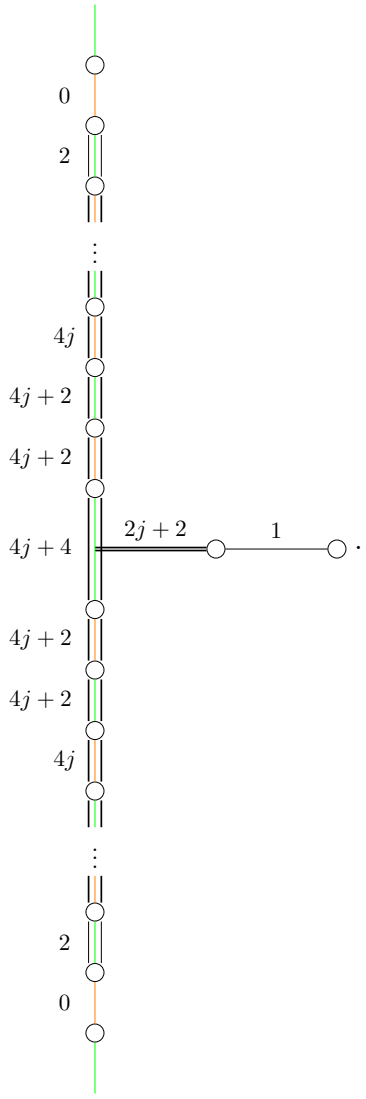

(4.21)

The numbers next to the brane segments on top of ON5 planes indicate the number of $\frac{1}{2}(0,1)5$-branes not accounting for the stuck $\frac{1}{2}(0,1)5$ involved in the $\widetilde{\mathrm{ON}}5^-$. From this brane

JHEP10(2025)144

web we can read the unitary-orthosymplectic magnetic quiver[14]

$$\mathsf{MQ}\left(\mathcal{T}_{X^{(1)}_{D_{2j+2}}}\right) =$$

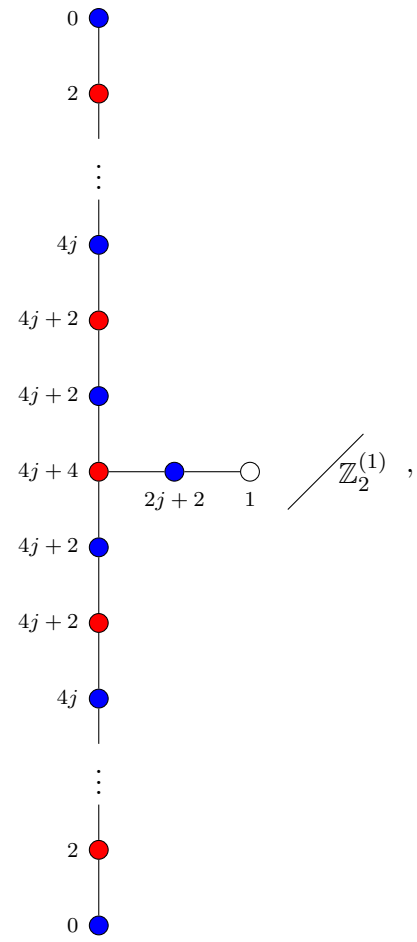

, (4.22)

from which we can identify the $\mathfrak{so}(4j+4) \times \mathfrak{so}(4j+4) \times \mathfrak{u}(1)^2$ global symmetry of the SCFT, which exists for $j \geq 1$. We have

$$\dim_{\mathbb{H}} \mathrm{CB}_{3d}\left(\mathsf{MQ}\left(\mathcal{T}_{X^{(1)}_{D_{2j+2}}}\right)\right) = 8j^2+15j+8 = (3j+4)+4(2j^2+3j+1) = \dim_{\mathbb{H}} \mathrm{HB}\left(\mathcal{T}_{X^{(1)}_{D_{2j+2}}}\right), \tag{4.23}$$

which matches table 3.

4.2.2 $X^{(1)}_{D_{2j+3}}$

The discussion of the brane web for the 5d SCFT associated to the $X^{(1)}_{D_{2j+3}}$ singularity is analogous to the previous section. We only present the infinite coupling brane web and

[14] For notation of quivers and types of gauge nodes, see appendix D.1.

JHEP10(2025)144

corresponding magnetic quiver:

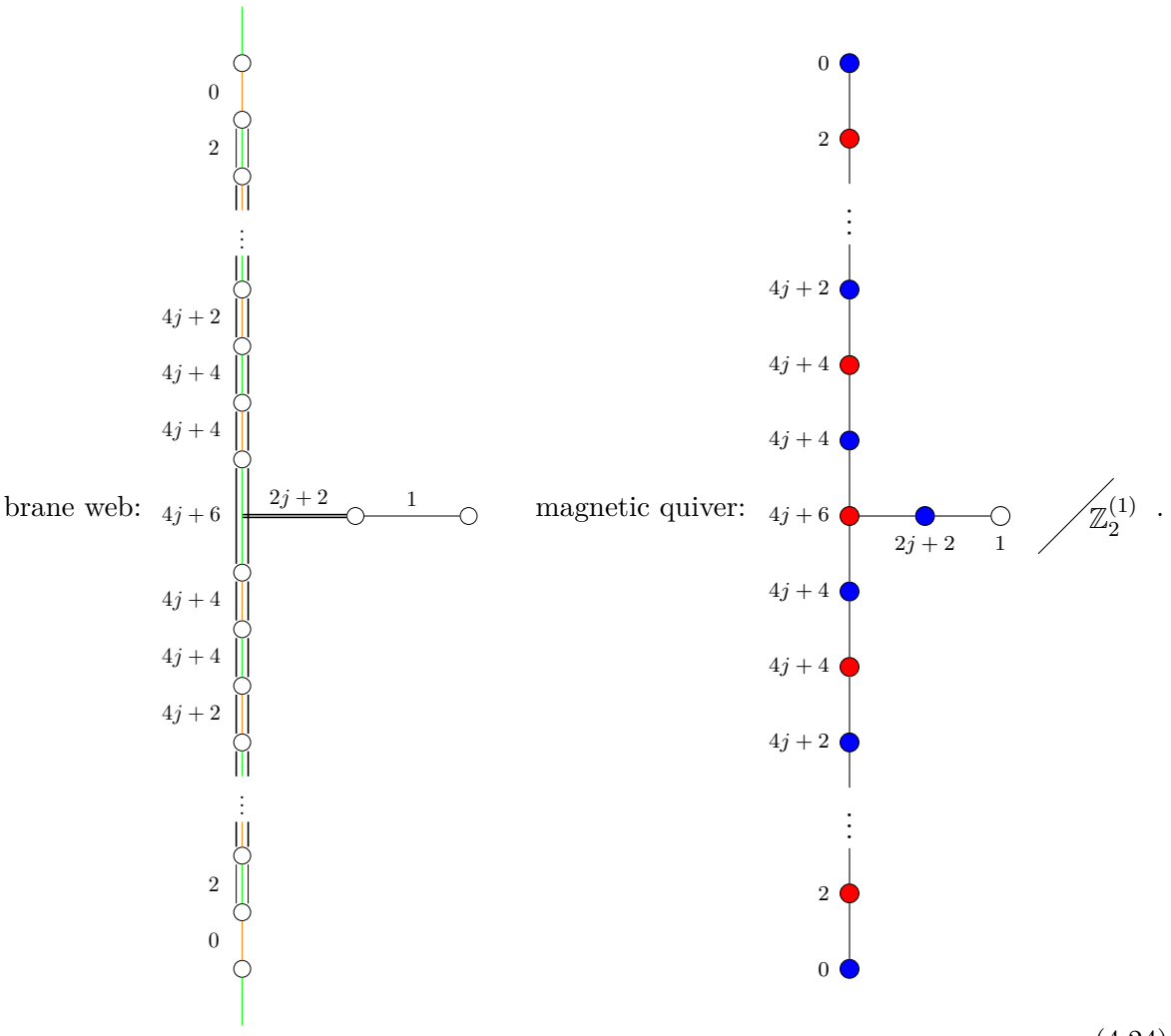

(4.24)

We note that, again, in the brane-web many D5 end on the same D7, and hence there exists a dual description, for the 5d conformal matter of type $X^{(1)}_{A_{2j}}$, in terms of a toric diagram with white dots. Again, this means that we can think to the procedure of passing from the aforementioned white-dots toric diagram to the singularity $X^{(1)}_{A_{2j}}$ as the geometric analogous of an Hanany-Witten move [38].

The Coulomb branch global symmetry of the magnetic quiver is $\mathfrak{so}(4j+6)\times\mathfrak{so}(4j+6)\times\mathfrak{u}(1)$ for $j \geq 1$, and E_7 for $j = 0$. We have

$$\dim_{\mathbb{H}}\mathrm{CB}_{3d}\left(\mathsf{MQ}\left(\mathcal{T}_{X^{(1)}_{D_{2j+3}}}\right)\right) = 8j^2 + 23j + 17 = \dim_{\mathbb{H}}\mathrm{HB}\left(\mathcal{T}_{X^{(1)}_{D_{2j+3}}}\right) , \tag{4.25}$$

which matches table 3.

The magnetic quiver for $\mathcal{T}_{X^{(1)}_{D_3}}$ is IR dual to the magnetic quiver for $\mathcal{T}_{X^{(1)}_{A_3}}$ [95], as is expected since $\mathfrak{su}(4) = \mathfrak{so}(6)$.

JHEP10(2025)144

4.2.3 $X^{(2)}_{D_{2j+2}}$

The discussion of the brane web for the 5d SCFT associated to the $X^{(2)}_{D_{2j+2}}$ singularity is analogous to the previous section. We only present the infinite coupling brane web and corresponding magnetic quiver:

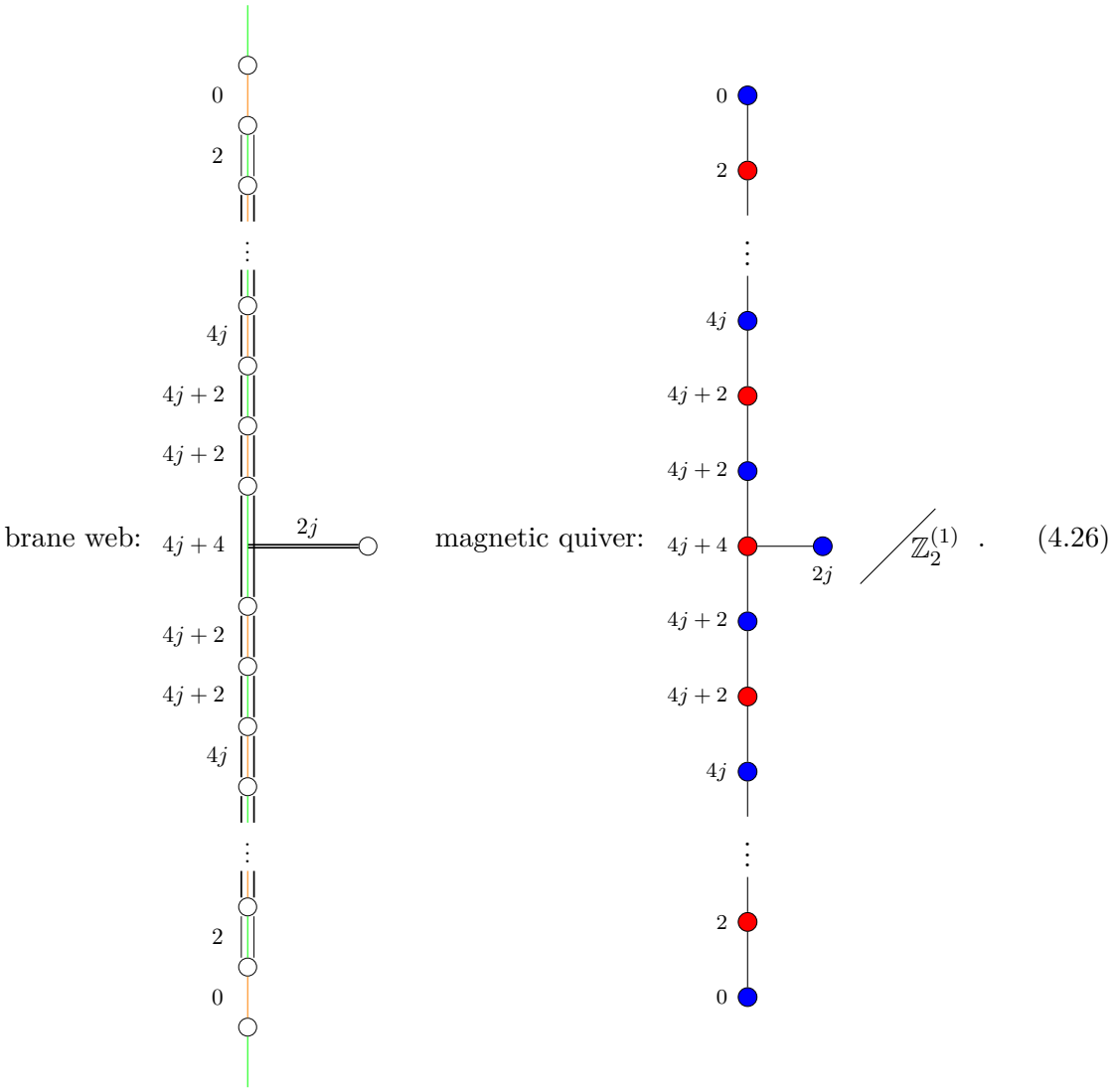

(4.26)

The Coulomb branch global symmetry of the magnetic quiver is $\mathfrak{so}(4j+4) \times \mathfrak{so}(4j+4)$ for $j > 1$, and E_8 for $j = 1$. We have

$$\dim_{\mathbb{H}} \mathrm{CB}_{3d}\left(\mathsf{MQ}\left(\mathcal{T}_{X^{(2)}_{D_{2j+2}}}\right)\right) = 8j^2 + 15j + 6 = \dim_{\mathbb{H}} \mathrm{HB}\left(\mathcal{T}_{X^{(2)}_{D_{2j+2}}}\right) , \tag{4.27}$$

which matches table 3.

4.2.4 $X^{(2)}_{D_{2j+3}}$

The discussion of the brane web for the 5d SCFT associated to the $X^{(2)}_{D_{2j+3}}$ singularity is analogous to the previous section. We only present the infinite coupling brane web and

corresponding magnetic quiver:

brane web:

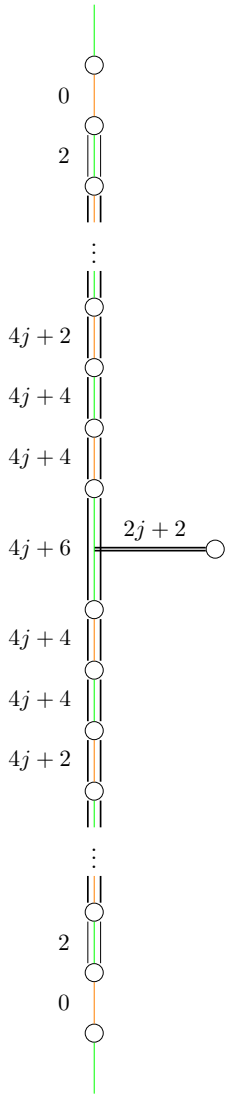

magnetic quiver:

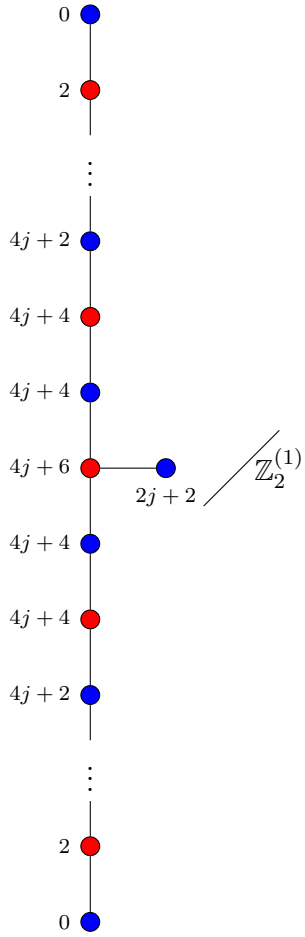

. (4.28)

The Coulomb branch global symmetry of the magnetic quiver is $\mathfrak{so}(4j+6) \times \mathfrak{so}(4j+6) \times \mathfrak{u}(1)$ for $j \geq 1$. For $j = 1$ the magnetic quiver has Coulomb branch $\mathbb{H}^{16}$ indicating that the SCFT consists of free hypers. We have

$$\dim_{\mathbb{H}} \mathrm{CB}_{3d}\left(\mathsf{MQ}\left(\mathcal{T}_{X^{(2)}_{D_{2j+3}}}\right)\right) = 8j^2 + 23j + 16 = \dim_{\mathbb{H}} \mathrm{HB}\left(\mathcal{T}_{X^{(2)}_{D_{2j+3}}}\right) , \tag{4.29}$$

which matches table 3.

4.2.5 $X^{(3)}_{D_j}$

The discussion of the brane web for the 5d SCFT associated to the $X^{(3)}_{D_2}$ singularity is analogous to the previous section. We only present the infinite coupling brane web and

JHEP10(2025)144

corresponding magnetic quiver:

brane web:

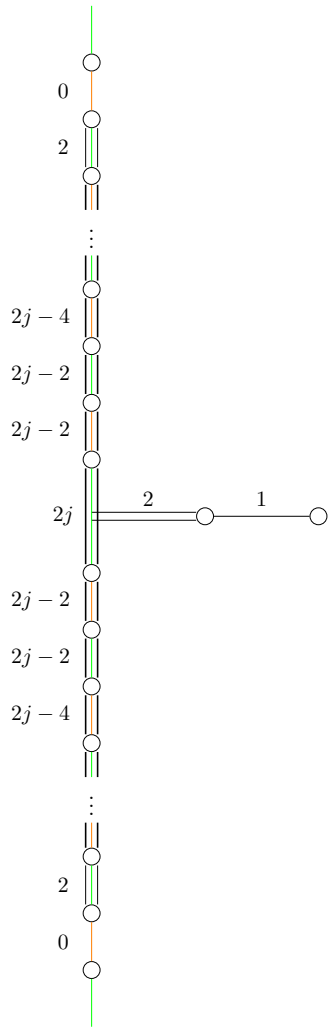

magnetic quiver:

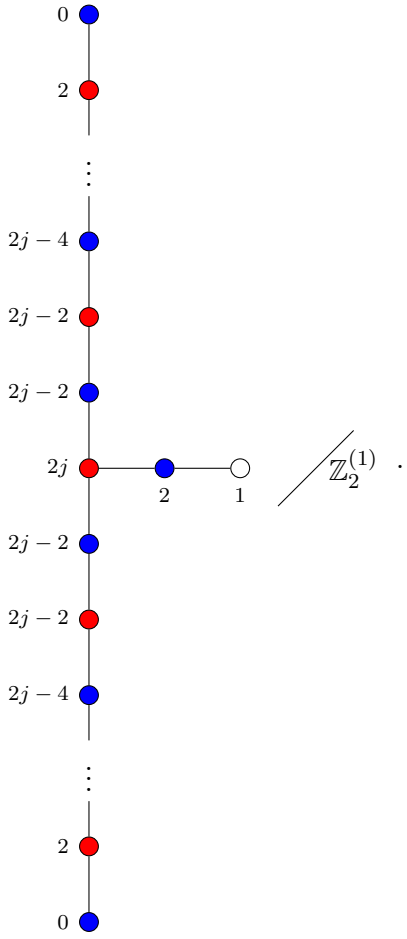

. (4.30)

The Coulomb branch global symmetry of the magnetic quiver is $\mathfrak{so}(4j) \times \mathfrak{su}(2)$[15] for $j \geq 3$, and E_7 for $j = 3$ [95]. We have

$$\dim_{\mathbb{H}} \mathrm{CB}_{3d}\left(\mathsf{MQ}\left(\mathcal{T}_{X^{(3)}_{D_j}}\right)\right) = 2j^2 - j + 2 = \dim_{\mathbb{H}} \mathrm{HB}\left(\mathcal{T}_{X^{(3)}_{D_j}}\right) , \tag{4.31}$$

which matches table 3.

4.3 Relation to class-$\mathcal{S}$ construction

We observe that all A- and D-type 5d conformal matter atoms can be constructed as worldvolume theories of 5-brane webs. The magnetic quivers read from these brane webs match exactly those read from the class-$\mathcal{S}$ construction (from puncture data). This further confirms that the identified toroidal reduction is the correct one.

[15] Notice that the global symmetry always enhances from the $\mathfrak{g} \times \mathfrak{g} \times F_{\text{rest}}$ type in this case.

JHEP10(2025)144

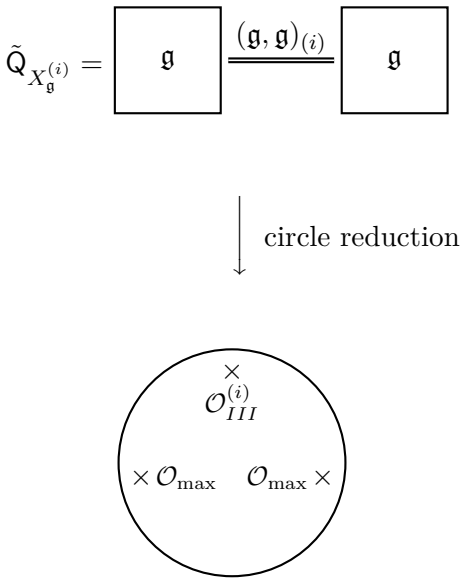

Figure 8. The conformal matter 5d theory of type $X_{\mathfrak{g}}^{(i)}$ and its 4d descendant realized as a class-$\mathcal{S}$ setup with three regular punctures. This corresponds to the vertical blue arrow in figure 1.

5 5d conformal matter molecules and class $\mathcal{S}$

In this section we naturally extend the construction presented in section 3 and determine the 4d descendants of the 5d SCFTs encoded by the complete intersections (2.6), that correspond to 5d conformal matter molecules (or, equivalently, to 5d generalized linear quivers). The 5d molecules in general admit a flavor symmetry of the form:

$$F_{UV} = \mathfrak{g} \times \mathfrak{g} \times F_{\text{rest}}. \tag{5.1}$$

It turns out that on a specific point of the extended CB of the 5d SCFT, corresponding to turning on some masses for F_{rest}, its circle reduction lends itself to a 4d $\mathcal{N} = 2$ class-$\mathcal{S}$ interpretation. Hence, we match the CB dimension across dimensional reduction in section 5.1, and we relate the dimension of the HB and the flavor symmetry of the 5d theory to the ones of its 4d descendant in section 5.2. In section (6) we then compute the brane-webs and magnetic quivers for the 5d conformal matter molecules.

5.1 4d reduction of 5d conformal matter molecules

The procedure to find the 4d descendant of a 5d generalized linear quiver (molecule) is straightforward: we start from the fundamental 5d conformal matter atoms of table 2, that specify the descendant of the 5d theory $X_{\mathfrak{g}}^{(i)}$ by means of a class-$\mathcal{S}$ setup. The latter is given by the 6d $\mathcal{N} = (2,0)$ theory of type $\mathfrak{g}$ compactified on a sphere with three appropriately chosen regular punctures. As previously remarked, there is a one to one correspondence between $X_{\mathfrak{g}}^{(i)}$ and the choice of the nilpotent orbit associated to the third puncture $\mathcal{O}_{III}^{(i)}$ (where we have explicitly highlighted the dependence on i, that can be read off from table 2).

Pictorially, we can represent the 5d theory and its 4d descendant as in figure 8. Notice that the sphere corresponds to an "edge" in the generalized 5d quiver. Consequently, in order

JHEP10(2025)144

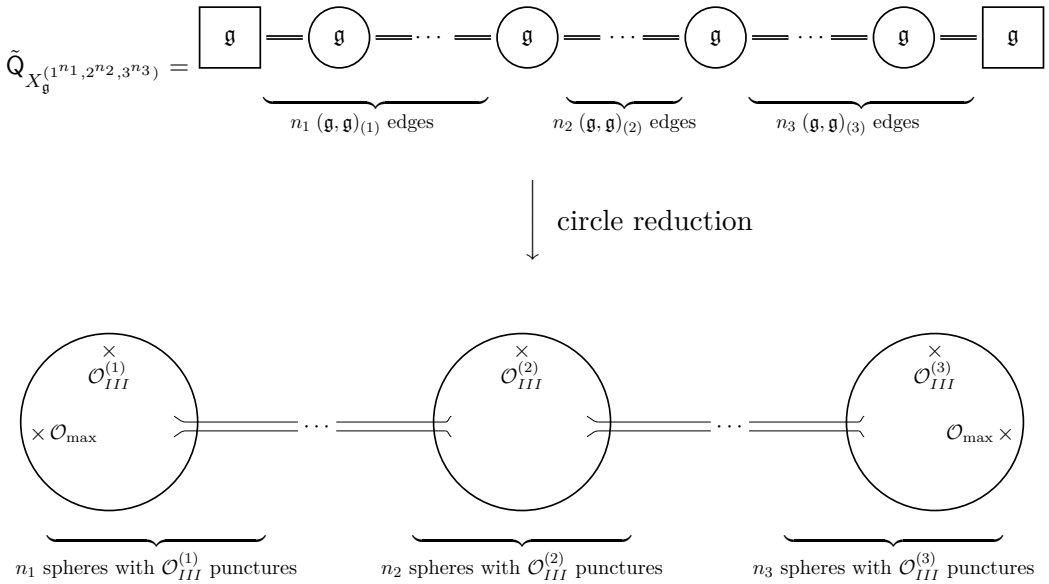

Figure 9. The generalized quiver with 5d conformal matter edges and its 4d descendant realized as a class-$\mathcal{S}$ setup with regular punctures. This corresponds to the blue arrow going to the bottom right in figure 2.

to construct the 4d descendants of the generalized 5d quiver theories $\tilde{\mathsf{Q}}_{X_{\mathfrak{g}}^{(1^{n_1},2^{n_2},3^{n_3})}}$ of figure 9 it suffices to consider as many class-$\mathcal{S}$ spheres as the number of edges of the 5d generalized quiver. Of course, we must choose the third puncture of each sphere in such a way to match the corresponding 5d conformal matter type $(\mathfrak{g},\mathfrak{g})_{(i)}$ of the corresponding edge. The gluing happens along the maximal punctures: all in all, we are left with a single sphere with two maximal punctures of type $\mathfrak{g}$, and as many non-maximal punctures as the number of edges, accounting for the extra flavor symmetry. Intuitively, we can represent this correspondence as in figure 9. Crucially, notice that the generalized quiver $\tilde{\mathsf{Q}}_{X_{\mathfrak{g}}^{(1^{n_1},2^{n_2},3^{n_3})}}$ does *not* correspond to the same extended CB phase as the quivers specified by our preferred resolution procedure of section 2.2. This will impact on the relation between the Higgs branch dimension of the 5d SCFT and the class-$\mathcal{S}$ reduction corresponding to the choice of resolution that yields $\tilde{\mathsf{Q}}_{X_{\mathfrak{g}}^{(1^{n_1},2^{n_2},3^{n_3})}}$. We will extensively comment on this in section 5.2. It is easy to see that the ranks of the 5d and 4d Coulomb branch match: in the 5d quiver, we have n_1, n_2, n_3 edges of type $(\mathfrak{g},\mathfrak{g})_{(1)}, (\mathfrak{g},\mathfrak{g})_{(2)}, (\mathfrak{g},\mathfrak{g})_{(3)}$, respectively, each contributing with r_1, r_2, r_3 to the total rank of the Coulomb branch. Each gauge node further adds $\mathrm{rank}(\mathfrak{g})$ to such rank. Hence we obtain:

$$\mathrm{rank}(\mathrm{CB})_{5d} = n_1 r_1 + n_2 r_2 + n_3 r_3 + (n_1 + n_2 + n_3 - 1)\mathrm{rank}(\mathfrak{g}). \tag{5.2}$$

From the 4d side, we have to consider the contribution of two maximal regular punctures of type $\mathfrak{g}$, as well as that of n_1, n_2, n_3 regular punctures of type $\mathcal{O}_{III}^{(1)}, \mathcal{O}_{III}^{(2)}, \mathcal{O}_{III}^{(3)}$, respectively. As a consequence of the choices exhibited in table 2, it is immediate to check that the dimensions d_i of the $\mathcal{O}_{III}^{(i)}$ orbits are such that:

$$d_i = 2(r_i + \mathrm{rank}(\mathfrak{g})) \qquad \text{for } i = 1, 2, 3. \tag{5.3}$$

JHEP10(2025)144

Then, employing (3.1), we can compute the CB dimension in the 4d class-$\mathcal{S}$ theory:

$$\begin{aligned}\text{rank}\,\text{CB}_{4d}\left(\mathcal{T}_{4d}\right) &= \frac{1}{2}\left(2\text{dim}(\mathcal{O}_{\text{max}}) + n_1\text{dim}(\mathcal{O}_{III}^{(1)}) + n_2\text{dim}(\mathcal{O}_{III}^{(2)}) + n_3\text{dim}(\mathcal{O}_{III}^{(3)})\right) - \text{dim}(\mathfrak{g}) \\ &= n_1 r_1 + n_2 r_2 + n_3 r_3 + (n_1 + n_2 + n_3 - 1)\text{rank}(\mathfrak{g}),\end{aligned} \tag{5.4}$$

that precisely agrees with (5.2).

As regards the flavor symmetry, we expect the 5d theory to possess at least the flavor symmetry (2.8), that we repeat here for convenience, sticking to the same conventions:

$$F_{UV} = \mathfrak{g} \times \mathfrak{g} \times F_{\text{rest}}. \tag{5.5}$$

From the 4d perspective, notice that the two maximal punctures give rise to the expected $\mathfrak{g}\times\mathfrak{g}$ factor, and that the remaining punctures should take care of the leftover flavor symmetry. A quick tracking of the factors shows that the 4d picture does not account for the rank of the global symmetry F_{rest} in the general case. We explain this symmetry breaking effect in the following section, where we also comment on the matching between the 4d and 5d HB dimensions.

5.2 5d conformal matter molecules and Higgs branch dimension

In this section, we are going to relate the Higgs branch dimension, as well as the flavor symmetries, of the 5d conformal matter molecules with those of their 4d class $\mathcal{S}$ descendants presented in figure 9. We add more details on the matching of the flavor symmetry in appendix C.

Let us start by noticing that, due to (3.6), the dimension of the HB for the candidate class $\mathcal{S}$ theory depicted in figure 6 scales linearly with the number of junctions of the generalized quiver of the corresponding 5d theory. More precisely, for the 4d theory corresponding to a quiver with n_1 junctions of type $i = 1$, n_2 of type $i = 2$ and n_3 of type $i = 3$, we have

$$\begin{aligned}\text{dim}_{\mathbb{H}}\text{HB}\left(\mathcal{T}_{4d}\right) &= \text{dim}(\mathfrak{g}) - \text{rank}(\mathfrak{g}) \\ &\quad + \frac{1}{2}\sum_i n_i \left(\text{dim}_{\mathbb{C}}(\mathfrak{g}) - \text{rank}(\mathfrak{g}) - \text{dim}_{\mathbb{C}}(\mathcal{O}_i^L)\right) + \text{rank}(\mathfrak{g}) \\ &= \text{dim}(\mathfrak{g}) + \frac{1}{2}\sum_i n_i \left(\text{dim}_{\mathbb{C}}(\mathfrak{g}) - \text{rank}(\mathfrak{g}) - \text{dim}_{\mathbb{C}}(\mathcal{O}_i^L)\right),\end{aligned} \tag{5.6}$$

where in the first step we singled out the contribution $\text{dim}(\mathfrak{g}) - \text{rank}(\mathfrak{g})$ coming from the full punctures, and the sum over i accounts for the other punctures.

We can now compute the HB dimension of the 5d theory. As explained in [9], M-theory on (2.6) admits a mass deformation to an ordinary quiver gauge theory phase. The gauge nodes of the quiver are of type $\mathfrak{su}(N_k)$, with $k = 1, \ldots, \text{rank}(\mathfrak{g})$ and intersect each other according to the $\mathfrak{g}$ Dynkin diagram. The quiver might also display some flavor nodes, again of type $\mathfrak{su}$ or of type $\mathfrak{u}(1)$. In particular, the ranks of the quiver gauge nodes scale linearly with the n_i [9] and hence the HB dimension of the quiver, $n_H - n_V$, scales *quadratically* with the n_i:

$$\text{dim}_{\mathbb{H}}\text{HB}\left(\mathcal{T}_{5d}\right) = n_H - n_V + \underbrace{\text{dim}(\mathfrak{g}) - \text{rank}(\mathfrak{g})}_{\textit{instantonic contribution}}, \tag{5.7}$$

JHEP10(2025)144

where we have separated, on the r.h.s., the HB contributions that can be counted at finite coupling from the quiver $(n_H - n_V)$ from those coming from the instantonic particles [83] (or, equivalently, from the M2-brane states described in section 3.2). We listed the $\dim_{\mathbb{H}}(\mathrm{HB})^{UV}_{5d}$ for all the conformal matter molecules in table 4, where we colored in red the explicit expressions for $n_H - n_V$. It is immediate to see that (5.7) and (5.6) can not be matched. The resolution of the puzzle, though, is straightforward and can be traced back to our choices of partial resolutions for the molecule geometries.

Indeed, we constructed the 4d class $\mathcal{S}$ as the circle reduction of the generalized quiver in figure 9. The generalized quiver phase is itself a partially resolved phase (different from the resolution presented in section 2.2) of M-theory on (2.6). Consequently, the generalized quiver is a valid description away from the origin of the 5d extended Coulomb branch of the SCFT, and holds only when the compact curves supporting the compact lines of $\mathfrak{g}$ Du Val singularities have a non-zero volume. It then follows that the M2-brane states[16] wrapped on the inflated compact curves have a non-vanishing BPS mass, and then some HB directions are lifted. We can count the unlifted HB dimensions as follows: the generalized linear quiver in figure 9 corresponds to a *partial resolution* of (2.6) displaying $n_1 + n_2 + n_3 - 1$ compact lines of $\mathfrak{g}$ singularities intersecting according to the $A_{n_1+n_2+n_3-1}$ Dynkin diagram. Furthermore, we have two non-compact lines of $\mathfrak{g}$ singularities intersecting the compact lines corresponding to the leftmost and to the rightmost nodes of the $A_{n_1+n_2+n_3-1}$ Dynkin diagram. In total, we have $n_1 + n_2 + n_3$ intersection points between these lines where the unlifted HB modes localize. As these intersection points are separated, we can count their contributions one by one using the third[17] column of table 3. The final HB dimension is obtained by subtracting the contributions coming from the $\mathfrak{g}$ gauge nodes, obtaining:

$$\begin{aligned}
\dim_{\mathbb{H}}\mathrm{HB}\left(\tilde{\mathrm{Q}}_{X_{\mathfrak{g}}^{(1^{n_1},2^{n_2},3^{n_3})}}\right) &= \sum_i n_i \dim_{\mathbb{H}}\mathrm{HB}\left(Q_{X_{\mathfrak{g}}^{(i)}}\right) - (N-1)\dim(\mathfrak{g}) \\
&= N(\dim(\mathfrak{g}) - \mathrm{rank}(\mathfrak{g})) + \frac{1}{2}\sum_i n_i \left(\dim_{\mathbb{C}}(\mathfrak{g}) - \mathrm{rank}(\mathfrak{g}) - \dim_{\mathbb{C}}(\mathcal{O}_i^L)\right) \\
&\quad + N\mathrm{rank}(\mathfrak{g}) - (N-1)\dim(\mathfrak{g}) \\
&= \dim(\mathfrak{g}) + \frac{1}{2}\sum_i n_i \left(\dim_{\mathbb{C}}(\mathfrak{g}) - \mathrm{rank}(\mathfrak{g}) - \dim_{\mathbb{C}}(\mathcal{O}_i^L)\right) \\
&= \dim_{\mathbb{H}}\mathrm{HB}(\mathcal{T}_{4d}),
\end{aligned} \tag{5.8}$$

where $N = n_1 + n_2 + n_3$ and, in the second step, we singled out the contribution $N(\dim(\mathfrak{g}) - \mathrm{rank}(\mathfrak{g}))$ of the maximal regular punctures.

We can use this result to understand the apparent mismatch between the flavor symmetries of the 5d SCFT associated to (2.6) and those of the 4d class $\mathcal{S}$ corresponding theory. Indeed, in order to obtain $\mathcal{T}_{4d}$, we turned on non-zero Kähler volumes for some $\mathbb{P}^1$'s that can be interpreted, by the usual geometric engineering dictionary, as real mass deformations for the UV fixed point. One can check that the M2 BPS states wrapped on such $\mathbb{P}^1$'s have a

[16] It is important not to confuse these M2 states with the ones appearing in section 3.2, as they are associated to different resolutions of the threefold singularity.

[17] This is equivalent to adding the contributions from the 5d instantonic particles to the second column of table 3.

JHEP10(2025)144

normal bundle that identifies them as HB modes. Consequently, such modes are lifted, and hence we expect to get a tinier 4d flavor group after dimensional reduction. By exploiting the usual geometric engineering dictionary, the Kähler volumes of $\mathbb{P}^1$s i

The final flavor group is expected to be the commutant, inside the initial flavor group, of the elements of the flavor algebra corresponding to the mass parameters. Stated differently, the class $\mathcal{S}$ flavor group is expected to coincide with the flavor group of the mass-deformed phase of the 5d SCFT corresponding to the generalized linear quiver, that, from a 5d perspective, gets enhanced at the UV fixed point to (2.8) only when all the compact $\mathbb{P}^1$'s are contracted. In analogy to the instanton particles in the quiver gauge theory setup, the M2 branes wrapping the resolved $\mathbb{P}^1$ enlarge, after the contraction, both the flavor symmetry of the theory and the Higgs branch dimensions. More specifically, we notice that, since the generalized linear quiver still displays two non-compact lines of *singular* $\mathfrak{g}$ singularities, the mass parameters that we turned on to reach the generalized linear quiver phase must come from the F_{rest} factor of the 5d flavor group. Consequently, the 4d punctures capture just the commutants, inside F_{rest}, of the mass parameters that we turned on. Indeed, we can check this statement as follows: a mass deformation for F_{rest} is a background field along $\mathfrak{h}' \subset \mathfrak{h} \subset F_{\text{rest}}$, with $\mathfrak{h}$ the Cartan subalgebra. This breaks the F_{rest} to the commutant of $\mathfrak{h}'$ (excluding $\mathfrak{h}'$ itself). We hence expect

$$\text{rank}(G_{III,4d}) = \text{rank}(F_{\text{rest}}) - N. \tag{5.9}$$

We check this formula for the most general molecule, highlighting the precise breaking pattern of the flavor symmetry, in section C.

To conclude, we note that (5.8) is an independent check of the fact that the candidate 4d class $\mathcal{S}$ theories are exactly those in figure 8 and figure 9, validating our construction. In table 4 we summarize the *full* UV quaternionic Higgs Branch dimensions for all molecules of 5d conformal matter. In other words, given the defining threefold (2.6), the HB dimension depends on the non-negative integers n_1, n_2, n_3 as in the column on the right of table 4.

6 5d conformal matter molecules, brane webs and magnetic quivers

In this section we explore the brane-web perspective on 5d conformal matter molecules. That is, we now turn to gauging a diagonal symmetry of two 5d conformal matter atoms of the same algebra directly in 5d, and then going to the UV fixed point, i.e. a 5d conformal matter molecule.

We first discuss the A-type conformal matter brane systems in some detail, and then present the D-type brane systems which behave completely analogously.

JHEP10(2025)144

Molecule class	$\dim_{\mathbb{H}}\mathbf{HB}\left(\mathcal{T}_{5d}\right)$
A_{2j+1}	$n_1^2(j+1)+2j+1+\underbrace{2(1+j)(1+2j)}_{\text{obstructed}}$
A_{2j}	$\left(n_1^2+2\right)j+\underbrace{2j(1+2j)}_{\text{obstructed}}$
D_{2j+2}	$(j+2)n_1^2+n_1\left(2jn_2+n_2+4n_3\right)+j\left(n_2^2+2\right)+2n_3\left(n_2+n_3\right)+2+\underbrace{4(1+j)(1+2j)}_{\text{obstructed}}$
D_{2j+3}	$(j+2)n_1^2+2n_1\left((j+1)n_2+2n_3\right)+(j+1)n_2^2+2j+2n_3^2+2n_2n_3+3+\underbrace{4(1+j)(3+2j)}_{\text{obstructed}}$
E_6	$3n_1^2+4n_1n_2+3n_1n_3+2n_2^2+2n_2n_3+n_3^2+6+\underbrace{72}_{\text{obstructed}}$
E_7	$4n_1^2+6n_1n_2+3n_1n_3+3n_2^2+2n_2n_3+n_3^2+7+\underbrace{126}_{\text{obstructed}}$
E_8	$4n_1^2+5n_1n_2+3n_1n_3+2n_2^2+2n_2n_3+n_3^2+8+\underbrace{240}_{\text{obstructed}}$

Table 4. UV Higgs branch dimension of 5d conformal matter molecules. We highlighted with brackets the HB modes that are obstructed after the partial resolution of section 2.2. Note that, for the $\mathfrak{g}=A$ case, in [9] we have just one type of 5d conformal matter atom, and hence just n_1 appears in the HB dimension formula.

6.1 A-type

6.1.1 $\boldsymbol{X}^{(\mathbf{1}^n)}_{\boldsymbol{A_{2j+1}}}$

$\boldsymbol{X}^{(\mathbf{1}^2)}_{\boldsymbol{A_{2j+1}}}$**.** Consider gauging the diagonal $\mathrm{SU}(2j+2)$ symmetry of two $(A_{2j+1},A_{2j+1})_{(1)}$ 5d conformal matter atoms:

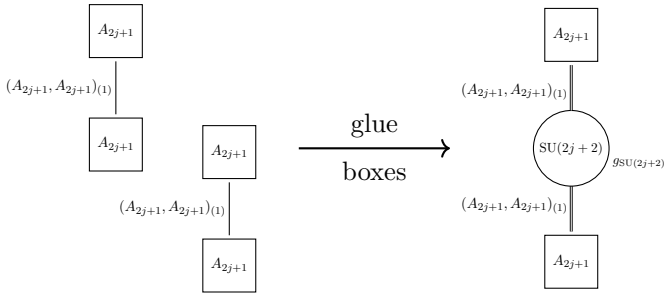

, (6.1)

where $g_{\mathrm{SU}(2j+2)}$ is the coupling of the gauged diagonal $\mathrm{SU}(2j+2)$ symmetry.

The brane web for the $(A_{2j+1},A_{2j+1})_{(1)}$ 5d conformal matter atom is given in 4.7. The two $\mathrm{SU}(2j+2)$ symmetries of the SCFT can be seen from the $[0,1]7$ branes which the (vertical) $(0,1)5$ branes end on.

JHEP10(2025)144

The diagonal SU$(2j+2)$ gauging can be done on the level of the brane web by 'gluing' the two webs corresponding to the two atoms together in the following way:

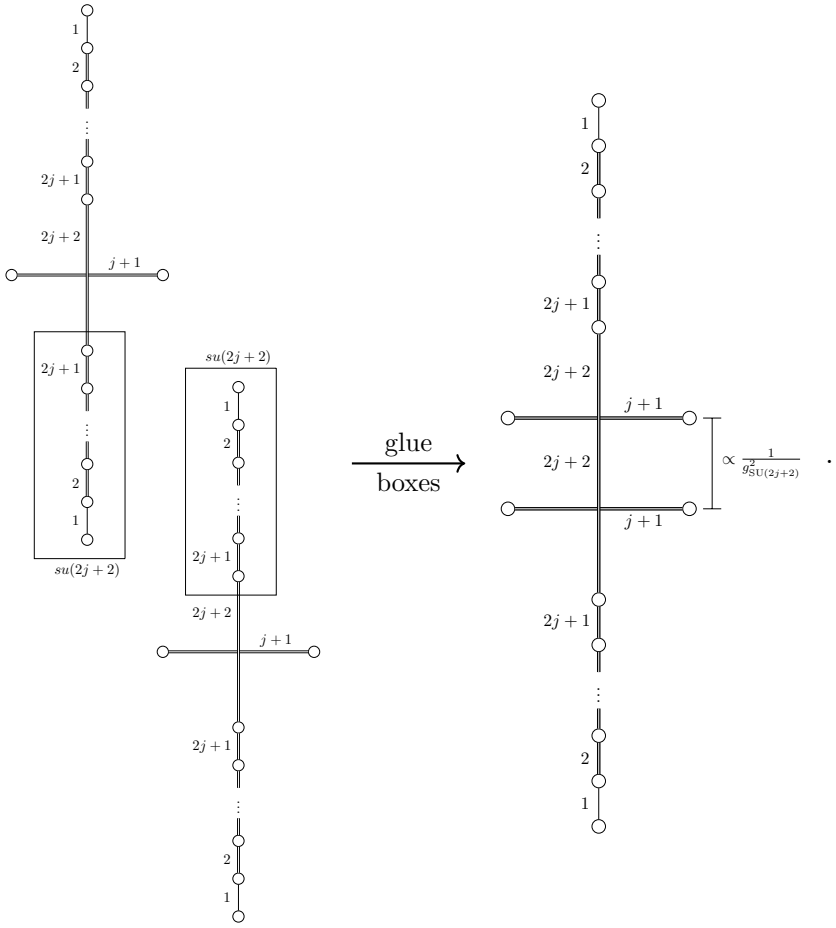

(6.2)

Note that this is the brane web for

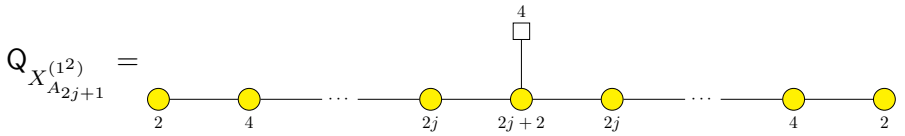

(6.3)

after taking all the couplings to infinity, but giving a mass m to two of the four flavours leaving the other two massless, where $m = \frac{1}{g^2_{SU(2j+2)}}$. This m corresponds to the mass deformation corresponding to the red line going to the right in figure 2.

JHEP10(2025)144

On the level of magnetic quivers this is realised by gauging a diagonal Coulomb branch symmetry (see for example [96] or [97, appendix B] how these are implemented):

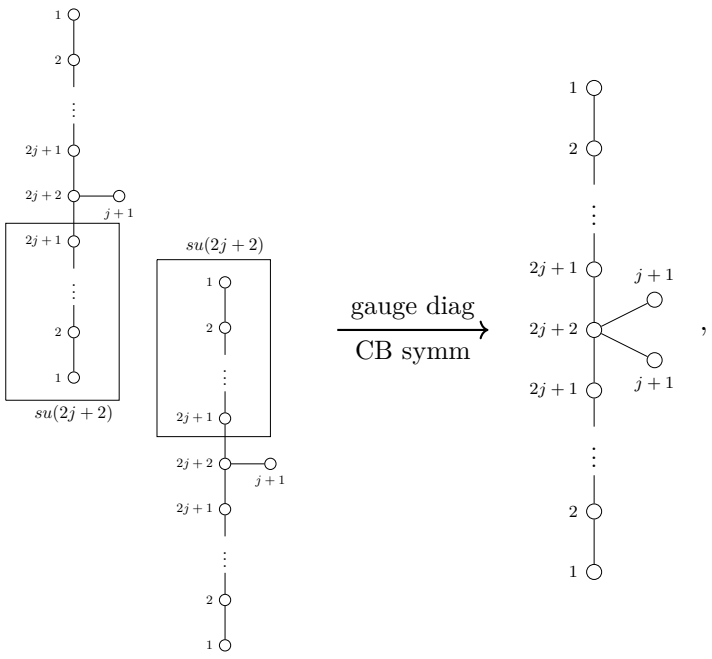

(6.4)

where the quiver on the r.h.s. of (6.4) can also be read straight from the brane web on the r.h.s. of (6.2).

The Higgs branch of the r.h.s. of (6.1) (at finite $g_{\mathrm{SU}(2j+2)}$) is obtained as a hyper-Kähler quotient of the product of the Higgs branches on the l.h.s. of (6.1) by $\mathrm{SU}(2j+2)$:

$$\mathrm{HB}\left(\text{r.h.s. (6.1)}\right) = \left(\mathrm{HB}\left(\text{l.h.s. 1 (6.1)}\right) \times \mathrm{HB}\left(\text{l.h.s. 2 (6.1)}\right)\right) /\!/\!/ \mathrm{SU}(2j+2)\,, \tag{6.5}$$

with dimension

$$\dim_{\mathbb{H}}(\mathrm{HB}(\text{r.h.s. (6.1)})) = \dim_{\mathbb{H}}(\mathrm{HB}(\text{l.h.s. 1 (6.1)})) + \dim_{\mathbb{H}}(\mathrm{HB}(\text{l.h.s. 2 (6.1)})) - (2j+2)^2 + 1\,. \tag{6.6}$$

JHEP10(2025)144

Infinite coupling. The SCFT engineered by $X^{(1^2)}_{A_{2j+1}}$ is realised by taking $\frac{1}{g^2_{\mathrm{SU}(2j+2)}} \to 0$ in the r.h.s. brane web of (6.2):

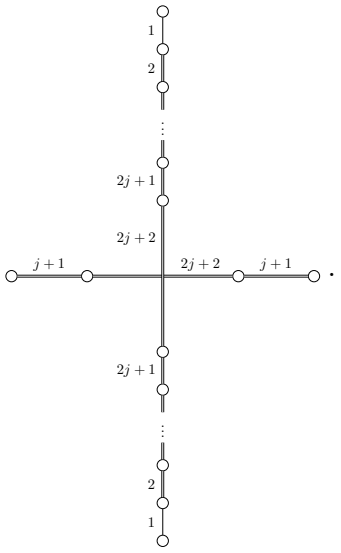

(6.7)

The magnetic quiver read from this web is

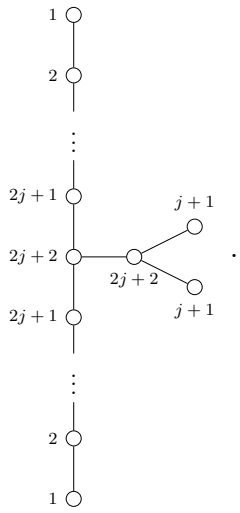

(6.8)

JHEP10(2025)144

$\boldsymbol{X^{(1^n)}_{A_{2j+1}}}$**.** Now consider gauging n $(A_{2j+1}, A_{2j+1})_{(1)}$ 5d conformal matter atoms, in order to obtain a generalised linear quiver. The corresponding brane web and magnetic quiver are:

brane web:

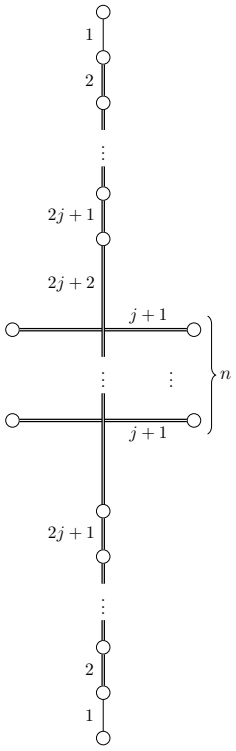

magnetic quiver:

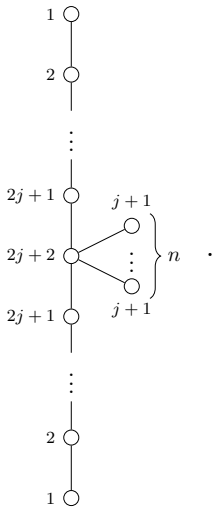

. (6.9)

Infinite coupling. Taking all the couplings of the generalised quiver to infinity realises the SCFT associated to the $X^{(1^n)}_{A_{2j+1}}$ singularity. The corresponding brane web is:

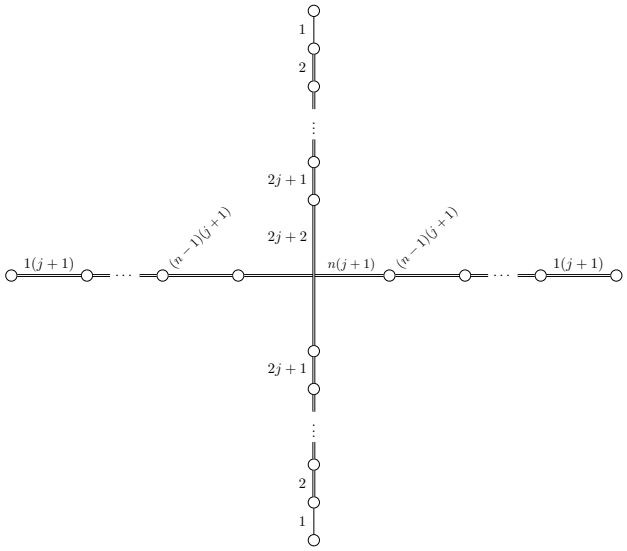

(6.10)

JHEP10(2025)144

from which we can read the magnetic quiver

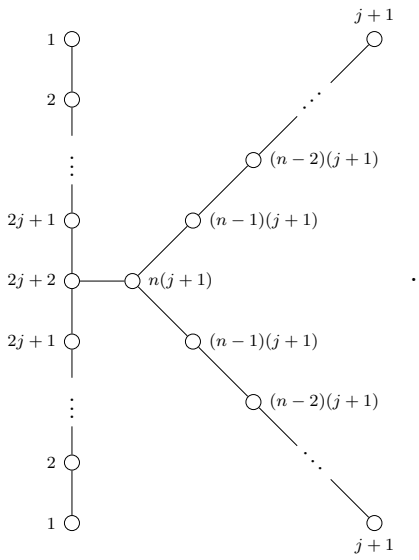

(6.11)

We notice that the quiver is not star-shaped, which would be the case for a magnetic quiver for a class-S theory with regular punctures [96], but rather it has two 'centers' stemming from the stack of NS5 branes and D5 branes in the middle of the brane web respectively. This suggests that the reduction to 4d is not a class-$\mathcal{S}$ theory with regular punctures.[18]

6.1.2 $X^{(1^n)}_{A_{2j}}$

Now consider gauging n $(A_{2j}, A_{2j})_{(1)}$ 5d conformal matter atoms, in order to obtain a generalised linear quiver. This case is completely analogous to the previous one. The

[18]This probably suggests a 4d-mechanism analogous to the one of [86, 98].

JHEP10(2025)144

corresponding brane web and magnetic quiver are:

brane web: 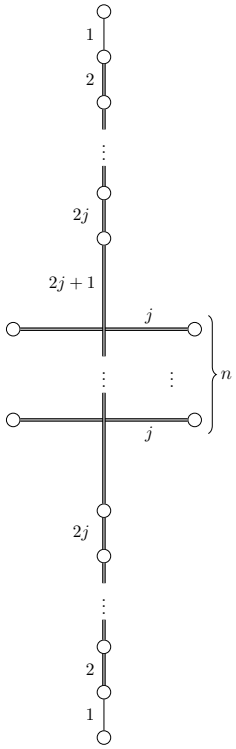

magnetic quiver: 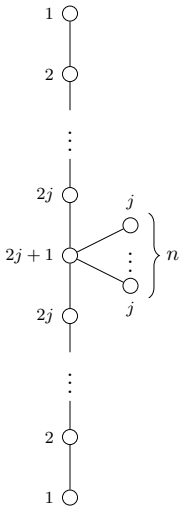

. (6.12)

Infinite coupling. Taking all the couplings of the generalised quiver to infinity realises the SCFT associated to the $X^{(1^n)}_{A_{2j}}$ singularity. The corresponding brane web is:

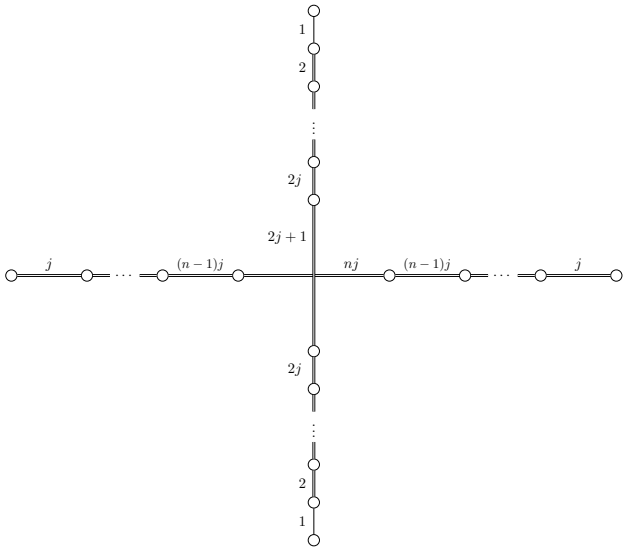

(6.13)

from which we can read the magnetic quiver

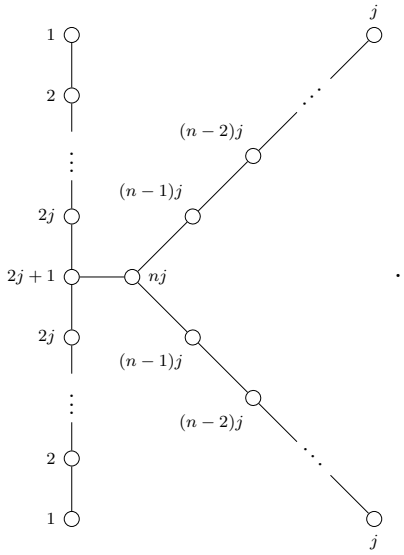

(6.14)

6.2 D-type

6.2.1 $X^{(1^{n_1},2^{n_2},3^{n_3})}_{D_{2j+2}}$

Let us now turn to D_{2j+2} conformal matter molecules. We start with building generalised quivers from $(D_{2j+2}, D_{2j+2})_{i\in\{1,2,3\}}$ conformal matter atoms by gauging diagonal $\mathrm{SO}(4j+4)$ symmetries:

$\tilde{\mathrm{Q}}_{X^{(1^{n_1},2^{n_2},3^{n_3})}_{D_{2j+2}}} =$ 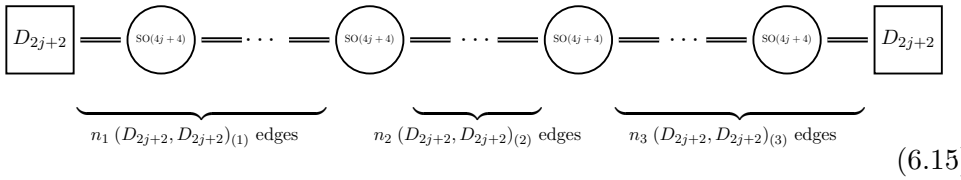

(6.15)

The infinite coupling SCFT will not depend on the order in which the atoms are gauge together, and neither will the finite coupling (of the $\mathrm{SO}(4j+4)$s) Higgs branch, therefore we fix the order above.

JHEP10(2025)144

The brane web is

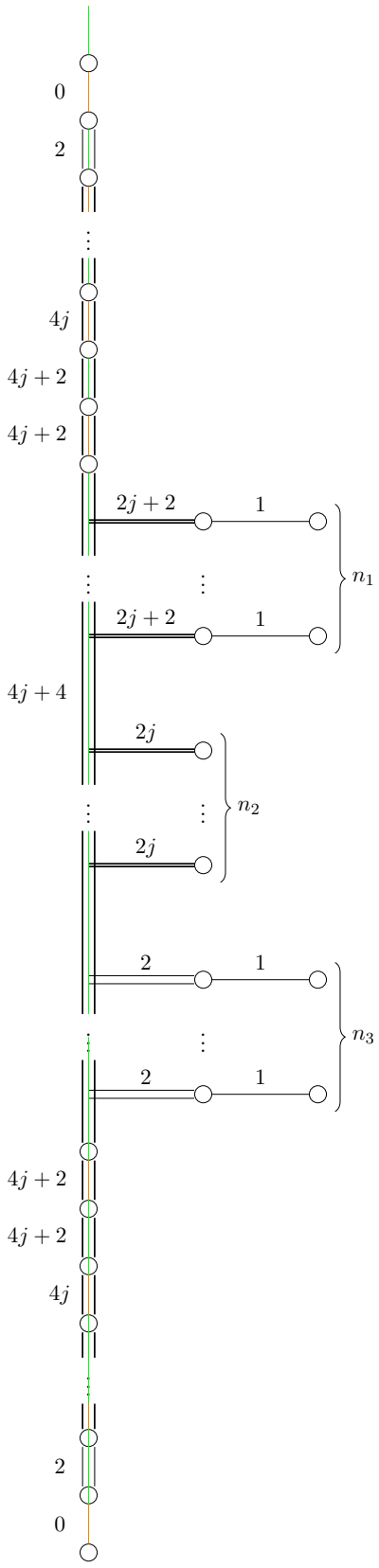

(6.16)

JHEP10(2025)144

and the magnetic quiver is

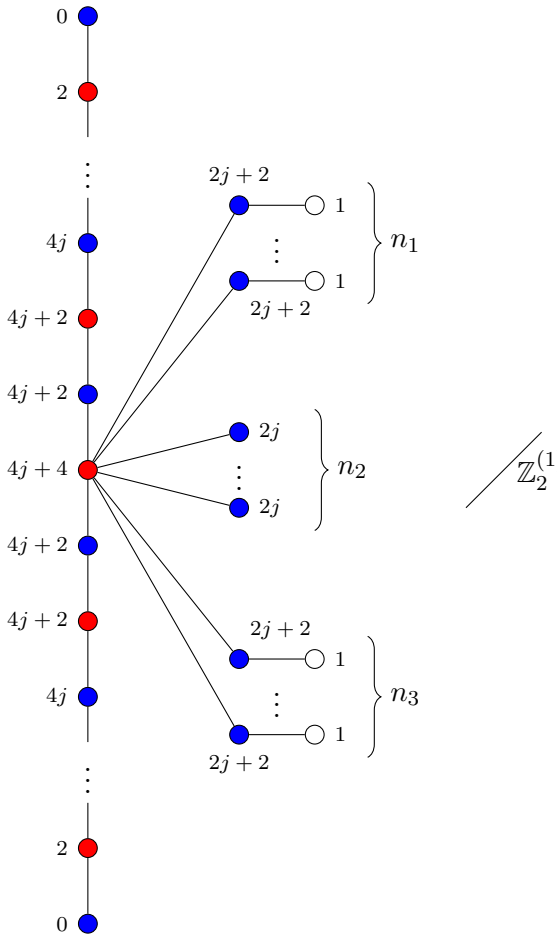

(6.17)

Infinite coupling. Taking all the couplings of the generalised quiver to infinity realises the SCFT associated to the $X_{D_{2j+2}}^{(1^{n_1},2^{n_2},3^{n_3})}$ singularity.

JHEP10(2025)144

The corresponding brane web is:

(6.18)

JHEP10(2025)144

from which we can read the magnetic quiver:

(6.19)

JHEP10(2025)144

6.2.2 $X^{(1^{n_1},2^{n_2},3^{n_3})}_{D_{2j+3}}$

Let us now turn to D_{2j+3} conformal matter molecules. We start with building generalised quivers from $(D_{2j+3}, D_{2j+3})_{i\in\{1,2,3\}}$ conformal matter atoms by gauging diagonal $\mathrm{SO}(4j+6)$ symmetries:

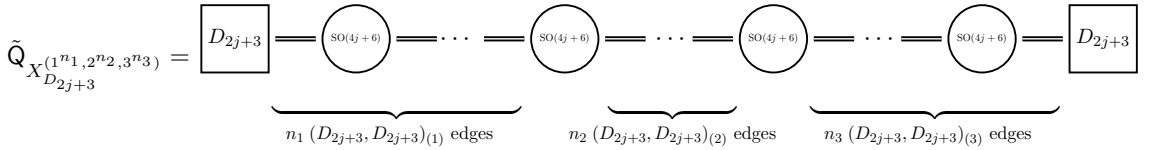

As before the infinite coupling SCFT will not depend on the order in which the atoms are gauged together [9], and neither will the finite coupling (of the $\mathrm{SO}(4j+6)$s) Higgs branch. Therefore we may fix the order above.

JHEP10(2025)144

The brane web is

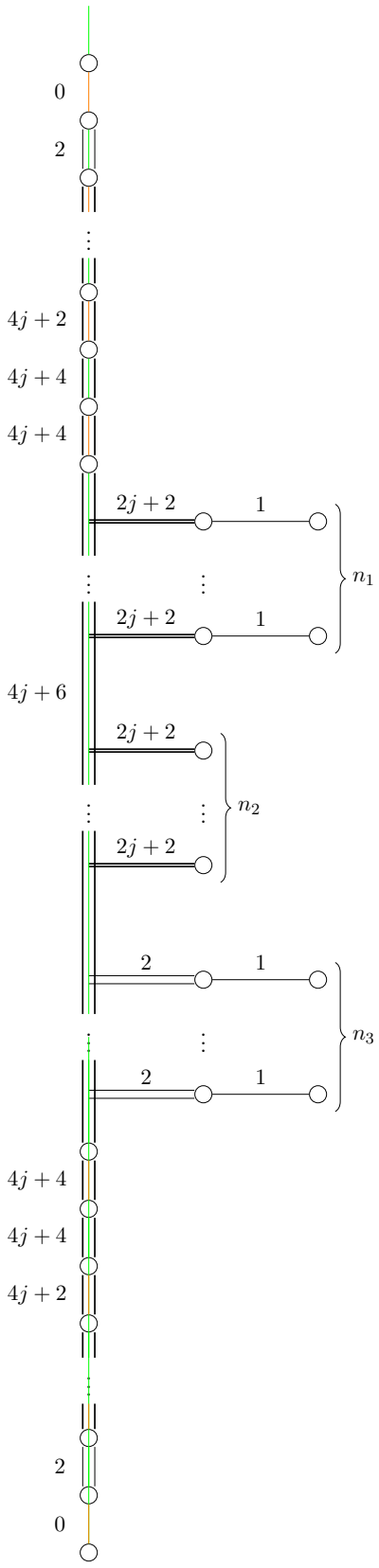

(6.20)

JHEP10(2025)144

and the magnetic quiver is

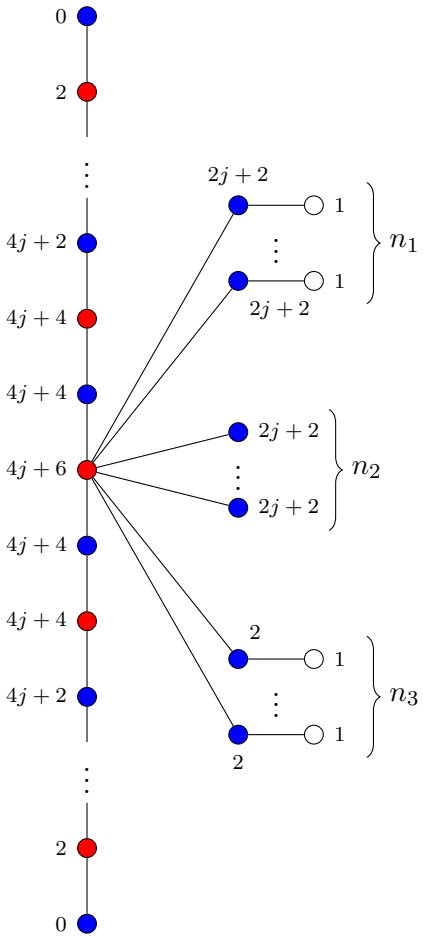

$$\mathbb{Z}_2^{(1)} \ . \tag{6.21}$$

Infinite coupling. Taking all the couplings of the generalised quiver to infinity realises the SCFT associated to the $X_{D_{2j+3}}^{(1^{n_1},2^{n_2},3^{n_3})}$ singularity.

JHEP10(2025)144

The corresponding brane web is:

(6.22)

JHEP10(2025)144

from which we can read the magnetic quiver:

(6.23)

JHEP10(2025)144

6.3 Relation to class−$\mathcal{S}$

We observe that all A- and D-type 5d conformal matter molecules can be constructed as worldvolume theories of 5-brane webs. The magnetic quivers read from these brane webs are not of the type obtained from class-$\mathcal{S}$ theories with regular punctures, which would be star-shaped. The deformations of conformal matter theories to generalized quivers $\tilde{\mathsf{Q}}$ produces magnetic quivers which match exactly those read from the class-$\mathcal{S}$ construction (from puncture data). This further confirms that the identified toroidal reduction is the correct one.

7 Outlook

In this work, we further characterised the 5d Conformal Matter SCFTs introduced in [9]. We specifically analysed three interconnected problems: the dimensional reduction of the aforementioned SCFTs, their (p, q)-web brane constructions and their magnetic quivers.

This work is situated at the intersection of a variety of tightly-related points of view on the geometric engineering landscape, and naturally paves the way for a plethora of possible developments:

1. One may ask, whether the 5d CM atoms (and molecules built thereof) introduced in [9], and studied in the present paper, are all the 5d SCFTs with at least $\mathfrak{g} \times \mathfrak{g}$ symmetry and a Dynkin quiver phase. In the upcoming paper [84] we answer this question by completing the classification and matching with corresponding CY singularities. Most of the results of this paper extend to the more general class, but we find also some new exotic hybrid 5d CM systems (new atoms that can be Higgsed to molecules).

2. The Higgs branch phase diagram, or Hasse diagram, of a 5d theory can be obtained from its brane web construction via magnetic quiver technology. On the geometric engineering side complex structure deformations achieve the same Higgsing. We address how to match such deformations with the Hasse diagram for specific theories in a further upcoming work [99]. The Higgs branch RG-flows between atoms are summarised in figure 10.

3. While first steps in reading magnetic quivers from geometry were made in [26–28], in general, it is still not clear how to precisely rephrase some aspects of the magnetic quiver analysis in the language of geometric engineering. Indeed, if on the one hand the geometric engineering allows in principle to study theories and Higgs branches that do not admit a (either electric or magnetic) quiver descriptions, it is less clear how to analyze fine aspects of the Higgs branches from a geometric perspective.

4. Our study leads to the prediction of the existence of new ADE families of 4d $\mathcal{N} = 2$ SCFTs with high rank and flavor symmetry at least $\mathfrak{g} \times \mathfrak{g}$. These models do not admit a Lagrangian nor a class-$\mathcal{S}$ realisation with regular punctures, which we predict from our magnetic quiver analysis (the magnetic quiver of these SCFTs is not of class-$\mathcal{S}$ type with regular punctures). We leave for the future the problem of characterizing these 4d SCFTs (a subset of which have been investigated by [86]), in particular to determine their CB dimensions, their conformal central charges and whether their flavor symmetries are gaugeable in 4d (which we expect to be the case).

JHEP10(2025)144

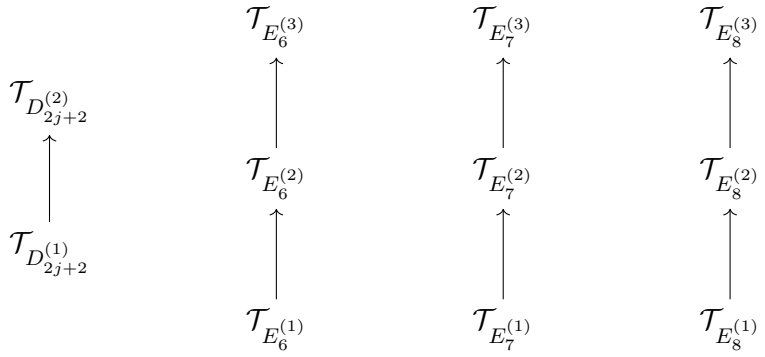

Figure 10. Higgsings between conformal matter atoms. (Many more phases exists in the Higgs branch of the conformal matter atom at the bottom of each flow, we omit them from this figure.)

Acknowledgments

We would like to thank Sergio Benvenuti, Antoine Bourget, Amihay Hanany, and Sakura Schäfer-Nameki for discussions as well as Shani Meynet for comments on an earlier version of the paper.

JFG is supported by the EPSRC Open Fellowship (Schäfer-Nameki) EP/X01276X/1. JFG and AS thank the "Simons Collaboration on Special Holonomy in Geometry, Analysis and Physics" for support during the initial stage of this project. The work of AS is funded by the VR Centre for Geometry and Physics (VR grant No. 2022-06593). The work of MDZ is supported by the European Research Council (ERC) under the European Union's Horizon 2020 research and innovation program (grant agreement No. 851931), the Simons Foundation Grant #888984 (Simons Collaboration on Global Categorical Symmetries) and by the VR project grant No. 2023-05590. MDZ also acknowledges the VR Centre for Geometry and Physics (VR grant No. 2022-06593).

A Quiver phases for 5d conformal atoms and molecules

In this appendix we collect the low energy quiver descriptions of 5d conformal matter atoms (and molecules) which were provided in [9]. It is important to remember that 5d SCFTs may have many different low energy Lagrangians (called UV duals), and the quivers provided here are very specific deformations of the 5d SCFTs in question.

JHEP10(2025)144

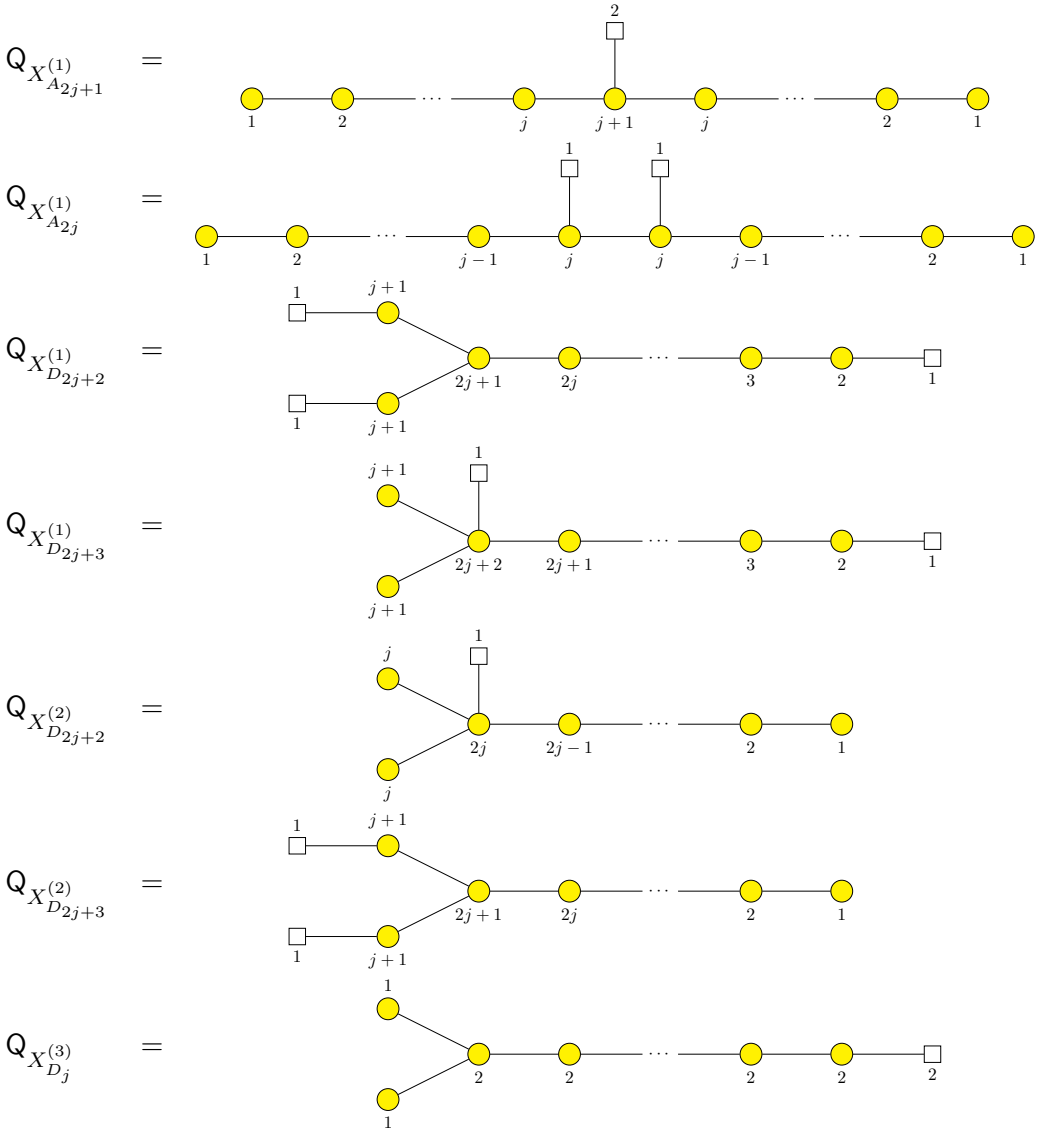

Table 5. Specific low energy quiver deformations of A/D-type 5*d* conformal matter atoms [9].

B Partial resolution of trinion theories

In this appendix we test the following statement:

> *Consider a 5d conformal matter singular threefold of the form (2.6), related to the algebra* $\mathfrak{g}$*, and perform the partial resolution of section 2.2: then, the M2-brane states wrapped on the singular* $\mathbb{P}^1$*'s trapped at the origin give rise to* $dim(\mathfrak{g}) - rank(\mathfrak{g})$ *HB modes for the corresponding 5d SCFT.*

We do so by examining a 5d SCFT that has been vastly studied in the literature, namely the $\mathbb{C}^3/(\mathbb{Z}_m \times \mathbb{Z}_m)$ "trinion" singularity. This is completely equivalent to considering 5d conformal matter theories. Indeed, we can employ the same resolution technique that we used to resolve the 5d conformal matter threefolds also to obtain a partial resolution of

JHEP10(2025)144

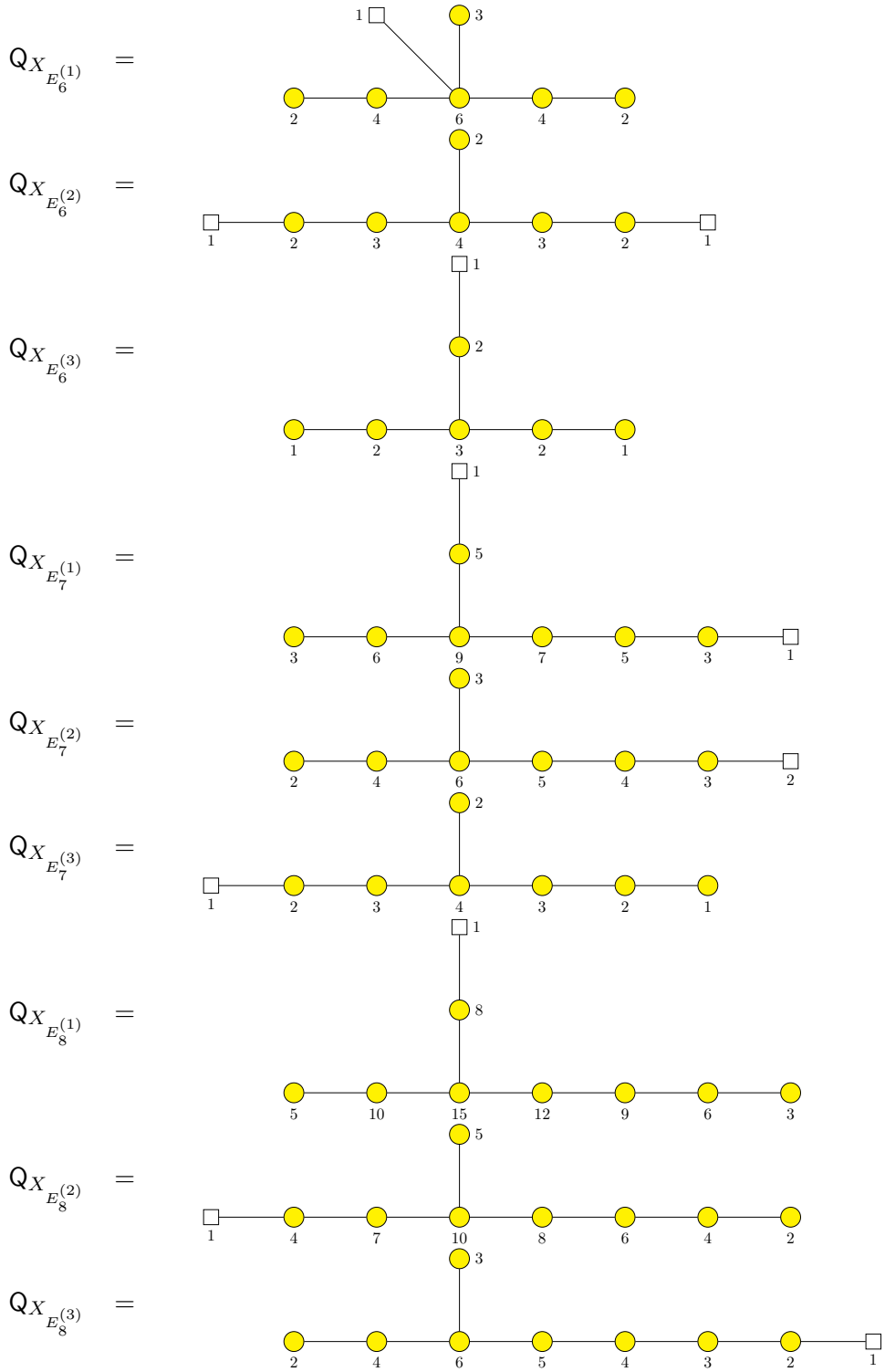

Table 6. Specific low energy quiver deformations of E-type 5d conformal matter atoms [9].

JHEP10(2025)144

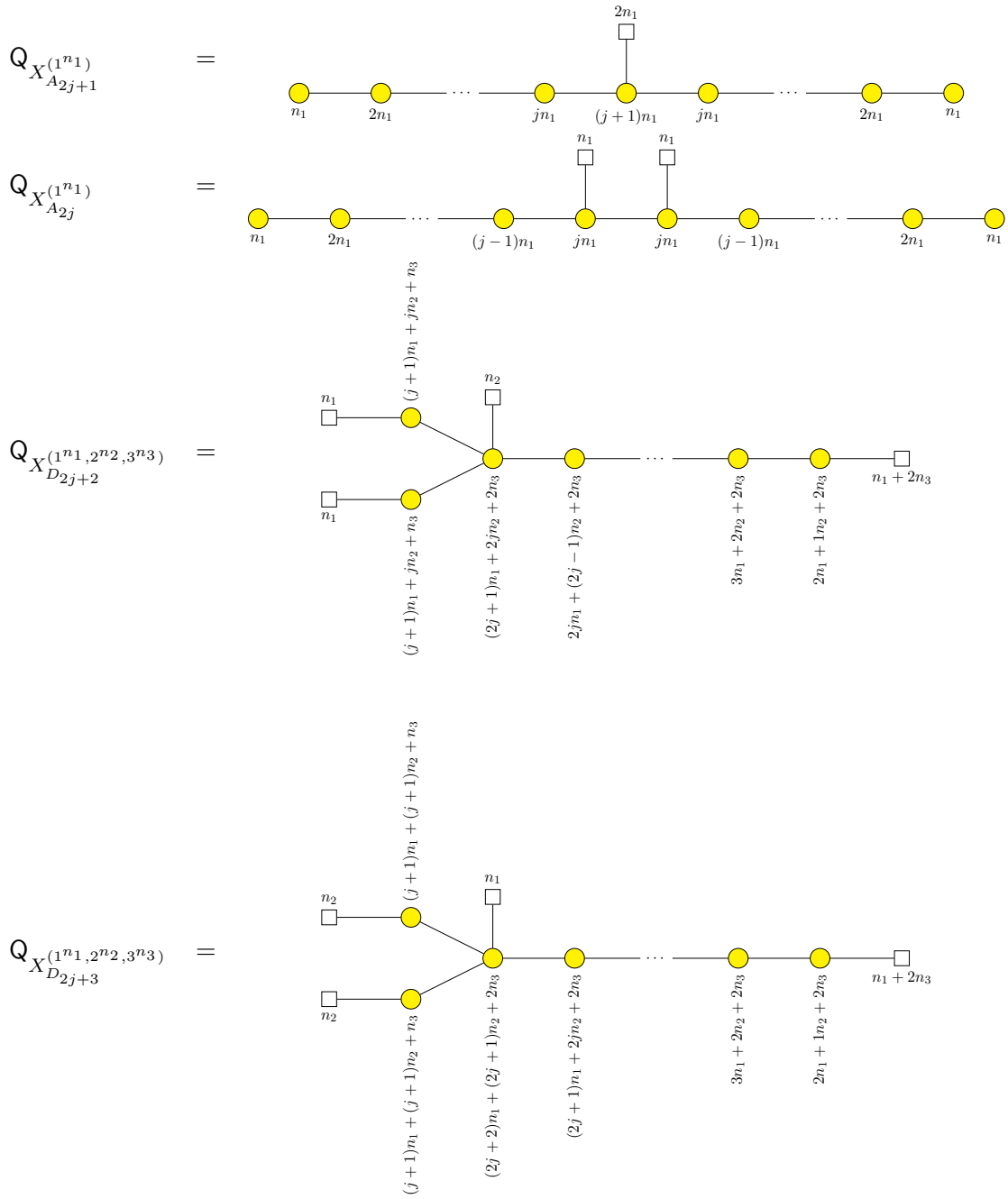

Table 7. Specific low energy quiver deformations of A/D-type $5d$ conformal matter molecules [9].

JHEP10(2025)144

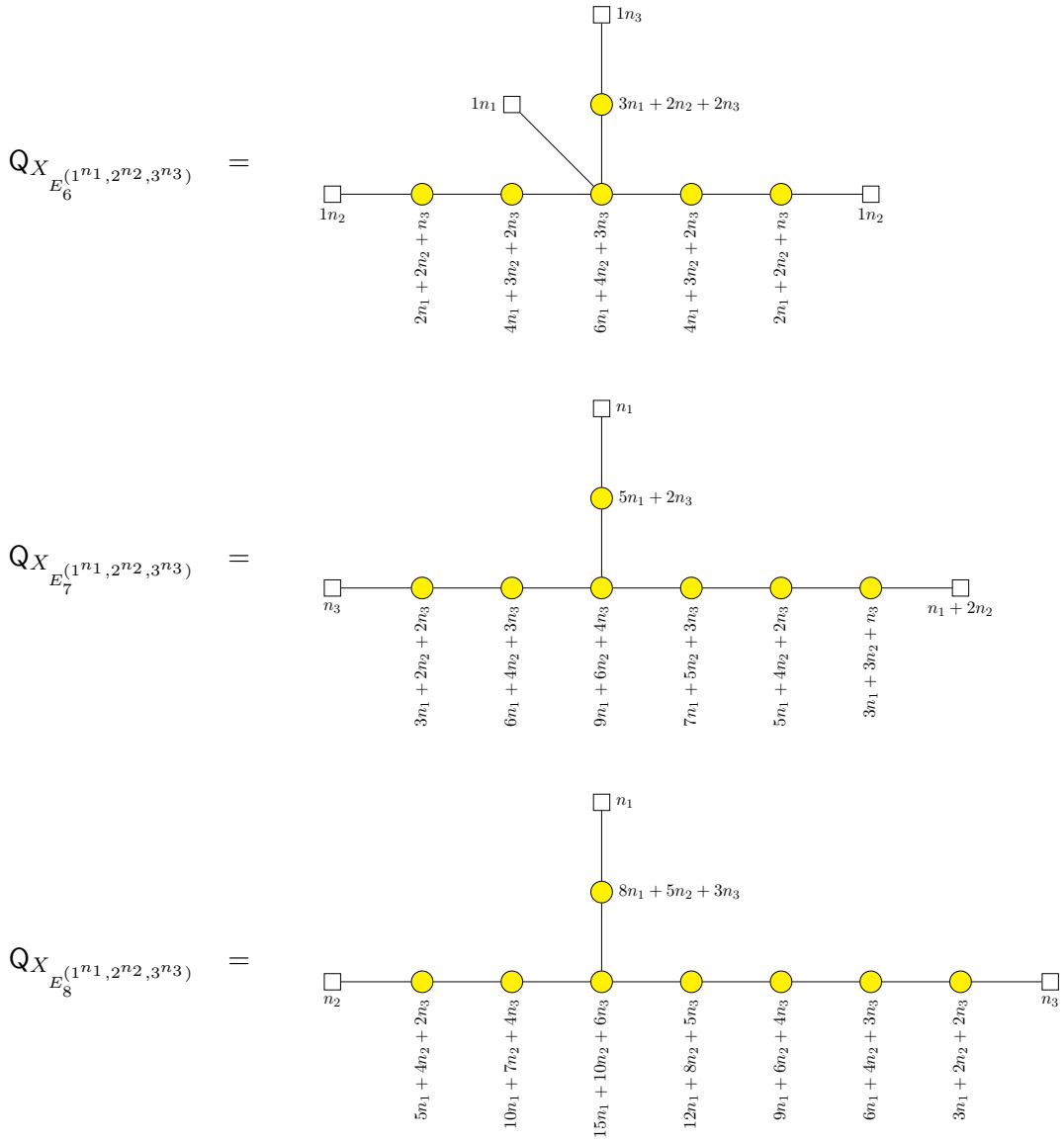

Table 8. Specific low energy quiver deformations of E-type $5d$ conformal matter molecules [9].

$\mathbb{C}^3/(\mathbb{Z}_m \times \mathbb{Z}_m)$. M-theory on $\mathbb{C}^3/(\mathbb{Z}_m \times \mathbb{Z}_m)$ is known to engineer a 5d trinions of type $\mathfrak{su}(m)$: a 5d SCFT with a flavor group at least of type $\mathfrak{su}(m) \times \mathfrak{su}(m) \times \mathfrak{su}(m)$. This can be geometrically guessed by the fact that the threefold displays three non-compact lines of A_{m-1} Du Val singularities. Performing a triangulation of the type called "allowed" in [100] and then taking the IIA limit [100] we get a gauge theory phase described by the ascending quiver in figure 11: We can again count the number of Higgs branch modes from the quiver, after tuning to zero the mass parameters of the $\mathfrak{su}(m)$ leftmost node of figure 11. Tuning to zero these mass parameters corresponds to going to the partially resolved phase depicted in figure 12, and the Higgs branch modes of the quiver correspond to complex deformations of the threefold that are not obstructed by the partial resolution.

JHEP10(2025)144

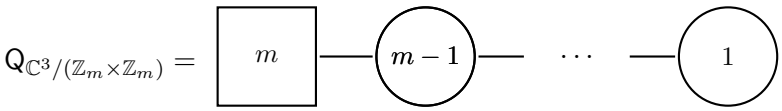

Figure 11. Quiver description of the low-energy gauge theory limit of M-theory on $\mathbb{C}^3/(\mathbb{Z}_m \times \mathbb{Z}_m)$. A round (resp. squared) node labeled with j corresponds to a $\mathfrak{su}(j)$ gauge (resp. flavor) node.

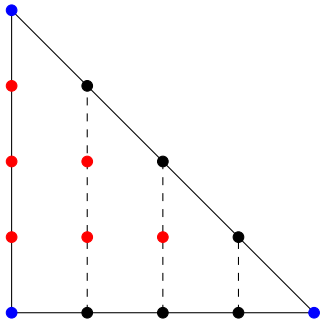

Figure 12. Toric diagram of the partial resolution of the $\mathbb{C}^3/(\mathbb{Z}_4 \times \mathbb{Z}_4)$ trinion that corresponds the quiver in figure 11 with all the zero-modes tuned to zero (keeping the gauge couplings finite). The red dots correspond to shrunk divisors, the black and the blue ones to inflated divisors. The black (resp. blue) divisors are non-compact and correspond to half-cigar bundles over compact (resp. non-compact) rational curves.

From the quiver, we obtain the following data

$$n_V = \frac{1}{6}(m-2)(m-1)(2m+3), \quad n_H = \frac{1}{3}m\left(m^2-1\right), \tag{B.1}$$

and hence

$$\dim_{\mathbb{H}}\mathrm{HB}\left(\mathsf{Q}_{\mathbb{C}^3/(\mathbb{Z}_m\times\mathbb{Z}_m)}\right) = n_V - n_H = \frac{1}{2}\left(m^2+m-2\right). \tag{B.2}$$

$\dim_{\mathbb{H}}\mathrm{HB}\left(\mathsf{Q}_{\mathbb{C}^3/(\mathbb{Z}_m\times\mathbb{Z}_m)}\right)$ corresponds to the number of complex deformations of the threefold that can still be performed when, from a generic triangulation respecting the structure of $\mathbb{C}^*$-fibration over the resolved A_{m-1} singularity (called "allowed" in [100]), we contract, as in figure 12, the volumes of the fibral curves inside the ruled surfaces inflated by the triangulation. We depicted this procedure graphically in figure 14, using the dual brane web, with the contracted curves being the oblique edges of the uppermost part of figure 14.

We can now relate (B.2) with the dimension of the 4d Higgs branch. In the case of M-theory on $\mathbb{C}^3/(\mathbb{Z}_m \times \mathbb{Z}_m)$, the corresponding 4d class-$\mathcal{S}$ theory is obtained from the 6d $(2,0)$ $\mathfrak{su}(m)$ theory, with three full punctures. One can use the methods of section 3 to find the number of 4d Higgs branch modes:

$$\dim_{\mathbb{H}}\mathrm{HB}\left(\mathcal{T}_{4d}\right) = \frac{1}{2}(m-1)(3m+2). \tag{B.3}$$

We then can eventually perform our check: we expect that, at the collision point, the M2-brane states supported on the $\mathbb{P}^1$'s of the non-compact lines get "transformed" into 5d Higgs branch modes. This number n_{missing} should then coincide with the mismatch between $\dim_{\mathbb{H}}\mathrm{HB}(\mathcal{T}_{4d})$

JHEP10(2025)144

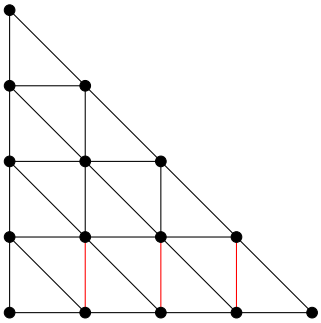

Figure 13. Toric diagram of the full resolution of the $\mathbb{C}^3/(\mathbb{Z}_4 \times \mathbb{Z}_4)$ trinion. The red edges correspond to the zero-section of the various Hirzebruch surfaces resolving the singularity and are naturally identified with the intersection with one of the three non-compact lines of A_3 singularities colliding at the origin of $\mathbb{C}^3/(\mathbb{Z}_4 \times \mathbb{Z}_4)$.

and $\dim_{\mathbb{H}}\mathrm{HB}\left(\mathsf{Q}_{\mathbb{C}^3/(\mathbb{Z}_m\times\mathbb{Z}_m)}\right)$, as the aforementioned $\mathbb{P}^1$'s are inflated in the partial resolution of figure 12, and the corresponding M2-brane states are massive. In fact, we can check that

$$n_{\text{missing}} = \dim_{\mathbb{H}}\mathrm{HB}\left(\mathcal{T}_{4d}\right) - \dim_{\mathbb{H}}\mathrm{HB}\left(\mathsf{Q}_{\mathbb{C}^3/(\mathbb{Z}_m\times\mathbb{Z}_m)}\right) = m^2 - m = \dim(\mathfrak{su}(m)) - \mathrm{rank}(\mathfrak{su}(m)), \tag{B.4}$$

as expected by our general argument. Indeed, one can complete the resolution in figure 12 to the full resolution depicted in figure 13. In this full resolution, the vertical lines of figure 12 have normal bundle $\mathcal{O}(-1) \times \mathcal{O}(-1)$. This can be shown by noticing that, if we contract them, we find a subdiagram of the toric diagram that is equivalent, up to $Sl(2,\mathbb{Z})$ moves, to the conifold one. The red vertical lines are the intersection of the non-compact $\mathbb{P}^1$-bundles resolving the non-compact line of A_{m-1} singularities corresponding to the horizontal external edge of the toric diagram in figure 13 with the Hirzebruch surfaces associated to the gauge nodes of figure 11. We then conclude that the M2 states wrapping the $\mathbb{P}^1$'s of the aforementioned non-compact line get trapped at the intersection point (as they have now a normal bundle without sections), and get transformed to 5d HB modes.

We can finally exhibit an alternative perspective considering the (p,q)-web picture dual to the toric diagram, shown in figure 14. From the image at the top, corresponding to the complete resolution of the singularity, one can readily see that the M2-brane modes trapped at the origin wrap the base $\mathbb{P}^1$'s of the red and blue divisors, as well as the green curve.[19] In the picture, these are nothing but horizontal segments, that have normal bundle $\mathcal{O}(-1) \oplus \mathcal{O}(-1)$, and thus are rigid. Shrinking the fibers produces the image at the center of figure 14, where the base $\mathbb{P}^1$'s are evident. The HB modes wrap precisely these singular $\mathbb{P}^1$'s. Notice that this partial resolution has explicitly broken the $\mathbb{Z}_3$ rotation symmetry of the fully resolved phase: in fact, the set of non-compact divisors labelled by I, II and III has been shrunk to a non-compact line supporting a A_3 singularity.

[19] Of course, a rotational $\mathbb{Z}_3$ symmetry is allowed in the choice of the base $\mathbb{P}^1$'s, in agreement with the symmetry of the brane web.

JHEP10(2025)144

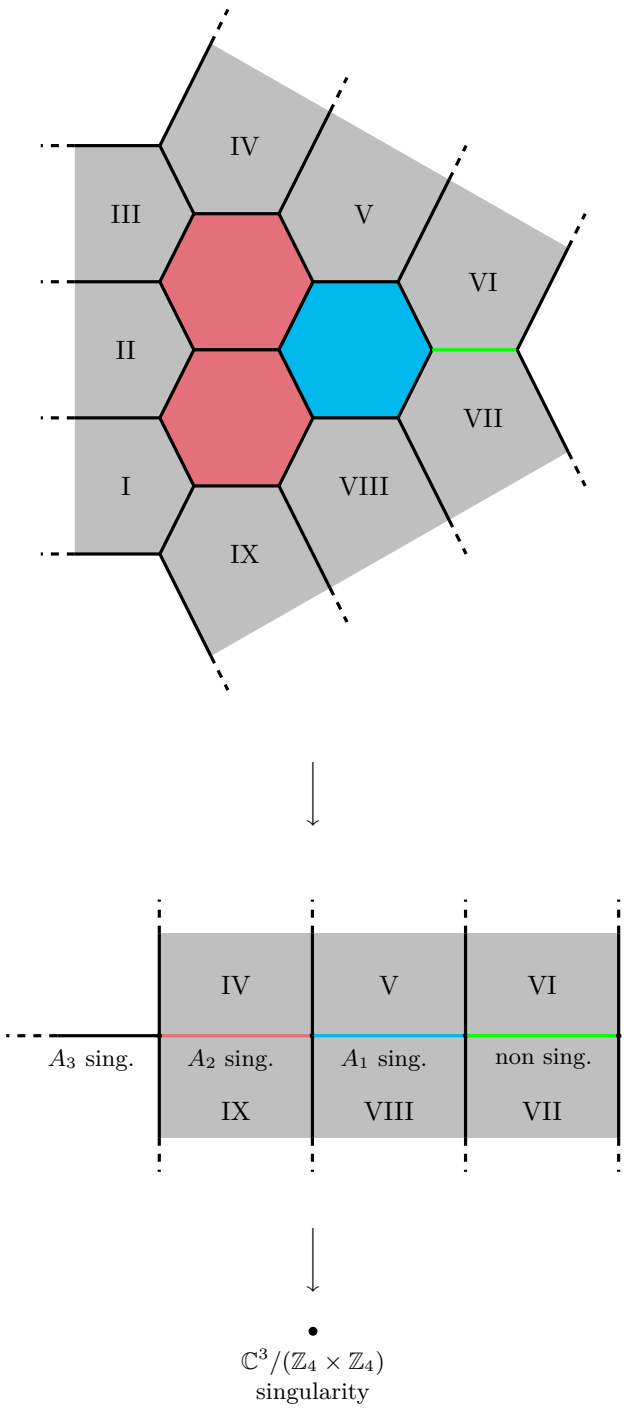

Figure 14. At the top, the fully resolved phase of the $\mathbb{C}^3/(\mathbb{Z}_4 \times \mathbb{Z}_4)$ singularity. In the center, the partially resolved phase corresponding to figure 11 in the main text. At the bottom, the SCFT phase, with no length scale remaining.

JHEP10(2025)144

C Breaking of the flavor symmetry

In this section, we quantitatively study the breaking of the flavor symmetry F_{rest} when we turn on the mass parameter needed to reach the generalized linear quiver phase of section 5.1. We are interested in the breaking of the flavor group that preserves the $\mathfrak{g} \times \mathfrak{g}$ factor. Consequently, we will always omit the $\mathfrak{g} \times \mathfrak{g}$ factor in what follows, as it is unaffected by the breaking procedure.

The flavor group unbroken by the mass vev coincides with the flavor group of the 4d class-$\mathcal{S}$ molecule, as the Higgs branch is preserved by toroidal reduction. We then want to study the breaking

$$F_{\text{rest}} \to F_{III,4d}, \tag{C.1}$$

where the 4d flavor group of the class S molecule reads $\mathfrak{g} \times \mathfrak{g} \times F_{III,4d}$.

Summing up the result, for all the type of $\mathfrak{g}$, we are going to show that

- the rank of the 4d flavor group is the one of the 5d conformal matter molecule, minus the number of mass parameters that we turned on to reach the generalized quiver phase.
- The breaking always happens as $F_{\text{rest}} \to F_{III,4d}$;
- We will use that the breaking of a $\mathfrak{su}(c_1 n_1 + c_2 n_2)$, with $c_1, c_2 \in \mathbb{N}$, factors as

  $$\mathfrak{su}(c_1 n_1 + c_2 n_2) \to \mathfrak{su}(c_1 n_1) \times \mathfrak{su}(c_2 n_2) \to \dots, \tag{C.2}$$

  where we denoted with the dots the corresponding factor of $F_{III,4d}$.
- The breaking of a factor $\mathfrak{su}(n_i)^{m_i}$ is always along the diagonal subgroup. One can explicitly check that a generic breaking along the diagonal combination of $\mathfrak{su}(n_i)^{m_i}$ breaks the group to a generic combination of the Cartan of the non-diagonal flavor transformations.
- We can guess the breaking of the abelian $\mathfrak{u}(1)$ factors in F_{rest} with a case-by-case analysis.

In general, we can geometrically understand this kind of diagonal breaking by turning off simultaneously two out of the three n_is. In this case, the $X_{\mathfrak{g}}^{(i)}$ becomes

$$\begin{cases} P(x_1, x_2, x_3) = 0, \\ uv = t^{n_k}, \\ t = x_k, \end{cases} \tag{C.3}$$

It then makes sense to talk about a "diagonal" breaking whenever we have a subfactor $\mathfrak{su}(\dots)^f$ in F_{rest}. Switching on a mass factor along the diagonal corresponds, in (C.3), to perform a diagonal resolution of the f lines of A-type singularities that is easy to check appear in (C.3), as it corresponds to perform a base-change type resolution now thinking of (C.3) as a base-change of the A_{k-1} singularity. Let us now consider the various cases in more details.

JHEP10(2025)144

First, we consider the A_{2j+1} case. In this case we have just one type of atom, $X^{(1)}_{A_{2j+1}}$, that we can combine in a molecule with n_1 junctions. From section 5.1 we get

$$F_{III,4d} = \mathfrak{u}(1)^{n_1+1} \Rightarrow \text{rank}(F_{III,4d}) = n_1 + 1. \tag{C.4}$$

On the other hand, in this case, the 5d flavor group is [9]

$$F_{\text{rest}} = \mathfrak{u}(2n_1), \quad \Rightarrow \quad \text{rank}(F_{\text{rest}}) = \text{rank}(F_{III,4d}) + (n_1 - 1), \tag{C.5}$$

This result is expected, as, to reach the generalized linear quiver phase, we gave a vev to $n_1 - 1$ mass parameters, represented by the Kähler volumes of the $\mathbb{P}^1$s supporting compact curves of A_{2j+1} singularities. To understand quantitatively the flavor breaking, we can decompose the $\mathfrak{su}(n_1) \times \mathfrak{su}(n_1)$ factor into its diagonal and antidiagonal part. The decomposition does not split the group as a direct product, and in particular all the elements not in the Cartan of the antidiagonal part are broken once we turn on a diagonal Cartan vev. Hence, we get

$$\mathfrak{su}(n_1) \times \mathfrak{su}(n_1) \times \mathfrak{u}(1) \to \mathfrak{u}(1)^{n_1-1} \times \mathfrak{u}(1) = \mathfrak{u}(1)^{n_1}. \tag{C.6}$$

Let us now consider the A_{2j} case; we again have just one kind of atom, $X^{(1)}_{A_{2j}}$ and any molecule with n_1 junctions have a trivial $F_{III,4d}$, hence

$$\text{rank}(F_{III,4d}) = 0. \tag{C.7}$$

The 5d flavor group is [9]

$$F_{\text{rest}} = \mathfrak{su}(n_1), \quad \Rightarrow \quad \text{rank}(F_{\text{rest}}) = n_1 - 1, \tag{C.8}$$

and hence again the rank of the class-$\mathcal{S}$ flavor group is the rank of the 5d F_{rest} minus the number of masses that we turned on to get the generalized quiver phase. In this case, to completely break F_{rest}, we have turned on a generic element on the Cartan $\mathfrak{h}_{\text{rest}} \subset F_{\text{rest}}$:

$$M = \sum_{i=1}^{2j} m_i \alpha_i^*, \tag{C.9}$$

with α_i the i-th dual root.[20] We can then consider the D_{2j} case. For this simple algebra, we have three different kind of atoms, $X^{(1)}_{D_{2j}}, X^{(1)}_{D_{2j}}$ and $X^{(3)}_{D_{2j}}$. We have [9]

$$\begin{aligned} F_{\text{rest}} &= \mathfrak{su}(n_1)^2 \times \mathfrak{su}(n_2) \times \mathfrak{su}(n_1 + 2n_3) \times \mathfrak{u}(1)^3, \quad \text{rank}(F_{\text{rest}}) = 3n_1 + n_2 + 2n_3 - 1, \\ F_{III,4d} &= \mathfrak{u}(1)^{2n_1} \times \mathfrak{su}(2)^{n_3}, \qquad \text{rank}(F_{III,4d}) = 2n_1 + n_3. \end{aligned} \tag{C.12}$$

[20] Let us define the "dual of the root α_j", an element of the Cartan $\mathfrak{h}_{\text{rest}}$ defined as

$$\left[\alpha_j^*, e_{\alpha_l}\right] = \delta_{jl} e_{\alpha_l}, \tag{C.10}$$

with e_{α_l} the root vector associated to the simple root α_l. Then, given the breaking

$$\mathfrak{u}(2n_1) \to \mathfrak{u}(1)^{n_1}. \tag{C.11}$$

JHEP10(2025)144

We can again verify that from (C.12) that

$$\text{rank}(F_{III,4d}) = \text{rank}(F_{\text{rest}}) - (n_1 + n_2 + n_3 - 1) = \text{rank}(F_{\text{rest}}) - n_{\text{masses}}. \tag{C.13}$$

The breaking pattern is first

$$\mathfrak{su}(n_1 + 2n_3) \to \mathfrak{su}(n_1) \times \mathfrak{su}(2n_2), \tag{C.14}$$

and then

$$\begin{aligned} \mathfrak{su}(n_1)^3 \times \mathfrak{u}(1) &\to \mathfrak{u}(1)^{2n_1}, \\ \mathfrak{su}(n_2) &\to \{1\}, \\ \mathfrak{su}(2n_3) &\to \mathfrak{su}(2)^{n_3}, \end{aligned} \tag{C.15}$$

where in the last lines we performed the breaking by turning on the following vev inside $\mathfrak{su}(2n_3)$:

$$M = \sum_{i=1}^{n_3-1} m_i \alpha^*_{2i}. \tag{C.16}$$

Finally, to match the class $\mathcal{S}$ molecule flavor group, we give mass to the leftover $\mathfrak{u}(1)^2$ factors.

For the D_{2j+1} case, we can proceed similarly, obtaining the following "accidental" 5d and 4d flavor groups

$$\begin{aligned} F_{\text{rest}} &= \mathfrak{su}(n_1) \times \mathfrak{su}(n_2)^2 \times \mathfrak{su}(n_1+2n_3) \times \mathfrak{u}(1)^3, \quad \text{rank}(F_{\text{rest}}) = 2n_1+2n_2+2n_3-1, \\ F_{III,4d} &= \mathfrak{u}(1)^{n_1} \times \mathfrak{u}(1)^{n_2} \times \mathfrak{su}(2)^{n_3}, \qquad \text{rank}(F_{III,4d}) = n_1+n_2+n_3 = \text{rank}(F_{III,4d}) - n_{\text{masses}}. \end{aligned} \tag{C.17}$$

The flavor symmetry breaking pattern is first

$$\mathfrak{su}(n_1 + 2n_3) \to \mathfrak{su}(n_1) \times \mathfrak{su}(2n_2), \tag{C.18}$$

followed by

$$\begin{aligned} \mathfrak{su}(n_1)^2 \times \mathfrak{u}(1) &\to \mathfrak{u}(1)^{n_1}, \\ \mathfrak{su}(n_2)^2 \times \mathfrak{u}(1) &\to \mathfrak{u}(1)^{n_2}, \\ \mathfrak{su}(2n_3) &\to \mathfrak{su}(2)^{n_3}, \end{aligned} \tag{C.19}$$

with the breaking in the last line being again (C.16). To match the 4d flavor group, we then give a mass to the $\mathfrak{u}(1)$ factor not appearing in (C.19).

We can then pass to the E_6 case. For the most general molecule, we have

$$\begin{aligned} F_{\text{rest}} &= \mathfrak{su}(n_1) \times \mathfrak{su}(n_2)^2 \times \mathfrak{su}(n_3) \times \mathfrak{u}(1)^3, \quad \text{rank}(F_{\text{rest}}) = n_1 + 2n_2 + n_3 - 1, \\ F_{III,4d} &= \mathfrak{u}(1)^{n_2}, \qquad \text{rank}(F_{III,4d}) = n_2 = \text{rank}(F_{\text{rest}}) - n_{\text{masses}}. \end{aligned} \tag{C.20}$$

The symmetry breaking $F_{\text{rest}} \to F_{III,4d}$ can be reached by turning on the generic Cartan element along the $\mathfrak{su}(n_1), \mathfrak{su}(n_3)$ factors, turning on a mass along two out of the three $\mathfrak{u}(1)$'s, and breaking

$$\mathfrak{su}(n_2)^2 \times \mathfrak{u}(1) \to \mathfrak{u}(1)^{n_2} \tag{C.21}$$

via turning on a diagonal combination along the two $\mathfrak{su}(n_2)$ factors.

JHEP10(2025)144

For the E_7 case, we have

$$\begin{aligned} F_{\text{rest}} &= \mathfrak{su}(n_1) \times \mathfrak{su}(2n_2 + n1) \times \mathfrak{su}(n_3) \times \mathfrak{u}(1)^2, \quad \text{rank}(F_{\text{rest}}) = 2n_1 + 2n_2 + n_3 - 1, \\ F_{III,4d} &= \mathfrak{u}(1)^{n_1} \times \mathfrak{su}(2)^{n_2}, \qquad \text{rank}(F_{III,4d}) = n_1 + n_2 = \text{rank}(F_{\text{rest}}) - n_{\text{masses}}. \end{aligned} \tag{C.22}$$

Again, the breaking goes as follows: first we break

$$\mathfrak{su}(2n_2 + n_1) \to \mathfrak{su}(n_1) \times \mathfrak{su}(2n_2), \tag{C.23}$$

we give mass to one of the two $\mathfrak{u}(1)$ factors, and finally we break

$$\begin{aligned} \mathfrak{su}(n_1)^2 \times \mathfrak{u}(1) &\to \mathfrak{u}(1)^{n_1}, \\ \mathfrak{su}(2n_2) &\to \mathfrak{su}(2)^{n_2}. \end{aligned} \tag{C.24}$$

Lastly, we have the E_8 case:

$$F_{\text{rest}} = \mathfrak{su}(n_1) \times \mathfrak{su}(n_2) \times \mathfrak{su}(n_3) \times \mathfrak{u}(1)^2, \quad \text{rank}(F_{\text{rest}}) = n_1 + n_2 + n_3 - 1, \tag{C.25}$$

with trivial $F_{III,4d}$, as expected being the rank of F_{rest} equal to the mass parameters needed to get to the generalized linear quiver phase. In this case, the breaking is compatible with the mass vev being a generic element in the Cartan subalgebra of F_{rest}.

D Notation for quivers and brane webs

In this appendix we briefly summarise the notation we use for quivers and brane webs.

D.1 Quivers

As is customary, we use square nodes for flavour groups, round nodes for gauge groups, and edges for bifundamental hypermultiplets (or half-hypermultiplets if the bifundamental representation is quaternionic). We colour the nodes white for unitary groups, yellow for special unitary groups (possibly with Chern-Simons level k), red for special orthogonal groups, and blue for compact symplectic groups:

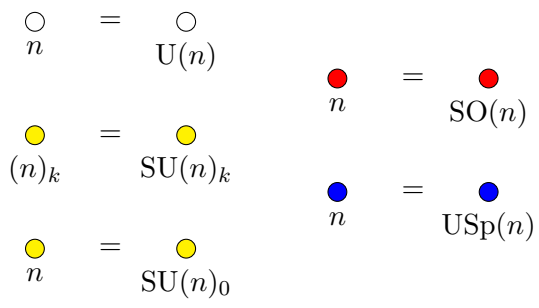

. (D.1)

Unframed quivers. If the quiver is unframed, i.e. there are no flavour nodes, then there can be a 1-form symmetry which can be gauged. (see e.g. [95], where the 1-form symmetry is referred to as 'H'.).

For an unframed quiver with only unitary gauge nodes there is a $\text{U}(1)^{(1)}$ 1-form symmetry which we always take to be gauged, and hence the true gauge group of the quiver is $\prod_i \text{U}(r_i)/\text{U}(1)$, where r_i are the ranks of the individual gauge nodes.

JHEP10(2025)144

Type IIB	x^0	x^1	x^2	x^3	x^4	x^5	x^6	x^7	x^8	x^9
(p,q)5-brane	×	×	×	×	×	angle α				
$[p,q]$7-brane	×	×	×	×	×			×	×	×

Table 9. Occupation of space-time directions of the (p,q)5-branes and $[p,q]$7-branes in Type IIB are denoted by ×. The angle α depends on the (p,q) charges and the axio-dilaton τ; $\alpha = \arg(p+\tau q)$. We set $\tau = i$ in the rest of the paper, s.t. $\tan(\alpha) = q/p$. Our 5d $\mathcal{N}=1$ theories exist as effective field theories living on fivebranes suspended between sevenbranes.

For an unframed quiver Q with only compact symplectic gauge nodes, and possibly even special orthogonal and/or unitary gauge nodes, there is a $\mathbb{Z}_2^{(1)}$ 1-form symmetry which may be gauged (or not). We denote the gauging of this 1-form symmetry by writing

$$\mathsf{Q} \Big/ \mathbb{Z}_2^{(1)} \quad . \tag{D.2}$$

D.2 Brane webs

We consider webs of (p,q)5-branes and $[p,q]$7-branes in Type IIB String Theory [15–17]. The occupied spacetime directions of the branes are summarised in table 9.

We depict brane webs by drawing the (x^5, x^6) plane:

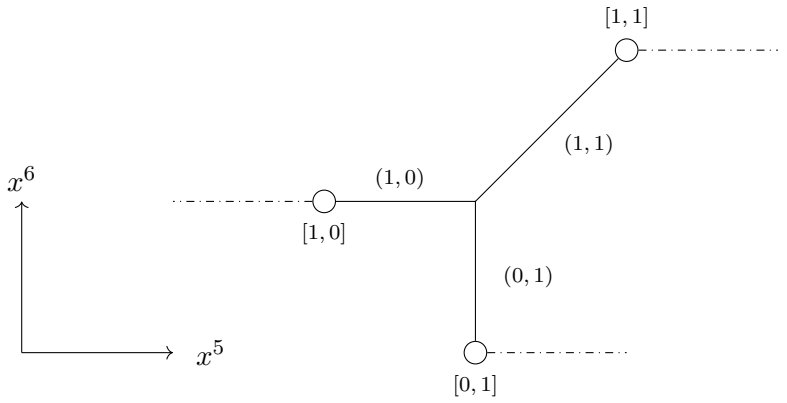

. (D.3)

A (p,q)5-brane ends on a $[p,q]$7-brane, or on a fivebrane vertex which preserves (p,q) charges. Multiple (p,q)5-branes can end on the same $[p,q]$7-brane as long as the s-rule [39, 49, 101, 102] is not violated.

Each $[p,q]$7-brane induces an $\mathrm{SL}(2,\mathbb{Z})$ monodromy cut (depicted by a dot-dash line) with associated monodromy matrix

$$M_{[p,q]} = \begin{pmatrix} 1-pq & p^2 \\ -q^2 & 1+pq \end{pmatrix} . \tag{D.4}$$

We usually don't draw the monodromy cuts of sevenbranes if they are oriented in such a way that they do not cross any fivebranes.

JHEP10(2025)144

An (r,s)5-brane crossing the monodromy cut of a $[p,q]$7-brane is affected in the following way:

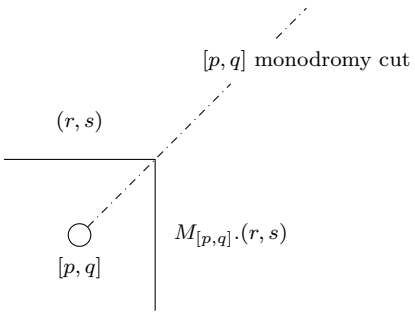

. (D.5)

When the (r,s)5-brane is pulled through the $[p,q]$7-brane, $|ps-qr|$ extra (r,s)5-branes are created via the Hanany-Witten effect:

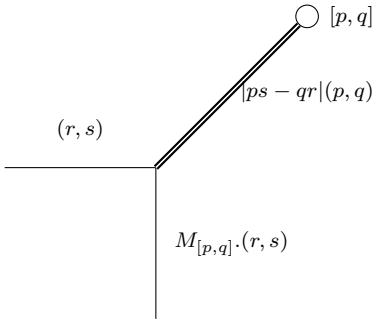

. (D.6)

We also study brane webs in the presence of orientifold 5-planes. In particular ON5$^-$ which we draw as a green line, and $\widetilde{\text{ON5}}^-$ (which corresponds to an ON5$^-$ with a stuck $\frac{1}{2}(0,1)5$ on top) which we draw as an orange line. An ON5$^-$ crossing a $\frac{1}{2}[0,1]$7-brane turns into an $\widetilde{\text{ON5}}^-$:

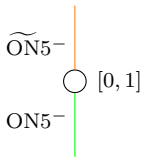

(D.7)

(suppressing the monodromy cut of the half sevenbrane, which is pointing upwards along the $\widetilde{\text{ON5}}^-$).

Data Availability Statement. This article has no associated data or the data will not be deposited.

Code Availability Statement. This article has no associated code or the code will not be deposited.

JHEP10(2025)144

References

[1] E. Witten, *String theory dynamics in various dimensions*, *Nucl. Phys. B* **443** (1995) 85 [hep-th/9503124] [INSPIRE].

[2] A. Strominger and M. Dine, *Open p-branes*, *Phys. Lett. B* **383** (1996) 44 [hep-th/9512059] [INSPIRE].

[3] E. Witten, *Five-branes and M-theory on an orbifold*, *Nucl. Phys. B* **463** (1996) 383 [hep-th/9512219] [INSPIRE].

[4] O.J. Ganor and A. Hanany, *Small E_8 instantons and tensionless noncritical strings*, *Nucl. Phys. B* **474** (1996) 122 [hep-th/9602120] [INSPIRE].

[5] N. Seiberg, *Nontrivial fixed points of the renormalization group in six-dimensions*, *Phys. Lett. B* **390** (1997) 169 [hep-th/9609161] [INSPIRE].

[6] N. Seiberg, *Five-dimensional SUSY field theories, nontrivial fixed points and string dynamics*, *Phys. Lett. B* **388** (1996) 753 [hep-th/9608111] [INSPIRE].

[7] D.R. Morrison and N. Seiberg, *Extremal transitions and five-dimensional supersymmetric field theories*, *Nucl. Phys. B* **483** (1997) 229 [hep-th/9609070] [INSPIRE].

[8] M.R. Douglas, S.H. Katz and C. Vafa, *Small instantons, Del Pezzo surfaces and type I-prime theory*, *Nucl. Phys. B* **497** (1997) 155 [hep-th/9609071] [INSPIRE].

[9] M. De Marco, M. Del Zotto, M. Graffeo and A. Sangiovanni, *Conformal matter*, *JHEP* **05** (2024) 306 [*Erratum ibid.* **08** (2024) 067] [arXiv:2311.04984] [INSPIRE].

[10] M. Del Zotto, J.J. Heckman, A. Tomasiello and C. Vafa, *6d conformal matter*, *JHEP* **02** (2015) 054 [arXiv:1407.6359] [INSPIRE].

[11] J.J. Heckman, D.R. Morrison, T. Rudelius and C. Vafa, *Atomic classification of 6D SCFTs*, *Fortsch. Phys.* **63** (2015) 468 [arXiv:1502.05405] [INSPIRE].

[12] L. Bhardwaj et al., *F-theory and the classification of little strings*, *Phys. Rev. D* **93** (2016) 086002 [*Erratum ibid.* **100** (2019) 029901] [arXiv:1511.05565] [INSPIRE].

[13] L. Bhardwaj, *Revisiting the classifications of 6d SCFTs and LSTs*, *JHEP* **03** (2020) 171 [arXiv:1903.10503] [INSPIRE].

[14] O.J. Ganor, D.R. Morrison and N. Seiberg, *Branes, Calabi-Yau spaces, and toroidal compactification of the N=1 six-dimensional E_8 theory*, *Nucl. Phys. B* **487** (1997) 93 [hep-th/9610251] [INSPIRE].

[15] O. Aharony and A. Hanany, *Branes, superpotentials and superconformal fixed points*, *Nucl. Phys. B* **504** (1997) 239 [hep-th/9704170] [INSPIRE].

[16] O. Aharony, A. Hanany and B. Kol, *Webs of (p,q) five-branes, five-dimensional field theories and grid diagrams*, *JHEP* **01** (1998) 002 [hep-th/9710116] [INSPIRE].

[17] O. DeWolfe, A. Hanany, A. Iqbal and E. Katz, *Five-branes, seven-branes and five-dimensional E_n field theories*, *JHEP* **03** (1999) 006 [hep-th/9902179] [INSPIRE].

[18] K.A. Intriligator, D.R. Morrison and N. Seiberg, *Five-dimensional supersymmetric gauge theories and degenerations of Calabi-Yau spaces*, *Nucl. Phys. B* **497** (1997) 56 [hep-th/9702198] [INSPIRE].

[19] N.C. Leung and C. Vafa, *Branes and toric geometry*, *Adv. Theor. Math. Phys.* **2** (1998) 91 [hep-th/9711013] [INSPIRE].

JHEP10(2025)144

[20] B.S. Acharya, *Confinement in five dimensions*, arXiv:2407.03171 [INSPIRE].

[21] D. Xie and S.-T. Yau, *Three dimensional canonical singularity and five dimensional N=1 SCFT*, *JHEP* **06** (2017) 134 [arXiv:1704.00799] [INSPIRE].

[22] P. Jefferson, H.-C. Kim, C. Vafa and G. Zafrir, *Towards classification of 5d SCFTs: single gauge node*, *SciPost Phys.* **14** (2023) 122 [arXiv:1705.05836] [INSPIRE].

[23] P. Jefferson, S. Katz, H.-C. Kim and C. Vafa, *On geometric classification of 5d SCFTs*, *JHEP* **04** (2018) 103 [arXiv:1801.04036] [INSPIRE].

[24] F. Apruzzi et al., *Fibers add flavor. Part I. Classification of 5d SCFTs, flavor symmetries and BPS states*, *JHEP* **11** (2019) 068 [arXiv:1907.05404] [INSPIRE].

[25] F. Apruzzi et al., *Fibers add flavor. Part II. 5d SCFTs, gauge theories, and dualities*, *JHEP* **03** (2020) 052 [arXiv:1909.09128] [INSPIRE].

[26] C. Closset, S. Schafer-Nameki and Y.-N. Wang, *Coulomb and Higgs branches from canonical singularities. Part 0*, *JHEP* **02** (2021) 003 [arXiv:2007.15600] [INSPIRE].

[27] C. Closset, S. Giacomelli, S. Schafer-Nameki and Y.-N. Wang, *5d and 4d SCFTs: canonical singularities, trinions and S-dualities*, *JHEP* **05** (2021) 274 [arXiv:2012.12827] [INSPIRE].

[28] C. Closset, S. Schäfer-Nameki and Y.-N. Wang, *Coulomb and Higgs branches from canonical singularities. Part I. Hypersurfaces with smooth Calabi-Yau resolutions*, *JHEP* **04** (2022) 061 [arXiv:2111.13564] [INSPIRE].

[29] A. Collinucci, M. De Marco, A. Sangiovanni and R. Valandro, *Higgs branches of 5d rank-zero theories from geometry*, *JHEP* **10** (2021) 018 [arXiv:2105.12177] [INSPIRE].

[30] A. Collinucci, A. Sangiovanni and R. Valandro, *Genus zero Gopakumar-Vafa invariants from open strings*, *JHEP* **09** (2021) 059 [arXiv:2104.14493] [INSPIRE].

[31] M. De Marco and A. Sangiovanni, *Higgs branches of rank-0 5d theories from M-theory on (A_j, A_l) and (A_k, D_n) singularities*, *JHEP* **03** (2022) 099 [arXiv:2111.05875] [INSPIRE].

[32] J. Tian and Y.-N. Wang, *5D and 6D SCFTs from $\mathbb{C}^3$ orbifolds*, *SciPost Phys.* **12** (2022) 127 [arXiv:2110.15129] [INSPIRE].

[33] C. Closset and H. Magureanu, *Partition functions and fibering operators on the Coulomb branch of 5d SCFTs*, *JHEP* **01** (2023) 035 [arXiv:2209.13564] [INSPIRE].

[34] A. Collinucci, M. De Marco, A. Sangiovanni and R. Valandro, *Flops of any length, Gopakumar-Vafa invariants and 5d Higgs branches*, *JHEP* **08** (2022) 292 [arXiv:2204.10366] [INSPIRE].

[35] M. De Marco, A. Sangiovanni and R. Valandro, *5d Higgs branches from M-theory on quasi-homogeneous cDV threefold singularities*, *JHEP* **10** (2022) 124 [arXiv:2205.01125] [INSPIRE].

[36] C. Closset and H. Magureanu, *Reading between the rational sections: global structures of 4d N=2 KK theories*, *SciPost Phys.* **16** (2024) 137 [arXiv:2308.10225] [INSPIRE].

[37] J. Mu, Y.-N. Wang and H.N. Zhang, *5d SCFTs from isolated complete intersection singularities*, *JHEP* **02** (2024) 155 [arXiv:2311.05441] [INSPIRE].

[38] A. Bourget, A. Collinucci and S. Schafer-Nameki, *Generalized toric polygons, T-branes, and 5d SCFTs*, *SciPost Phys.* **18** (2025) 079 [arXiv:2301.05239] [INSPIRE].

[39] F. Benini, S. Benvenuti and Y. Tachikawa, *Webs of five-branes and N=2 superconformal field theories*, *JHEP* **09** (2009) 052 [arXiv:0906.0359] [INSPIRE].

JHEP10(2025)144

[40] O. Bergman, D. Rodríguez-Gómez and G. Zafrir, *5-brane webs, symmetry enhancement, and duality in 5d supersymmetric gauge theory*, *JHEP* **03** (2014) 112 [arXiv:1311.4199] [INSPIRE].

[41] G. Zafrir, *Duality and enhancement of symmetry in 5d gauge theories*, *JHEP* **12** (2014) 116 [arXiv:1408.4040] [INSPIRE].

[42] H. Hayashi, S.-S. Kim, K. Lee and F. Yagi, *6d SCFTs, 5d dualities and Tao web diagrams*, *JHEP* **05** (2019) 203 [arXiv:1509.03300] [INSPIRE].

[43] H. Hayashi et al., *A new 5d description of 6d D-type minimal conformal matter*, *JHEP* **08** (2015) 097 [arXiv:1505.04439] [INSPIRE].

[44] O. Bergman and G. Zafrir, *5d fixed points from brane webs and O7-planes*, *JHEP* **12** (2015) 163 [arXiv:1507.03860] [INSPIRE].

[45] H. Hayashi, S.-S. Kim, K. Lee and F. Yagi, *Dualities and 5-brane webs for 5d rank 2 SCFTs*, *JHEP* **12** (2018) 016 [arXiv:1806.10569] [INSPIRE].

[46] H. Hayashi, S.-S. Kim, K. Lee and F. Yagi, *5-brane webs for 5d N=1 G_2 gauge theories*, *JHEP* **03** (2018) 125 [arXiv:1801.03916] [INSPIRE].

[47] H. Hayashi, S.-S. Kim, K. Lee and F. Yagi, *Rank-3 antisymmetric matter on 5-brane webs*, *JHEP* **05** (2019) 133 [arXiv:1902.04754] [INSPIRE].

[48] H. Hayashi, S.-S. Kim, K. Lee and F. Yagi, *Complete prepotential for 5d N=1 superconformal field theories*, *JHEP* **02** (2020) 074 [arXiv:1912.10301] [INSPIRE].

[49] O. Bergman and D. Rodríguez-Gómez, *The Cat's Cradle: deforming the higher rank E_1 and $\tilde{E}_1$ theories*, *JHEP* **02** (2021) 122 [arXiv:2011.05125] [INSPIRE].

[50] M. Del Zotto, J.J. Heckman and D.R. Morrison, *6D SCFTs and phases of 5D theories*, *JHEP* **09** (2017) 147 [arXiv:1703.02981] [INSPIRE].

[51] L. Bhardwaj and P. Jefferson, *Classifying 5d SCFTs via 6d SCFTs: rank one*, *JHEP* **07** (2019) 178 [*Addendum ibid.* **01** (2020) 153] [arXiv:1809.01650] [INSPIRE].

[52] L. Bhardwaj and P. Jefferson, *Classifying 5d SCFTs via 6d SCFTs: arbitrary rank*, *JHEP* **10** (2019) 282 [arXiv:1811.10616] [INSPIRE].

[53] L. Bhardwaj, *Do all 5d SCFTs descend from 6d SCFTs?*, *JHEP* **04** (2021) 085 [arXiv:1912.00025] [INSPIRE].

[54] L. Bhardwaj and G. Zafrir, *Classification of 5d N=1 gauge theories*, *JHEP* **12** (2020) 099 [arXiv:2003.04333] [INSPIRE].

[55] S. Cremonesi, A. Hanany and A. Zaffaroni, *Monopole operators and Hilbert series of Coulomb branches of 3d N=4 gauge theories*, *JHEP* **01** (2014) 005 [arXiv:1309.2657] [INSPIRE].

[56] S. Cremonesi, G. Ferlito, A. Hanany and N. Mekareeya, *Instanton operators and the Higgs branch at infinite coupling*, *JHEP* **04** (2017) 042 [arXiv:1505.06302] [INSPIRE].

[57] G. Ferlito and A. Hanany, *A tale of two cones: the Higgs Branch of $Sp(n)$ theories with $2n$ flavours*, arXiv:1609.06724 [INSPIRE].

[58] G. Ferlito, A. Hanany, N. Mekareeya and G. Zafrir, *3d Coulomb branch and 5d Higgs branch at infinite coupling*, *JHEP* **07** (2018) 061 [arXiv:1712.06604] [INSPIRE].

[59] S. Cabrera and A. Hanany, *Quiver subtractions*, *JHEP* **09** (2018) 008 [arXiv:1803.11205] [INSPIRE].

[60] S. Cabrera, A. Hanany and F. Yagi, *Tropical geometry and five dimensional Higgs branches at infinite coupling*, *JHEP* **01** (2019) 068 [arXiv:1810.01379] [INSPIRE].

JHEP10(2025)144

[61] S. Cabrera, A. Hanany and M. Sperling, *Magnetic quivers, Higgs branches, and 6d N=(1,0) theories*, *JHEP* **06** (2019) 071 [*Erratum ibid.* **07** (2019) 137] [arXiv:1904.12293] [INSPIRE].

[62] A. Bourget et al., *The Higgs mechanism — Hasse diagrams for symplectic singularities*, *JHEP* **01** (2020) 157 [arXiv:1908.04245] [INSPIRE].

[63] A. Bourget et al., *Brane webs and magnetic quivers for SQCD*, *JHEP* **03** (2020) 176 [arXiv:1909.00667] [INSPIRE].

[64] S. Cabrera, A. Hanany and M. Sperling, *Magnetic quivers, Higgs branches, and 6d N=(1,0) theories — orthogonal and symplectic gauge groups*, *JHEP* **02** (2020) 184 [arXiv:1912.02773] [INSPIRE].

[65] J.F. Grimminger and A. Hanany, *Hasse diagrams for 3d N=4 quiver gauge theories — inversion and the full moduli space*, *JHEP* **09** (2020) 159 [arXiv:2004.01675] [INSPIRE].

[66] A. Bourget et al., *Magnetic quivers from brane webs with O5 planes*, *JHEP* **07** (2020) 204 [arXiv:2004.04082] [INSPIRE].

[67] A. Bourget et al., *Magnetic quivers for rank 1 theories*, *JHEP* **09** (2020) 189 [arXiv:2006.16994] [INSPIRE].

[68] M. Akhond et al., *Five-brane webs, Higgs branches and unitary/orthosymplectic magnetic quivers*, *JHEP* **12** (2020) 164 [arXiv:2008.01027] [INSPIRE].

[69] A. Bourget et al., *S-fold magnetic quivers*, *JHEP* **02** (2021) 054 [arXiv:2010.05889] [INSPIRE].

[70] M. Van Beest, A. Bourget, J. Eckhard and S. Schäfer-Nameki, *(5d RG-flow) trees in the tropical rain forest*, *JHEP* **03** (2021) 241 [arXiv:2011.07033] [INSPIRE].

[71] J.J. Heckman, T. Rudelius and A. Tomasiello, *Fission, fusion, and 6D RG flows*, *JHEP* **02** (2019) 167 [arXiv:1807.10274] [INSPIRE].

[72] P.C. Argyres and M.R. Douglas, *New phenomena in SU(3) supersymmetric gauge theory*, *Nucl. Phys. B* **448** (1995) 93 [hep-th/9505062] [INSPIRE].

[73] O. Chacaltana and J. Distler, *Tinkertoys for Gaiotto duality*, *JHEP* **11** (2010) 099 [arXiv:1008.5203] [INSPIRE].

[74] O. Chacaltana and J. Distler, *Tinkertoys for the D_N series*, *JHEP* **02** (2013) 110 [arXiv:1106.5410] [INSPIRE].

[75] O. Chacaltana, J. Distler and Y. Tachikawa, *Nilpotent orbits and codimension-two defects of 6d N=(2,0) theories*, *Int. J. Mod. Phys. A* **28** (2013) 1340006 [arXiv:1203.2930] [INSPIRE].

[76] O. Chacaltana, J. Distler and Y. Tachikawa, *Gaiotto duality for the twisted A_{2N-1} series*, *JHEP* **05** (2015) 075 [arXiv:1212.3952] [INSPIRE].

[77] O. Chacaltana, J. Distler and A. Trimm, *Tinkertoys for the twisted D-series*, *JHEP* **04** (2015) 173 [arXiv:1309.2299] [INSPIRE].

[78] O. Chacaltana, J. Distler and A. Trimm, *Tinkertoys for the E_6 theory*, *JHEP* **09** (2015) 007 [arXiv:1403.4604] [INSPIRE].

[79] O. Chacaltana, J. Distler and A. Trimm, *Tinkertoys for the twisted E_6 theory*, arXiv:1501.00357 [INSPIRE].

[80] O. Chacaltana, J. Distler and A. Trimm, *Tinkertoys for the Z3-twisted D4 theory*, arXiv:1601.02077 [INSPIRE].

[81] O. Chacaltana, J. Distler, A. Trimm and Y. Zhu, *Tinkertoys for the E_7 theory*, *JHEP* **05** (2018) 031 [arXiv:1704.07890] [INSPIRE].

JHEP10(2025)144

[82] O. Chacaltana, J. Distler, A. Trimm and Y. Zhu, *Tinkertoys for the E_8 theory*, arXiv:1802.09626 [INSPIRE].

[83] K. Yonekura, *Instanton operators and symmetry enhancement in 5d supersymmetric quiver gauge theories*, *JHEP* **07** (2015) 167 [arXiv:1505.04743] [INSPIRE].

[84] A. Bourget, M. De Marco, M. Del Zotto, J.F. Grimminger and A. Sangiovanni, to appear.

[85] F. Apruzzi, S. Schafer-Nameki and Y.-N. Wang, *5d SCFTs from decoupling and gluing*, *JHEP* **08** (2020) 153 [arXiv:1912.04264] [INSPIRE].

[86] K. Ohmori, H. Shimizu, Y. Tachikawa and K. Yonekura, *6d N=(1,0) theories on S^1/T^2 and class S theories. Part II*, *JHEP* **12** (2015) 131 [arXiv:1508.00915] [INSPIRE].

[87] M. Martone and G. Zafrir, *On the compactification of 5d theories to 4d*, *JHEP* **08** (2021) 017 [arXiv:2106.00686] [INSPIRE].

[88] D.H. Collingwood and W.M. McGovern, *Nilpotent orbits in semisimple Lie algebras*, Routledge (2017) [DOI:10.1201/9780203745809].

[89] L. Bhardwaj, M. Hubner and S. Schafer-Nameki, *1-form symmetries of 4d N=2 class S theories*, *SciPost Phys.* **11** (2021) 096 [arXiv:2102.01693] [INSPIRE].

[90] E. Witten, *Nonperturbative superpotentials in string theory*, *Nucl. Phys. B* **474** (1996) 343 [hep-th/9604030] [INSPIRE].

[91] A. Sen, *A note on enhanced gauge symmetries in M and string theory*, *JHEP* **09** (1997) 001 [hep-th/9707123] [INSPIRE].

[92] A. Sen, *Dynamics of multiple Kaluza-Klein monopoles in M and string theory*, *Adv. Theor. Math. Phys.* **1** (1998) 115 [hep-th/9707042] [INSPIRE].

[93] B.S. Acharya, *M theory, G_2-manifolds and four-dimensional physics*, *Class. Quant. Grav.* **19** (2002) 5619 [INSPIRE].

[94] A. Hanany and A. Zaffaroni, *Issues on orientifolds: on the brane construction of gauge theories with $SO(2n)$ global symmetry*, *JHEP* **07** (1999) 009 [hep-th/9903242] [INSPIRE].

[95] A. Bourget et al., *Magnetic lattices for orthosymplectic quivers*, *JHEP* **12** (2020) 092 [arXiv:2007.04667] [INSPIRE].

[96] F. Benini, Y. Tachikawa and D. Xie, *Mirrors of 3d Sicilian theories*, *JHEP* **09** (2010) 063 [arXiv:1007.0992] [INSPIRE].

[97] A. Dancer, J.F. Grimminger, J. Martens and Z. Zhong, *Complex symplectic contractions and 3d mirrors*, *JHEP* **11** (2024) 116 [arXiv:2406.09626] [INSPIRE].

[98] K. Ohmori, H. Shimizu, Y. Tachikawa and K. Yonekura, *6d N=(1,0) theories on T^2 and class S theories. Part I*, *JHEP* **07** (2015) 014 [arXiv:1503.06217] [INSPIRE].

[99] M. De Marco, M. Del Zotto, J.F. Grimminger and A. Sangiovanni, to appear.

[100] C. Closset, M. Del Zotto and V. Saxena, *Five-dimensional SCFTs and gauge theory phases: an M-theory/type IIA perspective*, *SciPost Phys.* **6** (2019) 052 [arXiv:1812.10451] [INSPIRE].

[101] A. Hanany and E. Witten, *Type IIB superstrings, BPS monopoles, and three-dimensional gauge dynamics*, *Nucl. Phys. B* **492** (1997) 152 [hep-th/9611230] [INSPIRE].

[102] M. van Beest, A. Bourget, J. Eckhard and S. Schafer-Nameki, *(Symplectic) leaves and (5d Higgs) branches in the poly(go)nesian tropical rain forest*, *JHEP* **11** (2020) 124 [arXiv:2008.05577] [INSPIRE].

JHEP10(2025)144